

**INVESTIGATIONS OF EMBROIDERY ANTENNAS
ON POLYMER SUBSTRATE**

NGO QUANG BAO LOC, BEng.

**Thesis submitted to the University of Nottingham
for the degree of Master of Philosophy**

FEBRUARY 2016

Abstract

For everyday human life, people desire to stay connected via an advanced wireless network. Although cellular phone is worthy in various applications, people are likely to carry a wide range of mobile devices and constantly connect with each other. Future communication network requires a new class of front-ends electronic devices that are small, light-weight, conformal, multi-functional but also environment-friendly, inexpensive and good performance. In different aspects, once of the key factors to achieve this goal is to integrate the wireless antenna into garments as daily clothes and enhance its durability. Consequently, these wearable antennas need not only possess good RF performance characteristics but also mechanical structure which adaptable to conformity and durability. This dissertation presents a novel class embroidery patch antenna on polymer composite — polydimethylsiloxane (PDMS). By lamination and polymer integration, different structures and feeding techniques of fully embroidered polymer patch antenna with ground plane have been designed, fabricated and tested. Analysis of the effect of conductive patch weight as well as conductive characteristics using different embroidery structures on antenna performance has been carried out. The measured results show that although double embroidered layer on one side of fabric has similar conductivity and identical embroidery properties as two-sided embroidery, the antenna performs better using two-sided embroidery structure in term of reflection coefficient and gain measurement.

In respect of conductivity of embroidered layers, the thesis investigates a method to improve the conductivity of embroidered patches used in antennas on polymer composite. Nanopowders which include graphene, zinc oxide

(ZnO), aluminum oxide (Al_2O_3) and copper oxide (CuO) were dispersed in ethanol solvent to prepare as dyeing solutions. The effect of nanopowders on patches resistance has been studied. The measured results show that the patch conductivity improves 11.87% after 7 times dyeing with CuO and 8.14% after 10 times dyeing with ZnO. In contrast, graphene raises up the sheet resistance. The CuO and ZnO dyed conductive patch layers have been laminated and integrated on polymer substrate with embroidered ground plane to analyze the dyeing effect on antenna performance. Although dyeing effect reduces the resonant frequencies, the measured result indicates that dyed patch antennas perform better in term of reflection coefficient level.

List of Publications

Conferences:

[1] Loc Ngo Quang Bao, Pei Cheng Ooi and Jit Kai Chin, “The effect of different structures of embroidery patch antenna on polymer substrate with identical embroidery properties,” *IEEE International Symposium on Antennas and Propagation and USNC-URSI Radio Science Meeting (APSURSI)*, Memphis, Tennessee, USA, pp. 840-841, July 2014.

[2] Loc Ngo Quang Bao, Pei Cheng Ooi, Jit Kai Chin and Chuan Chin Pu, “Investigation of embroidery conductive layer dyed with graphene and ZnO,” presented in *19th International Symposium on Antennas and Propagation (ISAP)*, Taiwan, pp. 515-516, December 2014.

Journals:

[1] Loc Ngo Quang Bao, Pei Cheng Ooi, Jit Kai Chin and Chuan Chin Pu, “Embroidery Patch Antennas on Polymer Substrate with Identical Embroidery Properties,” submitted for review to the *IEEE Transaction on Antennas and Propagation*.

[2] Loc Ngo Quang Bao, Pei Cheng Ooi, Jit Kai Chin and Chuan Chin Pu, “Embroidery Patch Antennas Dyed with Nanopowders on Polymer Substrate,” submitted for review to the *IEEE Transaction on Antennas and Propagation*.

*Note: The papers are attached at the end of this dissertation for reference

Acknowledgements

I am deeply indebted to my supervisor, Dr. Pei Cheng Ooi, who has inspired me to undertake the work presented herein. I would like to appreciate her for her kindness and time spent throughout the years by carefully reviewing my work and manuscripts. Her constant encouragement, valuable suggestions, patience and guidance have been a valuable asset in my research.

I would also like to express my gratitude to my examiner Dr. Amin Malek Mohammadi for his thorough examination of my thesis. His valuable suggestions and comments have not only led to an improved thesis, but also will have significant impact on my future research path.

A special thank must be made to my co-supervisor Dr. Jit Kai Chin and Dr. Linus Lau from CST Malaysia for their time and advices on my research. Their willingness of listening to the electromagnetic problems has brought great discussion for my project.

I would also like to acknowledge my appreciation to Malaysia government, Ministry of Science, Technology and Innovation (MOSTI) for the sponsorship and the University of Nottingham Malaysia Campus for providing me laboratory and equipment that support me to finish my research.

Words seem not enough for me to express my heartfelt appreciation to my family, my mom Mrs. Thuy Nguyen and my sweetie Ms. Chuong Le for their encouragement, warm support through tough times and always. I am also pleased to send my regards to Ms. Nguyen Ngo for her assistance in drawing images, my perfect partners Ms. June, Dr. Renu, Dr. Cat, my VFT fellow together with all of my friends, 105 full house, my sisters and brothers in UN for their great kindness during my research journey.

Table of Contents

Abstract	i
List of Publications	iii
Acknowledgements	iv
Table of Contents	v
List of Figures	viii
List of Tables	xii
List of Abbreviations	xiii
CHAPTER 1	1
Introduction	1
1.1 Motivation of Research.....	1
1.2 Aims and Objectives.....	2
1.2.1 Scope of Work.....	2
1.2.2 Project Deliverables.....	4
1.2.3 Research Applications	5
1.3 Thesis Organization.....	6
CHAPTER 2	7
Literature Review	7
2.1 Fundamental Parameters of Antennas	7
2.1.1 Bandwidth	7
2.1.2 Return Loss and Reflection Coefficient.....	7
2.1.3 Radiation Pattern	8
2.1.4 Gain, Directivity and Efficiency	8
2.1.5 Polarization	8
2.1.6 Antenna Field Regions.....	9
2.2 Conformal Antenna	9
2.2.1 Textile and Fabric Antenna.....	10
2.2.2 Embroidery Antenna.....	16
2.2.3 Antenna Using Polymer Materials	25
2.2.4 Embroidery Antenna on PDMS Substrate	29
2.3 Summary.....	32

CHAPTER 3.....	34
Research Methods and Materials.....	34
3.1 Research Materials	34
3.1.1 Conductive Threads.....	34
3.1.2 PDMS Polymer Composite.....	37
3.2 Research Methods and Measurement Set-Ups.....	38
3.2.1 Embroidery Process.....	38
3.2.2 PDMS Preparation and Antenna Fabrication.....	39
3.2.3 Simulation Software and Setting.....	41
3.2.4 Measurement Set-Ups.....	41
3.3 Summary.....	46
CHAPTER 4.....	47
Embroidery Patch Antenna on Polymer Substrate with Identical Embroidery Properties	47
4.1 Introduction.....	47
4.2 Antenna Design and Characterization.....	47
4.2.1 Embroidery Structures	47
4.2.2 Design One – Microstrip-fed Rectangular Patch Antenna	48
4.2.3 Design Two – Microstrip-fed Polygon Patch Antenna.....	55
4.2.4 Design Three – SMA-fed Polygon Patch Antenna.....	56
4.3 Results and Discussion	58
4.3.1 Patch Resistance	58
4.3.2 Reflection Coefficient.....	60
4.3.3 Radiation Patterns.....	66
4.3.4 On-axis Gain	72
4.4 Summary.....	73
CHAPTER 5.....	75
Embroidery Patch Antennas Dyed with Nanopowders on Polymer Substrate.....	75
5.1 Introduction.....	75
5.2 Dyeing Solution Preparation.....	76
5.3 Embroidered Patch Resistance.....	78

5.4 Embroidery Patch Antennas Dyed with Nanopowder on PDMS substrate	82
5.5 Summary.....	87
CHAPTER 6.....	88
Conclusion and Future Work.....	88
References	90
Appendices	97

List of Figures

Figure 2.1 Literature review of conformal antenna	10
Figure 2.2 Geometry of the WLAN fabric antenna (redrawn from [11])	11
Figure 2.3 Weave pattern of the satin weave [13]	12
Figure 2.4 Geometry of rectangular ring textile antenna [14]	12
Figure 2.5 Measured phase angles of S21 for conductive polymer fabrics (left) and metal-coated fabrics (right) compared with a phase measured from a copper trace [15]	13
Figure 2.6 (a) Photograph of the various antenna structures bent with different radius, (b) Measured effect of antenna bending on S11 [16]	13
Figure 2.7 Photograph of the fabricated circular patch wearable antenna [9]	14
Figure 2.8 Photograph of proposed antenna [17]	14
Figure 2.9 Demonstration of the patch antenna flexibility [20]	15
Figure 2.10 Inkjet-printed textile antenna fabrication processes [21]	16
Figure 2.11 (a) Measurement set-up calibration, (b) Tag position on arm, (c) Tag-to-body separation increased with additional cotton fabric layers, (d) Embroidered tag model with different substrate thickness h on the human arm model [25].....	18
Figure 2.12 Sketch of patches and the stitch directions (redrawn from [26])	18
Figure 2.13 Photograph of embroidered patch antenna [23]	19
Figure 2.14 The prototype of embroidered Sierpinski carpet Antenna (a) Inner substrate, (b) Back view, (c) Front view [29]	20
Figure 2.15 The photograph of wearable antenna prototypes (a) Copper conducting sheet, (b) Embroidered conducting thread [30].....	21
Figure 2.16 Three manufactured antennas (from left to right): silver fabric, single-layer embroidery, dual-layer embroidery, the feeding structure can be attached to the antennas [31].....	22
Figure 2.17 Embroidered structures for wearable tag antenna ground planes (a) Embroidery 1, square density $3\lambda/100$, (b) Embroidery 2, square density $3\lambda/200$, (c) Embroidery 3, square density $9\lambda/1000$, (d) Embroidery 4, vertical line density $3\lambda/500$, (e) Embroidery 5, horizontal line density $3\lambda/500$, (f) Embroidery 6, vertical line densities $3\lambda/100$, $9\lambda/1000$ and $3\lambda/500$. The wavelength corresponds to 900 MHz [5].....	23

Figure 2.18	Conductive fabrics from LessEMF (a) copper, (b) argenmesh, (c) ripstop and (d) stretch [5].....	23
Figure 2.19	Reflection coefficient results of polypropylene based monopole antenna [36].....	26
Figure 2.20	Reflection coefficient results of proposed antenna in flat condition (left), and folded condition (right) [39].....	26
Figure 2.21	Photograph of printed antenna coil on PET substrate [40].....	27
Figure 2.22	Patch antenna (a) Copper mesh sandwiched inside PDMS, (b) The antenna prototype, bottom view [42].....	28
Figure 2.23	Tripod kettle antenna prototypes (a) before encapsulation in PDMS, (b) after encapsulation in PDMS [42].....	28
Figure 2.24	SC-based aperture-coupled patch antenna (all dimensions are in mm) [43].....	29
Figure 2.25	Printing process of single layer E-fiber RF circuit on PDMS [44].....	30
Figure 2.26	Prototype of embroidered transmission line on PDMS (a) One layer lamination on PDMS, (b) Fabricated microstrip line with ground plane, (c) Fabricated microstrip line under bending [44].....	30
Figure 2.27	Embroidered patch antenna mounted on (a) planar and (b) cylindrical surface respectively [46].....	31
Figure 2.28	E-fiber antenna array on PDMS-ceramic substrate (a) simulation geometry, (b) fabricated E-fiber array, (c) fabricated copper array [47].....	31
Figure 3.1	Conductive threads (a) monofilament, (b) bundled monofilament, (c),(d) nonconductive yarns twisted with conductive filaments [49].....	35
Figure 3.2	Photograph of studied conductive threads (a) Shieldex 40-22/7 + 110 PET 3ply, (b) Shieldex 33-17 PET 2ply and (c) Amberstrand 166.....	36
Figure 3.3	Photograph PDMS elastomer kit (a) silicone gel, (b) cross-link agent.....	37
Figure 3.4	(a) Photograph of embroidery machine, (b) Lock stitch formation.....	38
Figure 3.5	Photograph of PDMS fabrication process (a) Mixing silicone gel and cross-link agent, (b) Mixing composite thoroughly, (c) Degassing bubbles, (d), Fully-cured PDMS.....	39
Figure 3.6	Process of lamination and integration of embroidery antenna on PDMS substrate.....	40

Figure 3.7	Calibration set-up for reflection coefficient measurement.....	43
Figure 3.8	Calibration set-up for radiation pattern measurement.....	43
Figure 3.9	Photograph of reflection coefficient measurement set-up.....	43
Figure 3.10	Photograph of radiation pattern measurement set-up.....	44
Figure 3.11	Photograph of testing antenna mounted on tripod with foam supporter	44
Figure 3.12	Photograph resistance measurements by Fluke PM 6304	46
Figure 4.1	Three different embroidery structures.....	47
Figure 4.2	Microstrip-fed rectangular patch antenna geometry	50
Figure 4.3	Simulated reflection coefficient result of copper microstrip-fed rectangular patch antenna	52
Figure 4.4	Normalized simulated radiation patterns of copper microstrip-fed rectangular patch antenna at 2.35 GHz	53
Figure 4.5	Photograph of microstrip-fed rectangular patch antenna prototype	54
Figure 4.6	Microstrip-fed polygon patch antenna geometry	55
Figure 4.7	Photograph of microstrip-fed polygon patch antenna prototype .	55
Figure 4.8	SMA-fed polygon patch antenna geometry	56
Figure 4.9	Photograph of SMA-fed polygon patch antenna prototype.....	56
Figure 4.10	(a) Etching hole on ground plane, (b) Connectors with rubber tape	57
Figure 4.11	Measured reflection coefficient result of microstrip-fed rectangular patch antenna in different structures.....	61
Figure 4.12	Measured reflection coefficient result of microstrip-fed polygon patch antenna in different structures	63
Figure 4.13	Measured reflection coefficient result of SMA-fed polygon patch antenna in different structures.....	64
Figure 4.14	Normalized measured radiation patterns of antenna 1A at 3.23 and 4.63 GHz.....	67
Figure 4.15	Normalized measured radiation patterns of antenna 1B at 3.05 and 4.46 GHz.....	67
Figure 4.16	Normalized measured radiation patterns of antenna 1C at 3.25 and 4.48 GHz.....	68
Figure 4.17	Normalized measured radiation patterns of antenna 2A at 1.0 and 3.08 GHz.....	68

Figure 4.18 Normalized measured radiation patterns of antenna 2B at 1.17 and 3.18 GHz.....	69
Figure 4.19 Normalized measured radiation patterns of antenna 3A at 3.37 GHz	69
Figure 4.20 Normalized measured radiation patterns of antenna 3B at 3.61 GHz	69
Figure 5.1 Dyeing solution preparation process	77
Figure 5.2 Photograph of dyeing solution before and after sonicating process (a) Graphene, (b) ZnO, (c) CuO, (d) Al ₂ O ₃	77
Figure 5.3 Microscope zoom 4x view of dyeing solution.....	78
Figure 5.4 Microscope zoom 4x view of dyed embroidered antenna patch (a) origin without dyeing, (b) ZnO, (c) graphene, (d) CuO	79
Figure 5.5 SEM images of proposed embroidered patches after dyeing effect	80
Figure 5.6 Resistances of graphene, ZnO and CuO dyed patches.....	81
Figure 5.7 Microscope zoom 4x view of embroidered antenna patch (a) before immersion, (b) after 24 hours graphene immersion	82
Figure 5.8 Photograph of antenna prototype with front and back view (a) dyed with ZnO solution, (b) dyed with CuO solution.....	83
Figure 5.9 Measured reflection coefficient results of dyed embroidered patch antennas on PDMS substrate	84
Figure 5.10 Normalized measured radiation patterns of ZnO dyed antenna... ..	85
Figure 5.11 Normalized measured radiation patterns of CuO dyed antenna	86

List of Tables

Table 1.1 Project deliverables schedule	4
Table 3.1 Characteristics of studied conductive threads [51].....	36
Table 4.1 Parameters of the antenna – Design 1	52
Table 4.2 Parameters of the antenna – Design 2	56
Table 4.3 Parameters of the antenna – Design 3	57
Table 4.4 Characteristic of conductive patch layers	59
Table 4.5 Measured reflection coefficient comparison between three antenna designs with different structures	65
Table 4.6 Measured on-axis gain of proposed antennas	72
Table 5.1 Reflection coefficient comparisons between original and dyed patch antennas	84
Table 5.2 Measured On-axis gain of proposed antennas	87

List of Abbreviations

Acronym	Definition
3-D	Three-Dimensional
AMF	Asymmetric Meandered Flare
BAN	Body Area Network
LCP	Liquid Crystal Polymer
PDMS	Polydimethylsiloxane
PEN	Polyethylene Naphthalate
PET	Polyethylene Terephthalate
PIFA	Planar Inverted-F Antenna
PTFE	Polytetrafluoroethene
RF	Radio Frequency
RFID	Radio Frequency Identification
SAR	Specification Absorption Rate
SCs	Stretchable Conductors
SWNT	Single Wall Carbon Nanotube
TFT	Thin Film Transistors
TKA	Tripod Kettle Antenna
UHF	Ultra High Frequency
UWB	Ultra Wide Band

CHAPTER 1

Introduction

1.1 Motivation of Research

Advanced wireless communication systems and mobile electronic devices have become a part of everyday human life. People are likely to carry a range of portable devices and sensors which constantly communicate with each other and the outside world [1]. This forms up a modern network tending to the pervasive computing paradigm. As a result, future commercial systems require not only a new class of front-ends electronic devices that are small, light-weight, conformal, multi-functional but also environment-friendly, inexpensive and good performance.

For decades, the development in semiconductor technology has achieved great contribution in minimizing the size of transistors and integrated circuits. However, the microwave circuits, radio frequency (RF) electronics especially antennas still remain bulky with heavy metals, rigid surfaces and become the bottlenecks for such light-weight, conformity and system integration. Although radio-frequency identification (RFID) has gained its popularity due to the advantage of small, light-weight, environment-friendly and inexpensive with ink-jet printed capability [2, 3], future communication systems request for real-time signal transmitting and continuous frequency coverage [4]. As a result, antennas that are able to bear for mechanical loading, fully integration with structure, light-weight, flexible, robust and capable of body-worn application are highly attractive. In consequence, wearable and conformal antenna plays a key technology in establishing an efficient and reliable wireless communication

link between body-worn electronics and surrounding environment [5]. These antennas need not only possess good RF performance characteristics but also mechanical structure which adaptable to conformity and durability.

1.2 Aims and Objectives

Given the aforementioned demands, the aim of this project is to develop a novel class of good performance antenna that is light-weight, conformal and able to be integrated with garments as well as others flexible structures. The antenna fabrication process is inexpensive with environment friendly and conventional machinery.

The objectives of this project are to be achieved and described as below:

1. To develop the use of polymer as a substrate material for embroidery antenna.
2. Using silver-thread and conventional sewing machine to fabricate embroidery antenna on polymer substrate by lamination and multilayer integration techniques.
3. To analyze the effect of different structures of embroidery patch antenna on polymer substrate with identical embroidery properties.
4. To enhance conductivity of embroidered antenna layers by dying method with nanoparticles and study its effect on antenna performance.

1.2.1 Scope of Work

From the objectives of this project are to be achieved, the project scope of works are detailed as below:

1. Study the theoretical concept of microstrip patch antenna including the design structure, the performance parameters and the radiation characteristics.

2. Study the method of using antenna simulation software, CST microwave studio.
3. Literature review the history and development of conformal antennas which are textile antenna and polymer antenna.
4. Literature review for the research of embroidery antenna on polymer substrate.
5. Investigate the method of using conductive thread to embroider the conductive layers of microstrip patch antenna.
6. Investigate the method of using polymer as a substrate for microstrip patch antenna.
7. Fabricate the prototypes of embroidery microstrip patch antenna on polymer substrate.
8. Analyze the antenna performance through actual measurement with the result of conductivity, reflection coefficient, radiation pattern and gain.
9. Investigate the effect of different structures of embroidery patch antenna on polymer substrate with identical embroidery properties and make comparison of antenna performance. The analyzed results based on the investigation of the shape of the conductive embroidered patches and the embroidered structures.
10. Literature review the textile dyeing technique by using nanopowder solution.
11. Investigate the conductivity of embroidered patches when being dyed with graphene and metal oxide (ZnO, CuO, Al₂O₃) nanopowder solutions under different conditions.

12. Fabricate the prototypes of dyed embroidered patch antennas on polymer substrate.
13. Measure the antenna performance and investigate on the effect of dyed embroidered antennas with different conductive nanopowders through the result of conductivity, antenna reflection coefficient, radiation pattern and gain.
14. Research conclusion and future works discussion.

1.2.2 Project Deliverables

From the aforementioned project objectives and scope of work, the project deliverables are detailed as in Table 1.1.

Table 1.1 Project deliverables schedule

Items	Deliverables	Timestamps
1	- Design structure of 2.45 GHz microstrip-fed rectangular patch antenna based on theoretical ideal calculation.	October 2013
2	- Simulated operating frequency from the designed antenna structure to confirm the context of calculation and simulation.	November 2013
3	- Embroidered conductive layers of microstrip-fed rectangular patch antenna by using silver threads with the designed parameters.	November 2013
4	- Prototype of embroidery microstrip-fed rectangular patch antenna on polymer substrate.	December 2013
5	- First set of embroidery microstrip-fed rectangular patch antennas on polymer substrate with different embroidered structures.	January 2014
6	- Measured performance results of embroidery microstrip-fed rectangular patch antenna on polymer substrate with different embroidery structures.	March 2014
7	- Second set of embroidery microstrip-fed polygon patch antennas on polymer substrate with different embroidered structures.	April 2014
8	- Third set of embroidery SMA-fed polygon patch antennas on polymer substrate with different embroidery structures.	May 2014

9	- Measured performance results of embroidery microstrip-fed and SMA-fed polygon patch antennas on polymer substrate with different embroidery structures.	June 2014
10	- The effect result of different structures of embroidery patch antenna on polymer substrate with identical embroidery properties.	June 2014
11	- Dying solutions from dispersion of conductive nanopowders (graphene, ZnO, CuO, Al ₂ O ₃).	July 2014
12	- The effect of embroidery conductive layer dyed with graphene, CuO and ZnO dyeing solutions.	July 2014
13	- Prototypes of embroidery microstrip-fed rectangular patch antenna on polymer substrate dyed with ZnO and CuO dyeing solution.	August 2014
14	- Measured performance results of embroidery microstrip-fed rectangular patch antennas dyed with ZnO and CuO nanopowder solutions on polymer substrate.	October 2014
15	- Discussion on the antenna performance while dyed with conductive nanopowder solutions and compare with the original antenna without dyeing.	November 2014
16	- Project writing up, discussion and future work.	January 2015

1.2.3 Research Applications

This research has been supported by Malaysia Government, Ministry of Science, Technology and Innovation (MOSTI), project no 06-02-12-SF0213 to develop an application to measure gas and humidity in the atmosphere. The embroidery antenna on polymer composite is incorporated into sensors and used for sending the information received to another side which will display the data on the user interface. As mentioned in the project objectives and deliverables, this research presents a novel class embroidery patch antennas on polymer composite. The antenna characteristic is light-weight, conformal and able to be integrated with garments as well as others flexible structures. It can be sewed directly into daily clothes and reduces the obtrusiveness compared to rigid conventional radio antenna. According to [1], [4,5], these embroidery antennas

are ideal solution for mine workers, soldiers, marines and securities where the needs of lightweight, unobtrusive design and flexible mounting provide the most user-friendly and secured alternative to whip or bulk metal antennas. It can be also incorporated with health sensors and sewed into patients clothes to measure and monitor their heartbeat, pulses etc. The monitoring information can be transferred directly to doctors or person in charge in real time for immediate responses while the patients still get comfortable with their clothes and the embroidery antennas.

1.3 Thesis Organization

Chapter 2 of the thesis reviews a brief history and development of two main categories of flexible antennas which are textile antenna and polymer antenna together with antenna fundamental parameters. Researches of fabric antenna and embroidery antenna as well as antennas that used polymer as substrate material were also studied. It is then followed by the review of embroidery antenna on polymer substrate which is the main researched antenna category in this dissertation. Chapter 3 presents the research materials and method of antenna fabrication together with measurement set-ups. Chapter 4 provides a comparative study of the effect of different structure of embroidery patch antenna on polymer substrate with identical embroidery properties and similar electrical characteristics. Chapter 5 is concerned with enhancing the conductivity of embroidered layers by dyeing method with conductive nanopowders and demonstrates the effect on antenna performance. This dissertation concludes with Chapter 6, which is to summarize the main findings of the research and also provide some scopes for future investigations.

CHAPTER 2

Literature Review

Basic antenna terms and technical keywords are briefly reviewed in Section 2.1 of this chapter. Also reviewed are historical researches and developments of two main categories of flexible antennas which are textile antenna and polymer antenna in Section 2.2.

2.1 Fundamental Parameters of Antennas

2.1.1 Bandwidth

Bandwidth of an antenna is considered to be the “range of frequencies, on either side of a center frequency, where the antenna characteristics are within an acceptable value of those at the center frequency” [6]. The impedance bandwidth of narrowband antennas can be defined as $f_H - f_L$ or on a percentage basis as Equation (2.1), where $f_C = \frac{(f_H+f_L)}{2}$, f_H is the higher cutoff frequency and f_L is the lower cutoff frequency

$$\frac{(f_H-f_L)}{f_C} \times 100\% \quad (2.1)$$

2.1.2 Return Loss and Reflection Coefficient

Return loss is “a measure of the effectiveness of power delivery from a transmission line to antenna” while reflection coefficient is the negative of return loss [7], and is defined as,

$$\text{Reflection coefficient (dB)} = 10 \log_{10} \left(\frac{P_{ref}}{P_{in}} \right) \quad (2.2)$$

Where P_{in} and P_{ref} represent the power incident on the antenna and the power reflected back to the source.

2.1.3 Radiation Pattern

An antenna radiation pattern is defined as “a graphical representation of the radiation properties of the antenna as a function of space coordinates.” [6]. A directional antenna is defined as one having the property of radiating or receiving electromagnetic waves more effectively in some directions than others [8]. The radiation pattern is determined in the far-field region and is represented in the directional coordinates. One special type of directional pattern is an omni-directional pattern, which is defined as one having an essentially non-directional pattern in a given plane and a directional pattern in any orthogonal plane.

2.1.4 Gain, Directivity and Efficiency

$$\text{Gain (dB)} = \text{Directivity} \times \text{Radiation efficiency} \quad (2.3)$$

Equation 2.3 represents gain, directivity and radiation efficiency of an antenna. Directivity of an antenna is defined as the ratio of the radiation intensity in a given direction from the antenna to the radiation intensity averaged over all directions [8]. Therefore, antenna directivity quantifies its ability to direct energy. The radiation efficiency is the ratio of radiated power to input power. Antenna gain is the ratio of the intensity, in a given direction, to the radiation intensity that would be obtained if the power accepted by the antenna were radiated isotropically [8].

2.1.5 Polarization

Polarization of an antenna in a given direction is defined as the polarization of the wave transmitted by the antenna which is the orientation of the radiated electric field vector [8]. There are three different types of polarization which are linear, circular and elliptical polarizations. A pair of orthogonal polarizations,

which are co-polarization and cross-polarization, exists at each point on the radiation sphere. Co-polarization is the desired polarization and cross-polarization is the polarization orthogonal to the co-polarization [6].

2.1.6 Antenna Field Regions

The space surrounding an antenna is usually subdivided into three regions: (a) reactive near-field, (b) radiating near-field (Fresnel) and far-field (Fraunhofer) region [6].

Reactive near-field region is considered as the surrounding antenna region wherein the reactive field predominates [6]. The outer boundary of this region is taken at a distance $R < 0.62 \sqrt{\frac{D^3}{\lambda}}$ from the antenna surface, where λ is the wavelength and D is the largest dimension of the antenna [6].

The radiating near-field region is defined as the field between the reactive near-field region and the far-field region [6]. The outer boundary of this region is taken at a distance $R < 2D^2/\lambda$ from the antenna surface, where λ is the wavelength and D is the largest dimension of the antenna [6].

In measurement, most of antenna radiation pattern is measured in the far-field region. This is the region of the field where the angular field distribution is essentially independent of the distance from the antenna. The outer boundary of this region is taken at a distance $R > 2D^2/\lambda$, where λ is the wavelength and D is the largest dimension of the antenna [6].

2.2 Conformal Antenna

This section gives a literature review on flexible and conformal antenna regarding textile and polymer antenna. The hierarchical review is depicted in Figure 2.1.

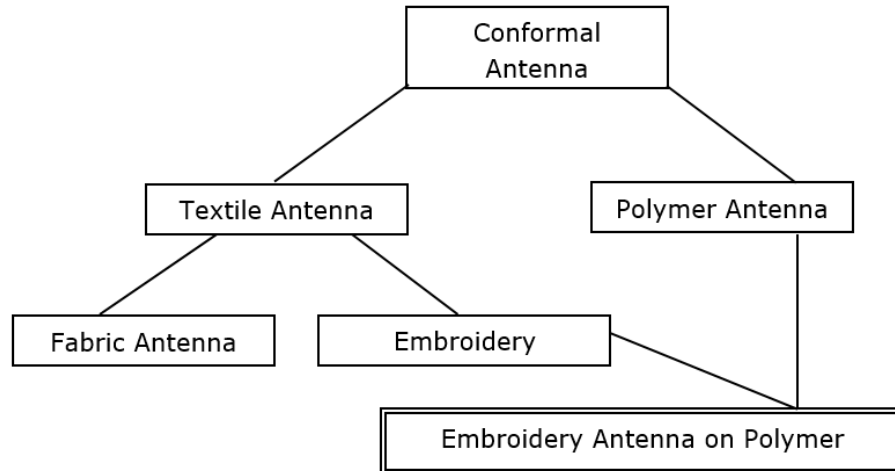


Figure 2.1 Literature review of conformal antenna

2.2.1 Textile and Fabric Antenna

Textile materials are an interesting candidate for flexible wearable antennas. They generally have a very low dielectric constant, which reduce the surface wave losses and improves the impedance bandwidth of the antenna [1]. Wearable antennas are most commonly designed and developed with microstrip configuration as it is conformal for integration into clothing [9].

In 2001, P.J. Massey proposed a planar inverted-F antenna (PIFA) operating at 900 MHz GSM band for mobile application [10]. The antenna was constructed using copper plated rip-stop nylon fabric for conductive surfaces and a shingle foam sheet spacer as the dielectric material.

Pekka Salonen designed a first fully compact fabric antenna for commercial smart clothing in 2003 [11]. The structure of the rectangular patch antenna is illustrated in Figure 2.2.

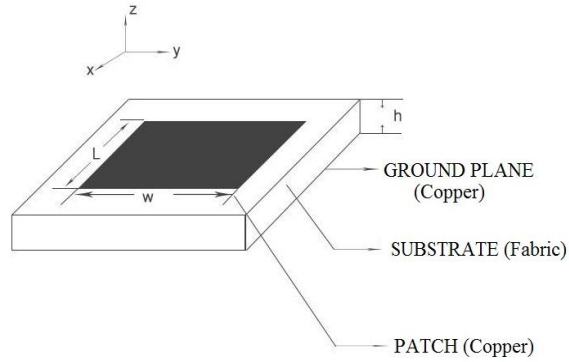


Figure 2.2 Geometry of the WLAN fabric antenna (redrawn from [11])

This WLAN antenna employed knitted copper fabrics for all conductive parts and 3 mm thickness fleece fabric for dielectric substrate with dielectric constant of 1.04.

In the subsequent year, the effect of conductive material on wearable patch antenna performance was studied in [12]. The authors used various conductive materials including solid copper tape (A), knitted copper fabric (B), vertically cut copper tape (C), horizontally cut copper tape (D), horizontally cut and soldered copper tape (E) and aracon fabric (F). The results showed that antennas A, B, C and E has similar results while antennas D and F has the worst performance since antenna D has discontinuities perpendicular to the surface current and antenna F has low conductive layers.

According to [13], Yuehui Ouyang *et al.* studied the effect of fabric patterns on electrotile patch antennas. The authors developed two different structures of woven conductive layers, one was with satin fabric face facing upwards and the other one was with metallic face facing up towards the air, both use Rogers board as substrate. The research was shown that the nonconductive fibers also affect the textile antenna performance. The weave pattern of woven antenna on satin is shown in Figure 2.3.

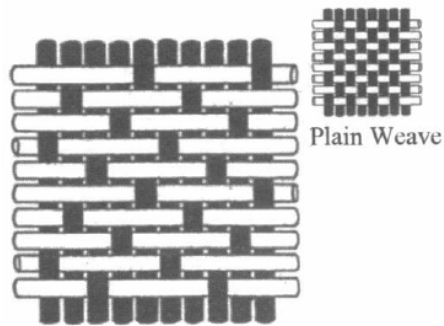


Figure 2.3 Weave pattern of the satin weave [13]

In 2006, A. Tronquo and others developed a single feed planar rectangular ring textile antenna for wireless body LANs operating at 2.5 GHz band [14]. The geometry of this antenna is shown in Figure 2.4. Fleece fabric substrate and electron conductive fabric were used for the development of this antenna.

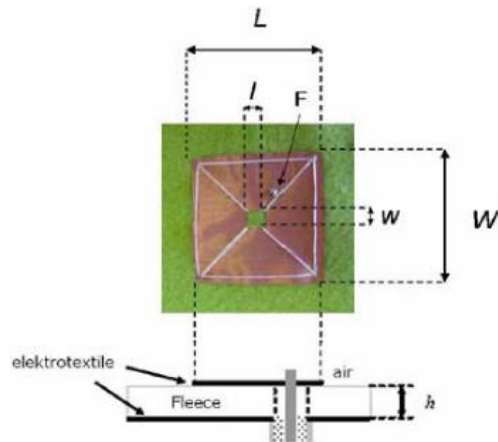


Figure 2.4 Geometry of rectangular ring textile antenna [14]

The effect of finite conductivity of conductive textiles on the electrical performance of soft wear antennas was introduced in [15]. The research was carried out with various textile microstrip lines. The measured results in Figure 2.5 show that the wave propagation velocity decrease according to the decrease of the fabric conductivity.

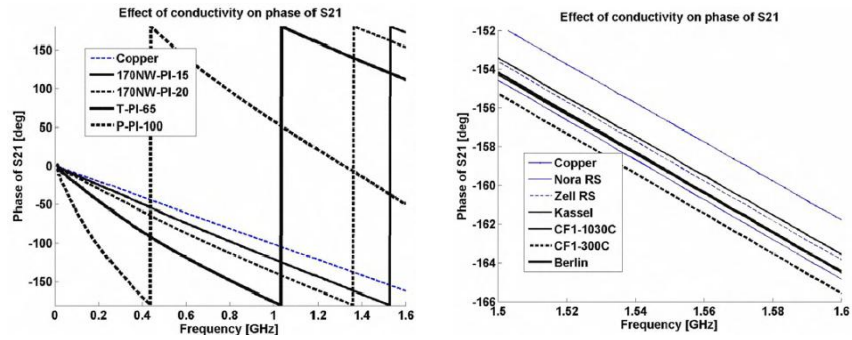
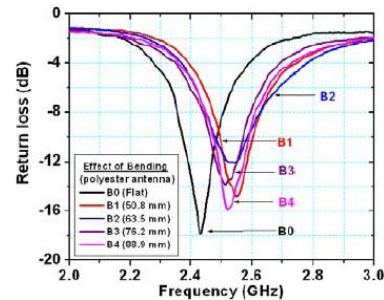


Figure 2.5 Measured phase angles of S21 for conductive polymer fabrics (left) and metal-coated fabrics (right) compared with a phase measured from a copper trace [15]

In wearable systems, antenna is made of flexible textile materials therefore it can be easily bent according to human body movements or the soft characteristic by itself. The antenna performance under bent condition was investigated by S. Sankaralingam in [16]. A polyester antenna was bent around curved surfaces of PVC pipes with different radius (50.8mm, 63.5mm, 76.2mm and 88.9mm).



(a)



(b)

Figure 2.6 (a) Photograph of the various antenna structures bent with different radius, (b) Measured effect of antenna bending on S11 [16]

Figure 2.6 (a) shows the photograph of the wearable antenna structures under bent condition. The measured S11 results were illustrated in Figure 2.6 (b). The deviations of resonant frequency and the reflection coefficient were affected by the bending. The more the antenna was bent, the more the resonant length gets reduced and so the resonant frequency gets shifted up [16].

A circular patch antenna was also designed and demonstrated in [9] by S. Sankaralingam *et al.* in 2011 for HiperLAN/2 application. The circular patch of the antenna were made from zelf fabric while the polyester fabric was applied for the substrate material. Photograph of the fabricated wearable antenna is shown in Figure 2.7.

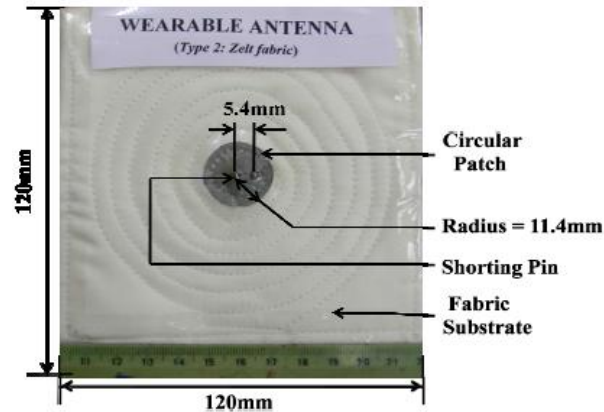


Figure 2.7 Photograph of the fabricated circular patch wearable antenna [9]

A year later, Ling Xu and others developed a dual-band microstrip antenna based on felt substrate [17]. Copper foils were used for the patch and the ground plane. Side-fed was chosen for the ease of fabrication and the simplicity of the matching process. The photograph of proposed antenna is shown in Figure 2.8.



Figure 2.8 Photograph of proposed antenna [17]

In addition to the advancement of wearable antenna applications, human body tissue gets exposed to the electromagnetic radiation. The amount of power absorbed by the human body and the risks to the human in long run are needed to be concerned. Therefore, a parameter called SAR (specification absorption

rate) is defined in [18]. The maximum value for SAR is 1.6 W/Kg for 1g of tissue.

In [19], Ginu George and others simulated a meander line wearable antenna with four different type of substrates (jeans, polycot, polyester and shieldit) while copper as radiating elements. The SAR value was measured when the designed antenna was placed on the arms of the human body. The calculated SAR value is 0.003 W/Kg on 1 g of tissue at 406 MHz band. This proved that wearable antennas are absolutely compatible for human daily use.

A wearable textile patch antenna for body area network (BAN) operating at 60 GHz was designed, constructed and tested by Nacer Chahat and others [20]. The antenna substrate was extracted from a shirt which has permittivity $\epsilon_r = 2$ and loss tangent $\tan\delta = 0.02$. The ground plane consists of Shieldit Super fabric while flexible copper foil was used for radiating patch and the feeding lines. Figure 2.9 demonstrates the patch antenna flexibility.



Figure 2.9 Demonstration of the patch antenna flexibility [20]

In 2014, an innovative technique of inkjet printing antennas on textiles was introduced by William G. Whittow *et al.* [21].

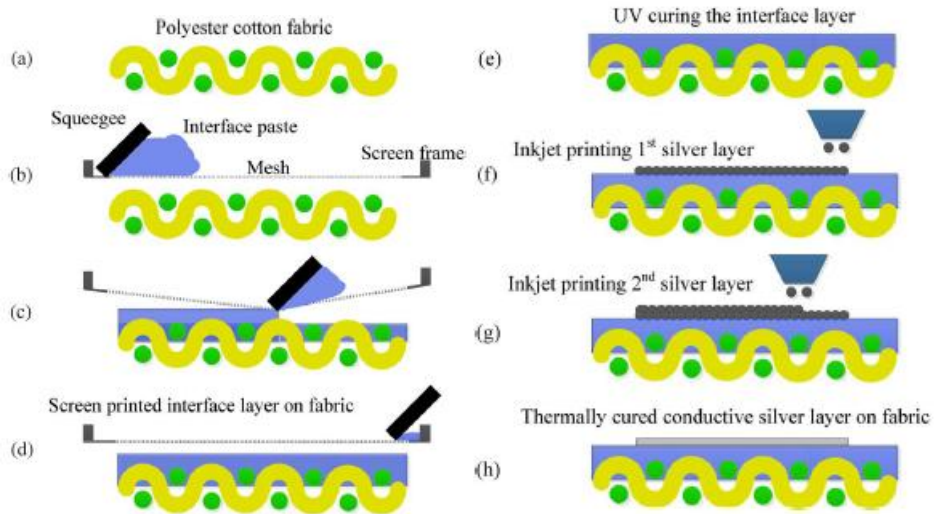


Figure 2.10 Inkjet-printed textile antenna fabrication processes [21]

Figure 2.10 shows the inkjet-printed textile antenna fabrication process. A screen-printed interface layer was firstly used to reduce the surface roughness of the polyester/cotton material that facilitated the printing of a continuous conducting surface. Silver ink was then applied by DMP 2831 printer to create inkjet-printed patch antennas. The substrate layer was made from felt fabric and attached to conducting nylon Nora Dell ground plane by using glue that is activated by ironing. The inkjet-printed side faced the ground plane and was connected to the probe via highly conductive silver epoxy paint.

2.2.2 Embroidery Antenna

The aforementioned researchers demonstrated the feasibilities of wearable antennas with high electromagnetic performance. The antennas promise to meet the requirement of flexibility and comfort to the user. Industries are continuously seeking for a class of wearable antennas that are compact, robust, mobile and cost effective. These antennas need not only possess good RF performance characteristics but also mechanical structure which is adaptable to

conformity and durability. Embroidery patch antenna is a potential candidate that meets the requirements. Computerized sewing machine can be used to fabricate textile antennas quickly and on mass manufacturing scales, highly flexible to change the design at minimal costs and time [22]. Using conductive threads in embroidery antenna can also provide high mechanical, robust structures with aesthetic patterns rather than unattractive attachments [23]. Conductive threads can be highly resistive and make embroidered surface become discontinuous with air gaps compared to bulk metal sheets. Researchers who have considered designing embroidery antennas using conductive threads are reviewed as follows.

In 2012, Shiyu Zhang *et al.* showed that the performance of embroidery antenna in term of reflection coefficient, bandwidth, gain, directivity and efficiency depend on stitches spacing of embroidered conductive threads [24]. Closer stitch spacing can improve the electrical connection between neighboring stitches and improve better antenna performance.

The on-body performance of embroidered dipole-type ultra-high frequency (UHF) RFID tags was studied in [25]. Six embroidered tag antennas which different sewing patterns were fabricated by embroidering directly on cotton ($\epsilon_r = 1.8$ and $\tan\delta = 0.018$) using computer aided sewing machine and conductive thread by Shieldex (110f34 dtex 2-ply HC). The researchers showed that the conductivity of embroidered tag antennas is mainly determined by the direction of sewed lines with respect to the direction of current flow in the structure of the antenna. Moreover, conductivity of the embroidered structure depends on the electrical properties of the used conductive thread. An embroidered dipole tag is designed utilizing the human arm and the embroidered tag models on $h =$

0.25 mm thick cotton fabric substrate using the Statex conductive sewing thread (4000 S/m and thickness is 0.2 mm) and NXP IC. The effect of tag-to-body separation was investigated by adding 0.25 mm thick cotton fabric layers between the body and the tag. The measurement set-up is shown in Figure 2.11.

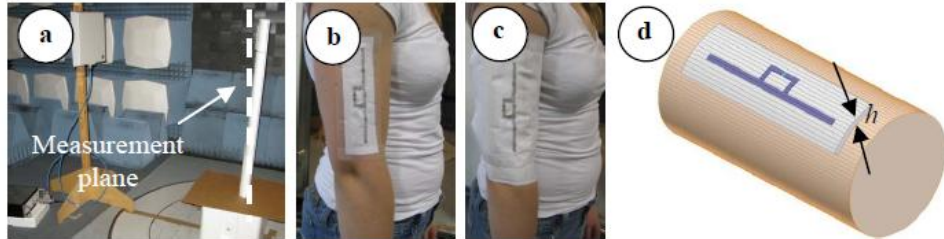


Figure 2.11 (a) Measurement set-up calibration, (b) Tag position on arm, (c) Tag-to-body separation increased with additional cotton fabric layers, (d) Embroidered tag model with different substrate thickness h on the human arm model [25]

The read range increases with increased tag-to-body separation. The reason is that when the tag is close to the body, the introduced losses from the body are more prominent compared to the case where additional fabric layers are used. The read range performance is sufficient for many body-centric wireless applications [25].

Researchers in [26] deeply focused on stitch direction and stitch density effects on performance of embroidered antennas. The definition of the stitch directions of the patch is illustrated in Figure 2.12 with vertical, horizontal and diagonal lines.

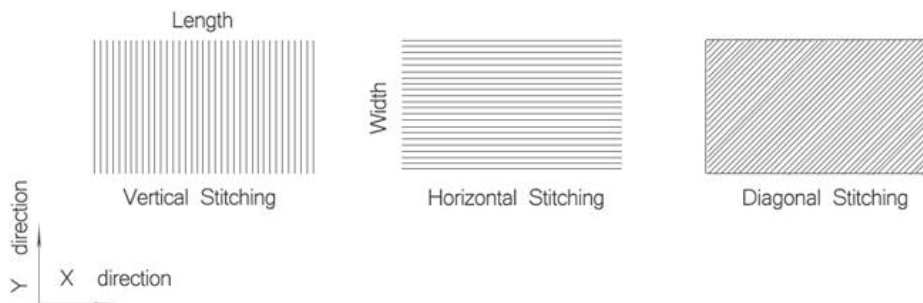


Figure 2.12 Sketch of patches and the stitch directions (redrawn from [26])

The embroidered patches were placed on Taconic RF-45 ($\epsilon_r = 4.5$ and $\tan\delta = 0.0037$) substrate with a copper ground plane. The best performance was achieved by the antenna has higher stitch density and embroidered in vertical thread direction.

Researchers in [23] pointed out the challenges of fabricating embroidery antenna using conductive threads. The antennas were embroidered on cotton fabric and placed on an FR4 substrate with a copper ground plane with the aid of non-conducting glue and plastic tape as shown in Figure 2.13.

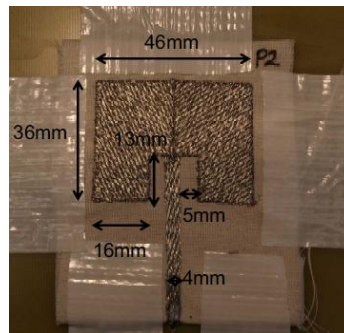


Figure 2.13 Photograph of embroidered patch antenna [23]

The challenges is designing antennas pattern with conductive threads to form up a continuous radiating surfaces while maintain their flexibility. Compared to conventional rigid antennas, embroidery antenna made from conductive threads has greater losses in electromagnetic performance.

Body-worn antenna needs not only to be simultaneously excellent in RF performance but also possess in attractive attire, conformity and lightweight. Lanlin Zhang and others fabricated an embroidered asymmetric meandered flare dipole antenna on a scarf [27]. Two successive layers were embroidered from silver-coated Amberstrand fibers to increase the conductivity while minimizing physical discontinuities. The scarf was made from polyester fabric and the embroidered antenna was tested on the front and back torso respectively.

Although the RF performance has been affected by human body, the embroidered antenna has successful demonstration and can be applied to body-worn applications due to its robust and reliable embroidery process.

Jung-Sim Roh *et al.* researched on the effect of different body postures while wearing an embroidered antenna [28]. A five-folded dipoles antennas were embroidered onto a polyester woven substrate ($\epsilon_r = 1.15$). The research shows that the bandwidth of wearable antenna could be larger when the antenna is placed closer to the human body.

To identify the effects of different fabric substrates on embroidered antenna, a Sierpinski carpet antenna was introduced by S.Ahmand and others in [29]. Two antennas were designed to operate at 2.45 GHz and the conductive embroidered layers were made from silver plated nylon thread which are created from single and multiple strands of conductive and nonconductive fibers. Meanwhile, the antenna substrate was made from the felt and denim fabrics which have dielectric constant of 1.361 and 1.666 respectively. The embroidery process was done by using computerized embroidery machines and the radiating elements were sewn to the felt and denim textile. The prototype of embroidered Sierpinski Carpet embroidered antenna is shown in Figure 2.14.

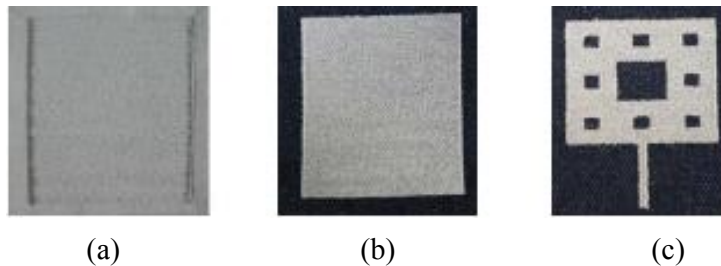


Figure 2.14 The prototype of embroidered Sierpinski carpet Antenna (a) Inner substrate, (b) Back view, (c) Front view [29]

The researchers have showed that the antenna bandwidth is affected by the thickness of the substrate, and denim fabric has given the best performance compared to fluffy surface of felt fabric.

An UWB fully textile wearable antenna was designed and analyzed in [30] by M. A. R. Osman *et al.* Conductive layers were embroidered by using silver plated nylon thread directly on flannel fabric for the top patch and the ground plane while isolated flannel fabric is used for substrate. Three layers of flannel fabric were stacked and sewn together to complete the antenna and enhance the bandwidth. A copper self-adhesive sheet is also used to make a copper antenna for reference. Figure 2.15 shows the photograph of the prototypes.

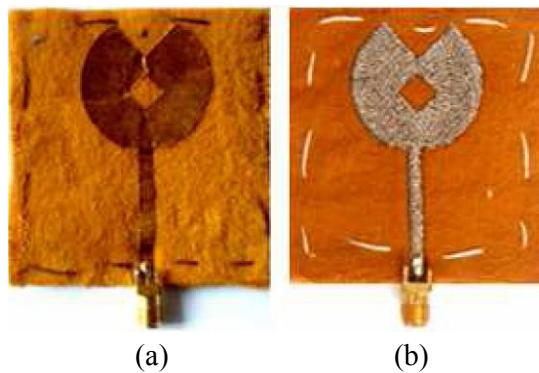


Figure 2.15 The photograph of wearable antenna prototypes (a) Copper conducting sheet, (b) Embroidered conducting thread [30]

In 2013, in order to make a better comparison between conductive fabric and embroidered antennas, Thosmas Kaufmann and others designed and constructed three different antennas with identical dipole pattern on Rogers RO4350 substrate and copper ground plane [31]. The first fabricated dipole antenna based on silver plated RipStop nylon fabric. It was tailored to shape and sewed with folded edges on a thin standard fabric sheet. The second antenna was embroidered only for the single upper layer by using conductive thread 117/17 2ply. The third dipole antenna was embroidered by using higher

conductive thread (234/34 4 ply) on both side of the fabric. All antennas were connected to feeding structure on one end and integrated into fabric of the antennas on the other end. The antennas are shown in Figure 2.16.

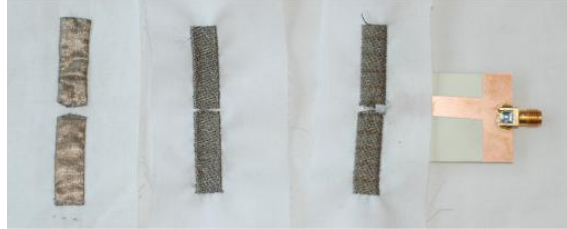


Figure 2.16 Three manufactured antennas (from left to right): silver fabric, single-layer embroidery, dual-layer embroidery, the feeding structure can be attached to the antennas [31]

In wearable antenna, ground plane is also playing an important role. An efficient and proper ground plane provides less energy impact on human body and electromagnetic waves should not penetrate the human body [5]. In aforementioned researches, most of researchers focused on antenna design, embroidered strategy, fabric substrate and conductive thread but less attention has been paid to embroidered ground planes for wearable patch antenna. In [5], Karoliina Koski *et al.* explored different types of embroidered ground planes affect the performance of RFID patch tag antenna. Several conductive fabrics are also applied for comparison purpose. The authors applied Shieldex silver thread which has lineal resistivity of $500 \pm 100 \Omega/\text{m}$ to fabricate six different ground plane structures, including squared structures with varying stitch densities as shown in Figure 2.17.

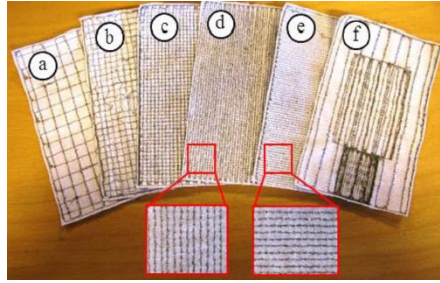


Figure 2.17 Embroidered structures for wearable tag antenna ground planes (a) Embroidery 1, square density $3\lambda/100$, (b) Embroidery 2, square density $3\lambda/200$, (c) Embroidery 3, square density $9\lambda/1000$, (d) Embroidery 4, vertical line density $3\lambda/500$, (e) Embroidery 5, horizontal line density $3\lambda/500$, (f) Embroidery 6, vertical line densities $3\lambda/100$, $9\lambda/1000$ and $3\lambda/500$. The wavelength corresponds to 900 MHz [5]

For comparison purpose, four LessEMF conductive fabrics which are copper polyester taffeta fabric (35% copper), argenmesh fabric (55% silver, 45% nylon), ripstop silver fabric and stretch fabric (silver plated 76% nylon 24% elastic fiber) were used to make conductive ground plane as shown in Figure 2.18.



Figure 2.18 Conductive fabrics from LessEMF (a) copper, (b) argenmesh, (c) ripstop and (d) stretch [5]

A copper reference tag antenna was implemented on Rogers 5880 substrate ($\epsilon_r = 2.2$ and $\tan\delta = 0.0009$) to analysis the effect of the ground planes. The researchers showed commercial conductive fabrics provides a better read ranges compared to embroidered structure. However, it is also possible to achieve high

performance embroidered ground planes by optimizing the embroidered pattern.

Aforementioned researches have visualized the performance of embroidery antenna through various investigations. The feasibility of embroidery antenna in garment integration for real life applications are also introduced in several researches such as an UHF asymmetric meandered flare (AMF) dipole antenna for integrating into scarves, handbags, shirts and coats is demonstrated in [32]. A GSM and Wi-Fi embroidered flare dipole antennas are validated on human phantom and sewn onto a jacket in [33]. As mentioned before, the wearable antennas need not only possess good RF performance characteristics but also mechanical structure which adaptable to conformity and durability [22]. Authors in [34] demonstrated the durability of embroidered wearable tags antenna by investigating various washing procedures. Conductive silver thread (Shieldex 110f34-dtex 2-ply HC) was used to embroider two dipole antenna tags on cotton fabric substrate. Tag 1 is washed by using hand wash at 30°C while tag 2 is applied washing program with 400 rpm at 40°C. Each antenna was washed three times and inserted the IC tag for read range measurement by silver epoxy. The results showed that the washing procedures have dissolved some of the silver ingredients of conductive thread, increased the resistance of the tag antenna and lowered the tag antenna radiation efficiency.

Daily body-worn applications require higher reliable antenna even after several washing times. The solution of using PDMS polymer with hydrophobic characteristic to cover the whole embroidered tag antenna was also introduced in [35]. Full polymer coating of the embroidered surface can help to improves the washing durability and maintain the antenna efficiency after multiple

washes. By this research, the authors have proved that the embroidered antennas are sensitive to washing. Proper solutions are requested to protect and maintain the antenna performance while integrating with garment for daily used.

2.2.3 Antenna Using Polymer Materials

Future body-worn antennas will be demanding in terms of system conformity and structure compatibility. As the antennas conform to the platform surface, they are bent and stretched. Obviously, the antennas must maintain functionality and withstand under mechanical forces such as pressures and vibrations. Flexible electronic have drawn significant attention in design, fabrication and testing of conformal antennas. Therefore, light weight, flexible and load-bearing materials are demanded to address these mechanical requirements. Polymer is a potential candidate that can satisfy these aspects.

A few flexible antenna technologies and researches have been conducted by numerous approaches of utilizing different polymer materials as flexible substrates. For instance, M.E. de Cos and F. Las Heras [36] designed and characterized a dual band CPW-fed monopole antenna using 0.45 mm thickness of polypropylene substrate ($\epsilon_r = 2.26$ and $\tan\delta = 0.002$). The polypropylene was then metallized, using simple adhesive aluminum foil and laser micromachining to pattern the shape of the CPW monopole antenna as shown in Figure 2.19 at its operating frequency.

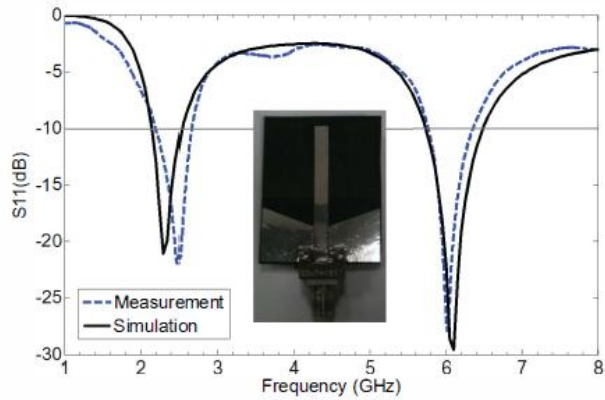


Figure 2.19 Reflection coefficient results of polypropylene based monopole antenna [36]

Haiwen Liu *et al.* [37] demonstrated a CPW-fed fishtail shaped antenna for WiMAX and X-band application. The bow-tie radiating components were printed on polytetrafluoroethene (PTFE) substrate ($\epsilon_r = 2.2$ and $\tan\delta = 0.0009$).

Other researchers also investigated on polymer antennas such as Ahmet Cemal Durgen *et al.* [38] introduced a novel flexible CPW bow-tie antenna mounted on flexible substrate polyethylene naphthalate (PEN) while radiating part was made from thin film transistors (TFT). Symeon Nikolaou *et al.* [39] developed from Vivaldi antenna design and fabricated an UWB slot antenna on liquid crystal polymer (LCP) substrate ($\epsilon_r = 3.1$ and $\tan\delta = 0.002$) with a $18\mu\text{m}$ thick copper layer. The measurement of reflection coefficient of proposed antenna in flat and folded condition is shown in Figure 2.20.



Figure 2.20 Reflection coefficient results of proposed antenna in flat condition (left), and folded condition (right) [39]

Polyethylene terephthalate (PET) substrate was used for printed antenna in research of Stanely Y. Y. Leung and others [40]. The octagonal planar coil antenna was printed by screen printer (DEK model 260) using silver-filled conductive polymer paste and cured procedures. The photograph of printed antenna coil on PET substrate is illustrated in Figure 2.21.

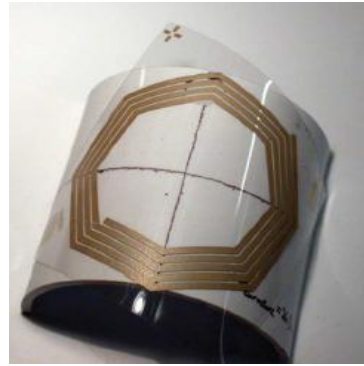


Figure 2.21 Photograph of printed antenna coil on PET substrate [40]

Among various types of polymers, polydimethylsiloxane (PDMS) is one of the most attractive and widely used materials for antenna applications because of its promising features, such as good chemical stability, low dielectric constant, low cost, cured at room temperature and eligible to be attached to other materials and performs system integration [41]. Numerous antenna researchers have used PDMS ($\epsilon_r \sim 3$ and $\tan\delta = 0.02$) as substrate material. For instance, Jovanche trajkovikj *et al.* [42] pointed that the electrical and mechanical properties of PDMS substrate can be adjusted by loading the PDMS with inclusions having low or high permittivity and/or density such as hollow glass, phenolic and silicate microspheres to control the permittivity and the rigidity. The authors took the advantage of initial low viscosity of PDMS to shape the antennas and substrates in in-house fabricated moulds. A patch antenna operating at 2.45 GHz was built by using copper-mesh sheets as conductive

parts. The antenna was completely encapsulated inside PDMS, with the copper mesh sandwiched between the substrate layers, which depicted in Figure 2.22.

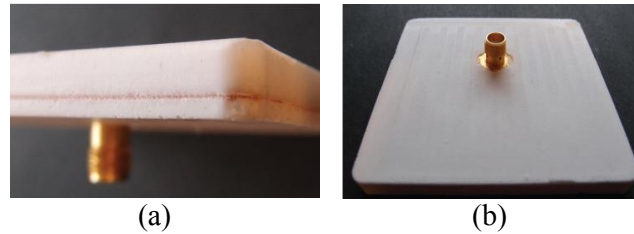


Figure 2.22 Patch antenna (a) Copper mesh sandwiched inside PDMS, (b) The antenna prototype, bottom view [42]

An UWB tripod kettle antenna (TKA) for short-range communication was also designed and fabricated in [42]. This antenna was completely encapsulated inside PDMS, thus showing the wide potential of this PDMS substrate, which can be patterned during viscosity form and cured to become high strength elastic polymer antenna material. The TKA antenna is shown in Figure 2.23.

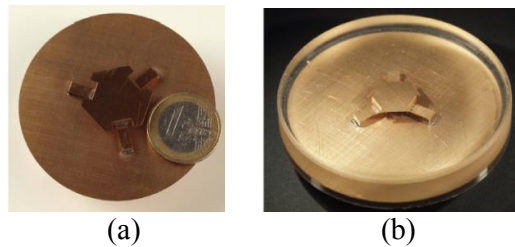


Figure 2.23 Tripod kettle antenna prototypes (a) before encapsulation in PDMS, (b) after encapsulation in PDMS [42]

For polymer antenna applications, flexible and stretchable characteristics are highly demanded. While other researchers relied mostly on metals materials for radiating parts such as copper, aluminum *etc.*, Riaz Ahmed Liyakath and others [43] introduced an aperture-coupled patch antenna, which was made from stretchable conductors (SCs) Zoflex FL45 conductive rubber on PDMS substrate as, shown in Figure 2.24.

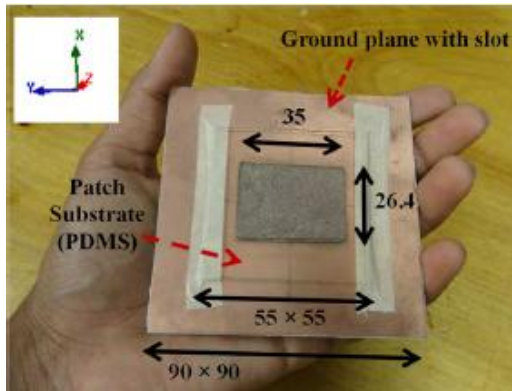


Figure 2.24 SC-based aperture-coupled patch antenna (all dimensions are in mm) [43]

2.2.4 Embroidery Antenna on PDMS Substrate

Conformal, lightweight, load-bearing antennas are critical for new generation communication system since conventional rigid antenna is not flexible and suitable for elastic surfaces integration. The aforementioned researches have proved that embroidered conductive layers and polymer materials such as PDMS are two potential candidates to develop a robust, high-strength, flexible, lightweight and low loss antennas for body-worn applications.

Numerous researchers have developed and investigated embroidery RF circuits and antennas on PDMS substrate to achieve a new generation of antenna for conformal and nonmetal RF electronics that satisfy the aforementioned requirements.

Zheyu Wang *et al.* [44] introduced a new printing technique based on polymer material and conductive fibers. The transmission line and the ground plane were embroidered by using a digitized sewing machine. Then, both conductive layers were laminated on partially cured PDMS tacky surfaces. Finally, two separated sub-layers were integrated by using fresh PDMS as glue, flowed by full curing. The printing process of single layer on PDMS was depicted in Figure 2.25 followed by the prototype of embroidered transmission

line after each fabricated stage is shown in Figure 2.26. It was seen that the final embroidered transmission line on PDMS substrate achieved mechanical flexibility and high strength properties.

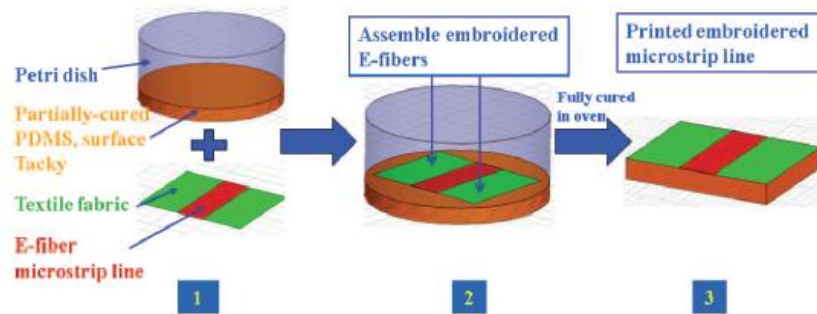


Figure 2.25 Printing process of single layer E-fiber RF circuit on PDMS [44]

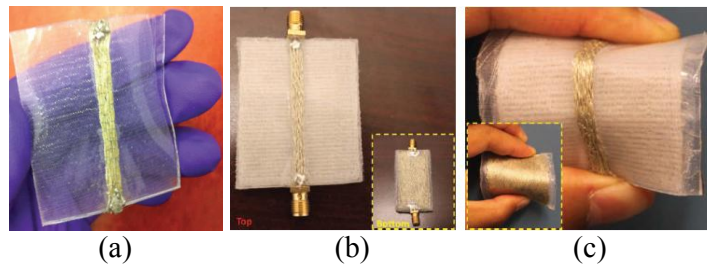


Figure 2.26 Prototype of embroidered transmission line on PDMS (a) One layer lamination on PDMS, (b) Fabricated microstrip line with ground plane, (c) Fabricated microstrip line under bending [44]

In 2006, Stavros Koulouridis *et al.* developed polymer-ceramic composite for microwave applications [45]. Low loss and highly flexible PDMS was used as substrates with initial permittivity of $\epsilon_r = 3.0$ and loss tangent of $\tan\delta < 0.02$. By adding ceramic powder from 0 vol% to 30 vol%, the permittivity of PDMS composite could be adjusted from $\epsilon_r = 3.0$ to $\epsilon_r = 13$, with a loss remained at $\tan\delta < 0.02$. Increasing the substrate permittivity plays a significant role in miniaturizing the size of antenna. Moreover, the research opened a method of adjusting permittivity of PDMS to achieve a wide range of dielectric constant for various future microwave applications.

In subsequent years, John L. Volakis first time introduced an embroidered rectangular patch antenna laminated on polymer-ceramic substrate [46]. The conductive patch layer was embroidered by using silver coated fibers then laminated and integrated on PDMS substrate which has 10vol% of ceramics, and had $\epsilon_r = 4.2$ and $\tan\delta = <0.01$. The antenna was put on copper ground plane and probe-fed by using silver epoxy composite. Figure 2.27 shows the antenna prototype mounted on planar and cylindrical surface respectively.

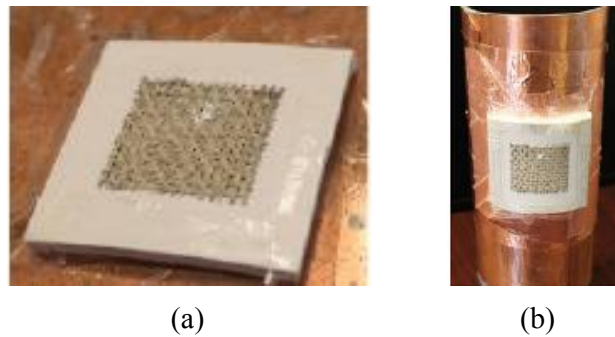


Figure 2.27 Embroidered patch antenna mounted on (a) planar and (b) cylindrical surface respectively [46]

Zheyu Wang *et al.* [47] fabricated and characterized an E-fiber antenna array by using aforementioned method of laminating embroidered conductive silver fibers on PDMS-ceramic substrate ($\epsilon_r = 4.2$ and $\tan\delta = <0.01$). Figure 2.28 shows the E-fiber antenna array prototype.

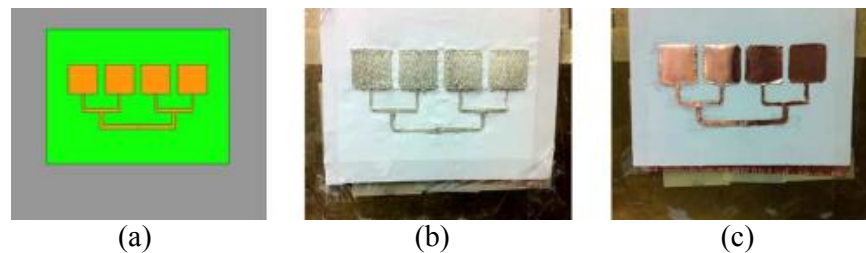


Figure 2.28 E-fiber antenna array on PDMS-ceramic substrate (a) simulation geometry, (b) fabricated E-fiber array, (c) fabricated copper array [47]

In recent years, a wideband embroidered conformal slot spiral antenna was designed and developed for radio frequency application from 300 to 3000 MHz

bandwidth [48]. The antenna substrate was PDMS with dielectric constant of $\epsilon_r \sim 3$ and the loss tangent of $\tan\delta < 0.01$. The authors have shown that the slot spiral retained its wide bandwidth and gain performance when conformed on a cylindrical surface. Importantly, the conformal spiral exhibited broader beam width and signal coverage due to the embroidered slot surfaces. The novel spiral slot antenna is highly attractive for wideband conformal RF applications.

2.3 Summary

In spite of best effort, review of such a huge realm in wearable and implantable antenna is remaining incomplete. However, from this review work, it is understood that textile materials are an interesting candidate for flexible wearable antennas, because fabric antennas can be easily integrated into clothes and researchers have shown the feasibility of textile antenna with strong mechanical structure and good RF performance for body-worn applications though fabric, embroidery antenna on fully textile as well as polymer substrate materials. Since 2003, fabric-based antennas have promised to meet the requirement of flexibility and comfort to the users. The aforementioned researchers showed many investigations and researches by changing the conductive fabric materials, antenna designs and others to obtain high levels of physical and electromagnetic performance and to minimize the effect of bending, crumpling or the presence of the user. The introduction of embroidery antenna has brought the textile antenna realm a revolution in term of compact, robust, mobile and cost effective structure. Computerized sewing machine can be used to fabricate textile antennas quickly and on mass manufacturing scales, highly flexible to change the design at minimal costs and time. Besides antenna designs and materials, the RF performance of embroidery antenna can also be

improved by considering the sewing techniques. Several researchers demonstrated that stitch direction, stitch spacing, stitch type, number of embroidered layers, relation of embroidered conductive thread on different substrates *etc.* will made significant effects on embroidery antenna performance. Conductive threads can be high resistance and make embroidered surface become discontinuous with air gaps compared to bulk metal sheets and cause different characteristic while comparing to metal antenna. This is the tradeoff between mass production for garment integration and metal rigid antenna. Demanding of wearable antenna that can withstand mechanical forces, load-bearing such as pressures and vibrations has brought up the application of polymer materials as antenna substrate. Among various types of polymers which have been introduced in different antenna applications, PDMS is a potential candidate because of its promising features, such as good chemical stability, low dielectric constant, low cost, can be cured at room temperature and eligible to be attached to other materials and performs system integration. PDMS has specialty while its permittivity can be adjustable, this can help to minimize the size of antenna and applied in different applications. Embroidery antenna on PDMS substrate was introduced in several researches since 2011 with numerous advantage characteristics and limitations. Therefore, further researches and investigation on this novel class of antenna are introduced and demonstrated in the following chapters of this thesis. The next chapter introduces about the research materials and method of antenna fabrication, as well as the measurement set-up.

CHAPTER 3

Research Methods and Materials

Embroidery antenna on PDMS substrate is potential candidate for this research due to its numerous aforementioned advantages in Chapter 2. Therefore, this chapter mainly focuses on the methods of processes and materials used for antenna fabrication. The first part will distinguish the conductive threads used for embroidery and PDMS material used as antenna substrate. The second part will analyze the fabrication process of antenna. Embroidery mechanism is introduced together with the lamination and integration method of PDMS material to complete the antenna structure. Antenna simulation software and measurement set-up for antenna prototypes are demonstrated in the following parts.

For reference, the structure parameters of rectangular patch antenna were theoretically calculated at the designed operating frequency and presented in Section 4.2.2. To validate the calculated antenna parameters at designed operating frequency, CST Microwave studio was used for simulating the copper antenna model. The calculated as well as simulated antenna parameters were then applied and referred to fabricate the embroidery antenna on polymer substrate prototypes. These antennas prototypes were investigated for further researches demonstrated in Chapter 4 and 5.

3.1 Research Materials

3.1.1 Conductive Threads

In embroidery process, conductive layers are embroidered from conductive threads. Depending on different electrical properties as well as wearability and

reliability characteristics, conductive threads are categorized into two main types which are multiple filament threads and monofilament threads as shown in Figure 3.1.

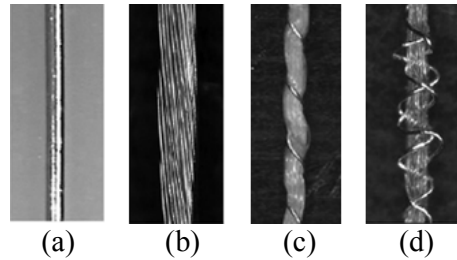


Figure 3.1 Conductive threads (a) monofilament, (b) bundled monofilament, (c),(d) nonconductive yarns twisted with conductive filaments [49]

The monofilament conductive thread composes of single metal plated fiber and can be bundle to become a thicker conductive thread. However, this type of threads may increase the surface stiffness and reduce the elasticity of embroidered layer. During the embroidery process, the conductive thread with high metal concentration can cause excess heat due to the strong friction and damage the needle [50]. The nonconductive yarns twisted with conductive filaments can assist to improve the strength of conductive thread which keep the thread more flexible and robust while maintain the conductivity.

Three different conductive threads with multiple filaments structure were applied in this research including Shieldex 40-22/7 + 110 PET 3ply, Shieldex 33-17 PET 2ply and Amberstrand 166 silver coated fibers. Figure 3.2 shows the photograph of these conductive threads and the characteristics, which are provided by manufacturers listed in Table 3.1.

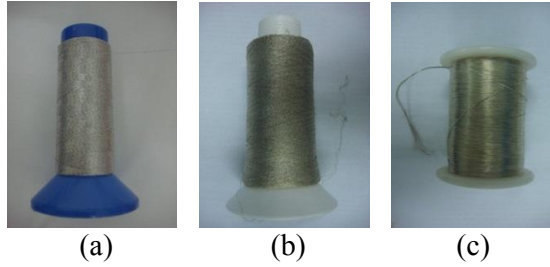


Figure 3.2 Photograph of studied conductive threads (a) Shieldex 40-22/7 + 110 PET 3ply, (b) Shieldex 33-17 PET 2ply and (c) Amberstrand 166

Table 3.1 Characteristics of studied conductive threads [51]

	Shieldex 40	Shieldex 33	Amberstrand 166
Fiber type	nylon + polyester	nylon	zylon PBO
Diameter	0.18 mm	0.17 mm	0.21 mm
Metal percentage by weight	16%	16%	82.5%
Weight	27,692.3 m/kg	39,915 m/kg	6,284.5 m/kg
Lineal resistance	800,000 Ohm/m	5905.5 Ohm/m	3.2808 Ohm/m
Structure description	7 silver plated nylon fibers twisted with 3x110 nonconductive polyester fibers	twist of 2x17 silver coated nylon fibers	bundle of 166 silver coated fibers

Choosing appropriate conductive thread for conventional embroidery machine is a challenge. Hairy finer threads have to be processed at slower speeds in order to reduce thread damages. Stiff threads and fine metal wires such as Shieldex 33 thread cannot go through the tension devices or cause breakages or jammed during embroidering process. The testing also found that thread containing abundant filaments is another problematic as it has a tendency to become wrapped around the tension devices and may not fit through the needle like Amberstrand 166 thread. Generally, only Shieldex 40 with nonconductive polyester supported fibers is suitable for the fabrication of embroidery antenna

by conventional sewing machine due to the familiarity with traditional embroidery threads.

3.1.2 PDMS Polymer Composite

Antennas for body-worn applications need not only possess good RF performance characteristics but also mechanical structure which adaptable to conformity and durability. Besides robust embroidered conductive layers, flexible and high strength material such as polymer is potential candidate for antenna substrate to enhance the durability and load-bearing characteristics. The literature review in Section 2.3 showed various types of polymers used as antenna substrate in different researches. PDMS is the most attractive and widely used material for RF applications because of its promising features, such as good chemical stability, low cost, cured at room temperature, eligible for system integration while transferring from viscosity to solid stage. Especially, electrical and mechanical properties of PDMS composite can be adjusted by doping with other materials to control the permittivity and rigidity [45], [46]. The PDMS material used for this research is Sylgard 184 Silicone Elastomer Kit which is provided by Dow Corning and has electrical properties of ($\epsilon_r \sim 3$, $\tan\delta < 0.02$). The elastomer kit consists of silicone gel and cross-link agent as shown in Figure 3.3.

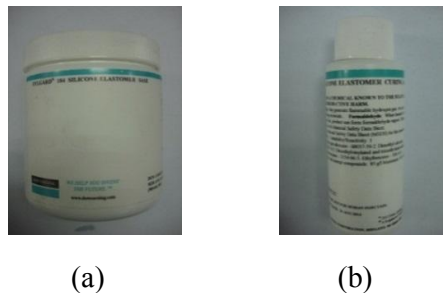


Figure 3.3 Photograph PDMS elastomer kit (a) silicone gel, (b) cross-link agent

3.2 Research Methods and Measurement Set-Ups

3.2.1 Embroidery Process

The embroidery machine used in this research is Brother Innov-IS 950. In sewing techniques, there are several different stitch types such as cross stitch, lock stitch, saddle stitch and others. For sewing machine, lock stitch is the most commonly utilized in embroidery. The lock stitch is created with an upper thread and a lower thread. The upper thread runs through a tension system and ends at the needle. Meanwhile, the lower thread is wound onto a bobbin, which is inside the lower basement of the machine. During the embroidery process, two individual threads will be interloped and perform the lock stitch as shown in Figure 3.4.

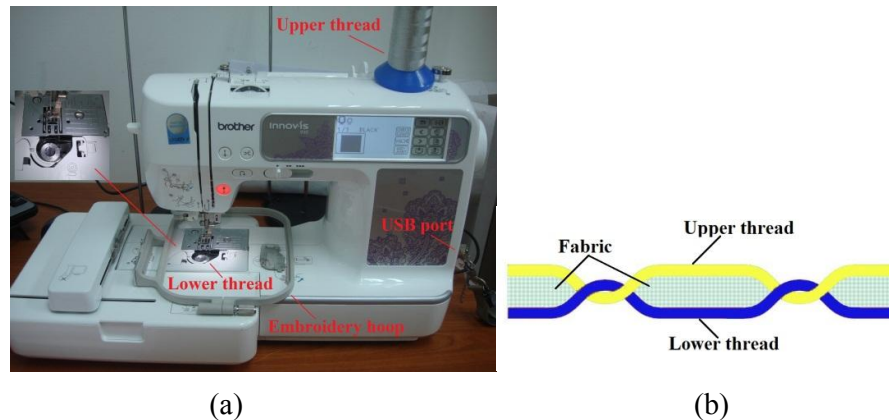


Figure 3.4 (a) Photograph of embroidery machine, (b) Lock stitch formation. Antennas are designed using Embird Studio embroidery software. Images can be imported for using as an embroidery objects or manually created by software tools. Depending on designing purpose, the embroidery objects can be manipulated with various parameters before it is filled with desired stitch type, compiled and transferred to embroidery machine through USB connection. For the stitch spacing in the computerized embroidery, a moderate setting of 0.4 mm has been selected. There is a trade-off between mechanical elasticity and

conductivity, as selecting too dense embroidery can lead to a very stiff pattern and might be difficult to manufacture. In order to support the embroidery process, the conductive thread was embroidered on very thin cotton fabric with 0.25 mm thickness. The minimal thickness of the fabric minimizes its effect on the antenna performance and its loss is very small compared to the losses of the sewing thread [52].

3.2.2 PDMS Preparation and Antenna Fabrication

Elastomeric PDMS polymers are usually formed from viscous liquid PDMS silicone gel and a cross-link agent (curing agent). According to the information of manufacturer, the mixing mass-based ratio of viscous liquid and cross-link agent is 10:1, which means that, for example, 10g of silicone gel is mixed with 1g of cross-link agent. The mixture is mixed thoroughly for approximately 10 minutes and then degassed for 15-20 minutes to remove possible air bubbles. The ready PDMS composite is let to be fully cured at room temperature within 48 hours or 30 minutes at 100°C on hot plate depending on the amount of the polymer composite [53]. The photograph of PDMS polymer fabrication process is shown in Figure 3.5.

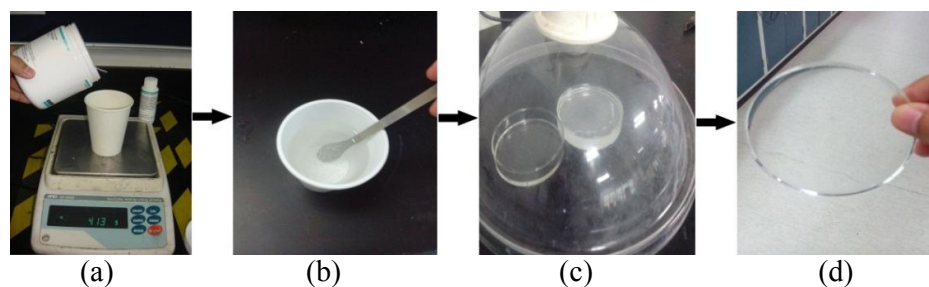


Figure 3.5 Photograph of PDMS fabrication process (a) Mixing silicone gel and cross-link agent, (b) Mixing composite thoroughly, (c) Degassing bubbles, (d), Fully-cured PDMS

Refer to technique was introduced in [54], Figure 3.6 shows the fabrication process of embroidery antenna on PDMS substrate by integration and

lamination method. Firstly, the PDMS viscous mixture is prepared as in Figure 3.5 (a), (b). Then the mixture was poured into a handmade mold to achieve half of the desired substrate thickness. Because the antenna substrate thickness is thin, the bubbles can be automatically removed without degassing. Then, the mold was put on hot plate to shorten the curing time and frequently checked the sticky surface of the polymer. A key advantage of PDMS substrate is its good affinity to other materials prior to curing. Therefore, ready embroidered conductive layers (ground plane and patch) were laminated on half-cured PDMS to achieve strong adhesive before put into fully-cured. After the lamination, two PDMS sides were flipped over and integrated together by using fresh PDMS as a natural adhesive to form the complete embroidered antenna on PDMS substrate. Silver epoxy will be then applied to connect SMA connector with the antenna body to make it ready for measurement.

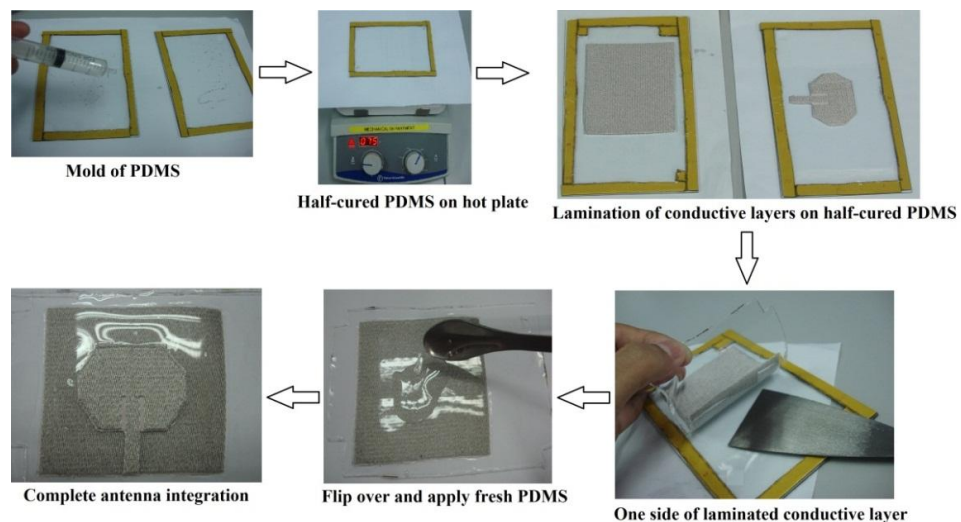


Figure 3.6 Process of lamination and integration of embroidery antenna on PDMS substrate

All antennas in this research are fabricated on 2 mm thick PDMS substrate which has dielectric constant of $\epsilon_r \sim 3$.

3.2.3 Simulation Software and Setting

The simulation for this project is performed by using a three-dimensional (3-D) electromagnetic field simulation software for high frequencies, the CST Microwave Studio. The software is highly recommended to obtain the fast and accurate analysis of high frequency electronics devices [55]. Based on different numerical methods, the software provides powerful solver modules such as transient solver, frequency domain solver and eigenmode solver. The transient solver based on finite integration technique, is general purpose time domain solver and used in this work as it is able to obtain the broadband frequency domain results like S-parameters. This transient solver is also time-effective since field results for many frequencies can be obtained from one single simulation run [55].

3.2.4 Measurement Set-Ups

In this research, resistance of conductive patch, reflection coefficient, gain and radiation pattern measurements were performed in the university's antenna testing laboratory. The main equipment used in the measurements reported in this research are:

1. Agilent 8757D Scalar network Analyzer: to perform signal measurement of transmission and reflection characteristics. This scalar network analyzer allows you to measure the signal quickly and accurately in the frequency range from 0.01 to 18 GHz [56].
2. Agilent E8257D PSG Analog Signal Generator: to generate output signal with the specified frequency ranges from 250 KHz to 20 GHz [57].

3. Agilent 83017A Microwave System Amplifier: to amplify the signal, provide power to recover system losses and boost up the RF power with 25 dB gain. This amplifier is applicable for bandwidth from 0.5 to 26.5 GHz which allows user to eliminate the need for crossover networks or multiple bias suppliers [58].
4. Fluke PM6304 Digital Meters: to measure the resistance of conductive layers.
5. Agilent 85027B Directional Bridge: to make modulated or unmodulated scalar reflection measurements with the scalar network analyzer. The bridge has a frequency range of 10 MHz to 26.5 GHz, a test port connector and a RF input port connector [59].
6. Agilent 11667B Power Splitter: to be used in network analyzer system for leveling or to supply a reference signal for ratio measurements. With the frequency range from DC to 26.5 GHz, the splitter contains one input signal arm and two output arms which have power level equally and simultaneously [60].
7. Agilent 85025E Detector: to detect RF signal and provides a square wave signal for analyzer to interpret and display. This detector operates from 0.01 to 26.5 GHz, and can detect the RF signal in both DC and AC mode [61].

a. Calibration Procedure

Before measurement, system calibration is required to characterize the systematic errors and eliminate the effects from unexpected sources. For reflection measurement, the equipment needs to be connected as shown in Figure 3.7 with point X is linked to the calibration standards, SHORT and then

OPEN to cancel the mismatch coming from the circuit. For radiation pattern measurement, points X and Y need to be connected together to establish a THRU connection, and thus achieve 0 dB as reference, as shown in Figure 3.8.

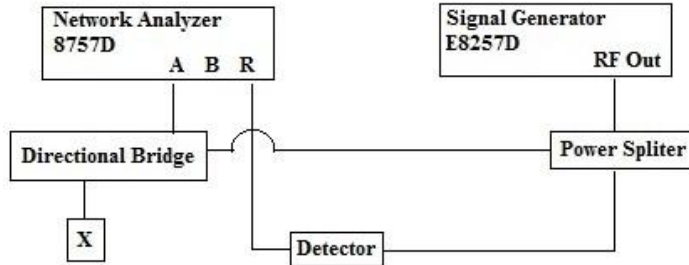


Figure 3.7 Calibration set-up for reflection coefficient measurement

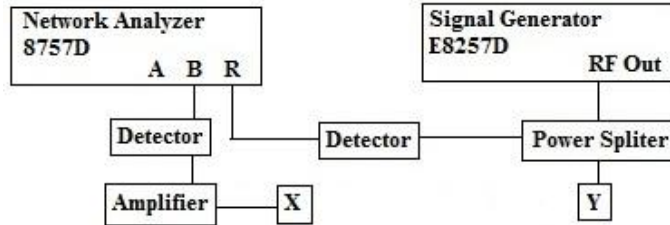


Figure 3.8 Calibration set-up for radiation pattern measurement

b. Reflection Coefficient Measurement

Once the reflection measurement calibration is performed, the OPEN is disconnected from point X and replaced by the antenna under test. A photograph of reflection coefficient measurement set-up is given in Figure 3.9.



Figure 3.9 Photograph of reflection coefficient measurement set-up

c. Radiation Pattern Measurement

After the radiation pattern calibration is conducted as described in above Section, the test antenna is connected to point X as shown in Figure 3.8 and mounted over a tripod on a computerized positioner system. Meanwhile, a standard pyramidal horn is used as the transmitting antenna and connected to point Y. A software is programmed to rotate the positioner for 360 degree while the measurement result is taken and recorded during each degree. Figure 3.10 and 3.11 show the photographs of pattern measurement set-up.



Figure 3.10 Photograph of radiation pattern measurement set-up



Figure 3.11 Photograph of testing antenna mounted on tripod with foam supporter

In this research work, the antennas were measured in a semi-rectangular anechoic chamber available at the university. The chamber is designed to minimize electromagnetic interference and simulate free-space conditions to

maximize the volume of the quiet zone [6]. However, due to the imperfect condition of the chamber having walls that are not fully covered with RF absorbers, the measured radiation patterns indicate with slightly deviations in its drawing which are represented in Chapter 4 and 5.

d. Gain Measurement

The gain-transfer method is the most commonly used method to characterize the gain of an antenna [6]. This method is one in which the unknown gain of the test antenna is measured by comparing it to that of a gain-standard antenna (usually a standard-gain horn antenna). Two sets of measurement data are required. First, the received power (P_{Test}) of the test antenna is recorded. Next, the test antenna is replaced by the standard-gain horn and the received power (P_{SGH}) is recorded. During both the sets, the arrangement needs to remain unchanged (apart from replacing the receiving antennas), and the input power to the transmitted antenna remains the same. The gain of the test antenna in decibel (dB) is given as [62].

$$G_{Test} = G_{SGH} + 10\log\left(\frac{P_{Test}}{P_{SGH}}\right) \quad (3.1)$$

Where, G_{SGH} is the power gain of the gain-standard antenna, P_{Test} is the power received with the test antenna and P_{SGH} is the power received with the gain-standard antenna.

e. Resistance Measurement

The resistance of embroidered layers was measured by Fluke PM6304 to determine the conductivity of reference points of measurement. Figure 3.12 shows the photograph of resistance measurement set-up.



Figure 3.12 Photograph resistance measurements by Fluke PM 6304

3.3 Summary

Research materials of conductive threads and PDMS polymer were introduced. Embroidery process and antenna fabrication procedure by lamination and integration of embroidered conductive layers on PDMS substrate were demonstrated. The simulation software and the measurement set-up for various antenna parameters such as resistance, reflection coefficient, radiation pattern and gain were also reviewed. The detail of antenna design and main research with novel investigations is reported in the remaining chapters of this dissertation.

CHAPTER 4

Embroidery Patch Antenna on Polymer Substrate with Identical Embroidery Properties

4.1 Introduction

While much effort has been directed toward the study of embroidered antenna on PDMS substrate, reported in Section 2.2.4, relatively little is understood about them in term of the performance effects from embroidered structures with identical embroidered characteristic. This chapter presents of first fully embroidered patch antenna on PDMS substrate with ground plane. The structures vary with the patch design, feeding techniques, patch weights and conductive characteristics with identical embroidered and electrical properties. Antenna performance analysis has been carried out through various parameters. The effect of different structures of embroidery patch antenna on polymer substrate with identical embroidery properties is represented.

4.2 Antenna Design and Characterization

4.2.1 Embroidery Structures

There are three different patch layers (A, B and C) and hence different structures have been embroidered differently using conductive thread and normal thread from bobbin, as shown in Figure 4.1.

2-sided embroidery patch	1-sided embroidery patch	1-sided embroidery patch
PDMS substrate	1-sided embroidery patch	Non conductive side
2-sided embroidery ground	Non conductive layer	PDMS substrate
Structure A	Non conductive layer	2-sided embroidery ground
	PDMS substrate	Structure C
	2-sided embroidery ground	
	Structure B	

Figure 4.1 Three different embroidery structures

The conductive layers have been embroidered by using Shieldex 40-22/7 + 110 PET 3 ply which has mentioned characteristics in Table 3.1 in Section 3.1.1. The embroidery process was mentioned in Section 3.2.1. All three structures are having the same two-sided ground plane and embroidered by conventional computerized sewing machine. The embroidered conductive layers were set up with moderate 0.4 mm stitch spacing. Figure 4.1 shows structures A and B hence have the same amount of conductive thread. Meanwhile, structure C has less conductive material.

To analyze the performance effect of embroidery patch antenna on polymer substrate with identical embroidery properties, three different patch designs (microstrip-fed rectangular patch, microstrip-fed polygon patch and SMA-fed polygon patch) antennas were fabricated and tested on 2 mm thick PDMS substrate which has dielectric constant of $\epsilon_r \sim 3$ by using lamination and integration method mentioned in Section 3.2.2.

4.2.2 Design One – Microstrip-fed Rectangular Patch Antenna

According to [63], microstrip-fed rectangular patch antenna is the typical planar antenna which consists of a conducting patch on one side of a dielectric substrate and a ground plane on the other side. Compared to many other antennas such as wire or horn antennas, microstrip antenna size and volume are relatively small. Its structure is simple and inexpensive to manufacture. Combining these features with planar structure and light weight, the microstrip patch antenna can be considered as a low profile antenna. In addition, by choosing appropriate width (W) and length (L) of rectangular patch, the antenna resonant frequency can be designed.

a. Basic Operating Mechanism

The primary source of microstrip antenna radiation is the electric fringing fields between the edges of the conductor element and the ground plane behind it. According to [6], when the microstrip patch is energized, a charge distribution is established on the upper and lower surfaces of the patch, as well as on the surface of the ground plane. The charge distribution is controlled by attractive and repulsive mechanism. The attractive mechanism is between opposite charges on the bottom side of the patch and the ground plane which maintains the charge concentration on the bottom of the patch. The repulsive mechanism is between like charges on the bottom surface of the patch, which tends to push charges around its edges. The movement of these charges creates corresponding electromagnetic excitation and causes antenna radiation [6]. Most practical microstrips the height-to-width ratio is very small, the attractive mechanism dominates and most of the charge concentration and current flow remain underneath the patch [63]. In microstrip patch antenna radiation, a loss mechanism has to be introduced in [6]. Deriving from the attractive mechanism of charges between the patch and the ground plane separated by a dielectric substrate, a dielectric loss is introduced. Refer to [64], dielectric loss is the dissipation of energy through the movement of charges in an alternating electromagnetic field. The dielectric loss of material is defined by its loss tangent, $\tan\delta$. For dielectrics with small loss, this $\tan\delta$ is $\ll 1$. Yuehui Ouyang and W. J. Chappell have proved that when there is a non-conductive surface is placed between the patch and the substrate, the dielectric loss will be increased since most of the charges are not concentrated at the bottom of the patch. There

is lacking of attractive force with the ground plane through dielectric substrate which leads to poor reflection coefficient [49].

b. Rectangular Patch Antenna Parameters Calculation

Figure 4.2 shows the front view of the microstrip-fed rectangular patch antenna with two points X and Y are the references points for measuring the patch resistance. For reference, the structure parameters of a rectangular patch antenna were calculated and applied for a simulated copper model on CST software for validation of the designed operating frequency.

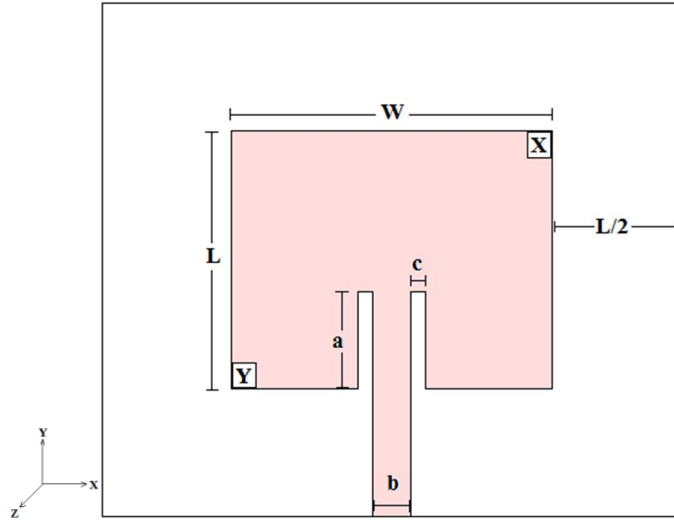


Figure 4.2 Microstrip-fed rectangular patch antenna geometry

With initial value of dielectric constant ϵ_r , thickness of the substrate h and the designed resonant frequency f_r , the antenna structure parameters of W and L can be theoretically obtained from following equations [6]:

$$W = \frac{v_0}{2f_r} \sqrt{\frac{2}{\epsilon_r + 1}} \quad (4.1)$$

where v_0 is the free-space velocity

$$\epsilon_{reff} = \frac{\epsilon_r + 1}{2} + \frac{\epsilon_r - 1}{2} \left[1 + 12 \frac{h}{W} \right]^{-1/2} \quad (4.2)$$

$$\frac{\Delta L}{h} = 0.412 \frac{(\epsilon_{reff}+0.3)\left(\frac{W}{h}+0.264\right)}{(\epsilon_{reff}-0.258)\left(\frac{W}{h}+0.8\right)} \quad (4.3)$$

$$L = \frac{1}{2f_r \sqrt{\epsilon_{reff}} \sqrt{\mu_0 \epsilon_0}} - 2\Delta L \quad (4.4)$$

The microstrip-fed rectangular patch antenna is theoretically designed for operating frequency at $f_r = 2.45$ GHz. The dielectric constant of PDMS is known as $\epsilon_r = 3$ and the substrate thickness of embroidery patch antenna is fabricated with $h = 2$ mm. The width of rectangular patch is calculated by solving equation (4.1).

$$W = \frac{v_0}{2f_r} \sqrt{\frac{2}{\epsilon_r + 1}} = \frac{3 \times 10^8}{2 \times 2.45 \times 10^9} \sqrt{0.5} = 0.043292 \text{ (m)} = 43.292 \text{ (mm)}$$

The value of ϵ_{reff} and ΔL can be calculated from equation (4.2) and (4.3) above.

- $\epsilon_{reff} = \frac{\epsilon_r+1}{2} + \frac{\epsilon_r-1}{2} \left[1 + 12 \frac{h}{W}\right]^{-\frac{1}{2}}$

$$= 2 + \left[1 + 12 \frac{2}{43.292}\right]^{-1/2} = 2.80208 \text{ (mm)}$$
- $\frac{\Delta L}{h} = 0.412 \frac{(\epsilon_{reff}+0.3)\left(\frac{W}{h}+0.264\right)}{(\epsilon_{reff}-0.258)\left(\frac{W}{h}+0.8\right)}$

$$= \frac{0.412 \times 3.102088 \times 21.910125}{2.544088 \times 22.44612} = 0.490368$$

$$\text{so, } \Delta L = 0.490368 \times 2 = 0.980737 \text{ (mm)}$$

The length of rectangular patch is calculated by solving equation (4.4).

$$L = \frac{1}{2f_r \sqrt{\epsilon_{reff}} \sqrt{\mu_0 \epsilon_0}} - 2\Delta L$$

$$= \frac{3 \times 10^8}{2 \times 2.45 \times 10^6 \times \sqrt{2.80208}} - 2 \times 0.980737$$

$$= 34.613 \text{ (mm)}$$

The aforementioned calculation shows that the rectangular patch antenna which has the length ($L = 34.613$ mm) and the width ($W = 43.292$ mm) theoretically operates at 2.45 GHz when fabricated on a 2 mm thick dielectric substrate with $\epsilon_r = 3$. A microstrip transmission line is connected directly to the rectangular patch as connector to fully characterize the antenna performance. The microstrip line is designed to have 50Ω input impedance (which is the usual connector characteristic impedance). The microstrip line dimensions can be obtained from determined antenna operating frequency f_r , substrate thickness h and the dielectric constant ϵ_r [6]. The microstrip-fed rectangular patch antenna parameters are calculated as in Table 4.1.

Table 4.1 Parameters of the antenna – Design 1

Parameters	W	L	a	b	c
Value (mm)	43.292	34.613	13	5	2

c. Simulation of Microstrip-Fed Rectangular Patch Antenna

A copper model of microstrip-fed rectangular patch antenna was simulated on CST Microwave Studio with calculated parameters shown in Table 4.1 to validate the 2.45 GHz operating frequency. Figure 4.3 and 4.4 show the simulated reflection coefficient result and normalized radiation pattern of copper microstrip-fed rectangular patch antenna respectively.

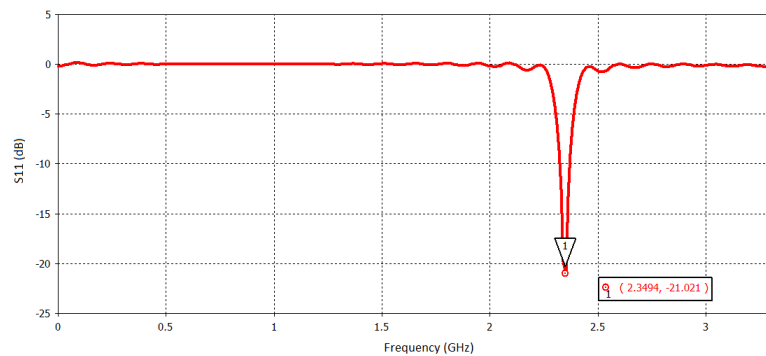


Figure 4.3 Simulated reflection coefficient result of copper microstrip-fed rectangular patch antenna

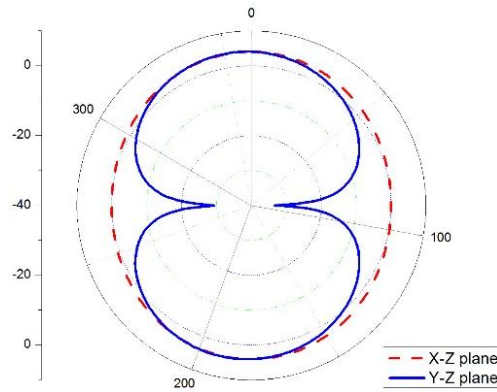


Figure 4.4 Normalized simulated radiation patterns of copper microstrip-fed rectangular patch antenna at 2.35 GHz

Applying the calculated parameters, the simulated resonant frequency of copper microstrip-fed rectangular patch antenna is 2.35 GHz while the theoretical designed operating frequency is 2.45 GHz. This is due to the difference between conductive material used in ideal theory which has perfect electric conductance [6] and the copper material used in simulation for actual usage. However, the simulated operating frequency has provided the validation for the calculated antenna parameters. The simulated radiation pattern result in Figure 4.4 illustrates that on the x-z and y-z plane, the copper microstrip-fed rectangular patch antenna has strongest radiation at its origin angle, and this completely agrees with the patch antenna radiation characteristic in [6]. The simulated result shows that near omni-directional radiation pattern can be obtained with back-lobe representation (angles from 180° to 360°) due to the finite ground plane effect. It has been assumed in the analysis and design of patch antenna that the size of ground plane is theoretically infinite. In microstrip patch antenna theory, an infinitely large ground plane would prevent any radiation towards the back of the antenna [6]. The effect of a finite ground plane on radiation fields has been studied by Huang in [63]. The research shows that if the size of the ground plane is increased, the ripples in the main pattern diminish and a finite

ground plane gives rise to radiation in the backward direction. In actual usage, only a finite size ground plane can be implemented to reduce the antenna size and the ground plane extension. However, finite ground plane give rise to diffraction of radiation from the ground plane resulting in changes in radiation pattern and increase the ripples in the radiation pattern [63].

The operating frequency and the radiation pattern of simulated copper microstrip-fed rectangular patch antenna are represented by applying the calculated antenna parameters in Table 4.1. The prototype of embroidery microstrip-fed rectangular patch antenna on polymer substrate is introduced in the following section.

d. Embroidery Microstrip-Fed Rectangular Patch Antenna on polymer substrate

Due to the limitation of CST microwave software simulation according to the special characteristics of embroidery antenna with incontinuous surface unlike copper, the calculated parameters in Table 4.1 were applied and referred to fabricate the embroidery antenna on polymer substrate prototypes. Figure 4.5 illustrates the photograph prototype of the microstrip-fed rectangular patch antenna on polymer substrate.



Figure 4.5 Photograph of microstrip-fed rectangular patch antenna prototype
The conductive layers of proposed antenna were embroidered precisely by computerized sewing machine as mentioned in Section 3.2.1. The antenna

prototypes were fabricated by following the process in Section 3.2.2. The antennas measurement and discussion will be demonstrated in Section 4.3.

4.2.3 Design Two – Microstrip-fed Polygon Patch Antenna

In order to make a better comparison and validation on the research concept, another design of microstrip patch antenna was proposed. Figure 4.6 shows the front view of the microstrip-fed polygon patch antenna geometry and Figure 4.7 shows the photograph of the antenna prototype.

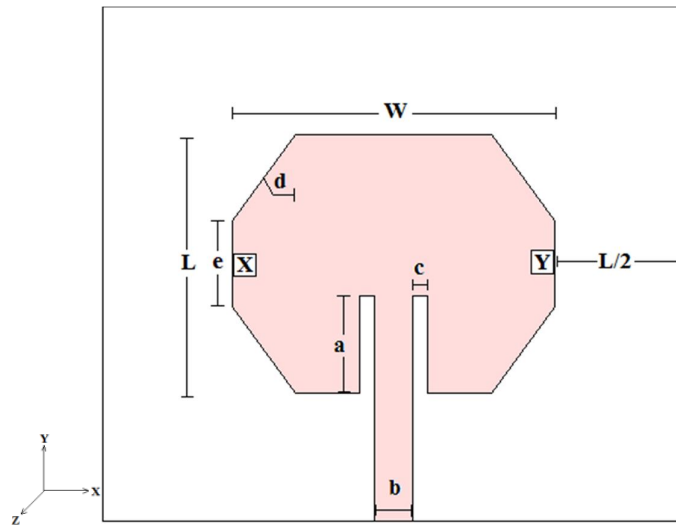


Figure 4.6 Microstrip-fed polygon patch antenna geometry



Figure 4.7 Photograph of microstrip-fed polygon patch antenna prototype

Following the aforementioned parameters of microstrip-fed rectangular patch antenna, the microstrip-fed polygon patch antenna parameters are illustrated in

Table 4.2. Two points X and Y in Figure 4.6 are the references points for measuring the patch resistance.

Table 4.2 Parameters of the antenna – Design 2

Parameters	W	L	a	b	c	d	e
Value (mm)	43.292	34.613	13	5	2	14.37	11.53

4.2.4 Design Three – SMA-fed Polygon Patch Antenna

The changing in feeding method was also investigated to validate the research concept of embroidery patch antenna on polymer substrate with identical embroidery properties. A SMA feeding was applied to polygon patch antenna. Figure 4.8 shows the front view of the SMA-fed polygon patch antenna geometry and Figure 4.9 shows the photograph of the antenna prototype.

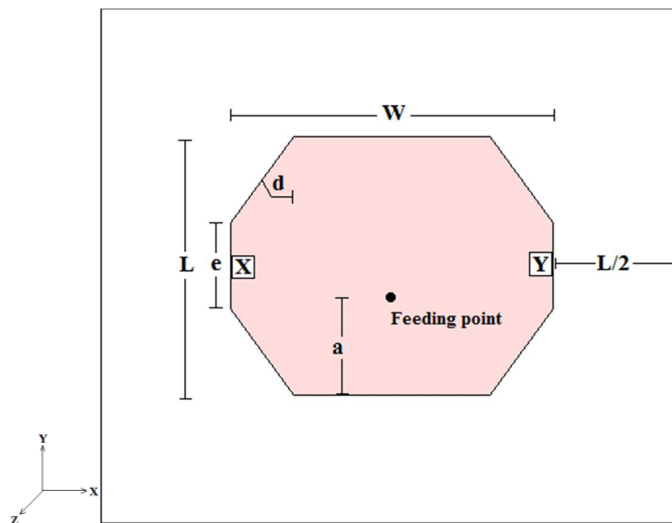


Figure 4.8 SMA-fed polygon patch antenna geometry

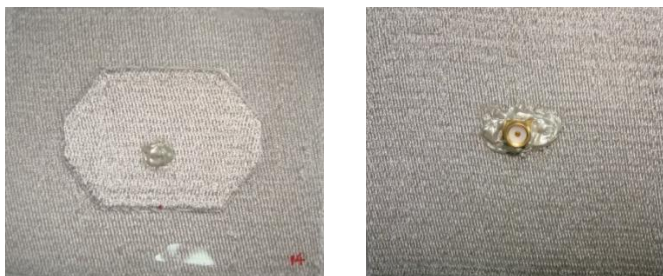


Figure 4.9 Photograph of SMA-fed polygon patch antenna prototype

The SMA-fed polygon patch antenna parameters are illustrated in Table 4.3.

Two points X and Y in Figure 4.8 are the references points for measuring patch resistance.

Table 4.3 Parameters of the antenna – Design 3

Parameters	W	L	a	d	e
Value (mm)	43.292	34.613	13	14.37	11.53

Besides difficulty caused by alignment of two PDMS layers during antenna integration process, there is another challenge of patch antenna with SMA feeding from the ground plane. The embroidered layer with 0.4 mm stitch spacing is quite close and this cause short-circuit while the center pin of SMA connector touches the conductive threads of the 2-sided ground plane before it goes through the PDMS substrate and reaches the patch layer. To overcome this situation, a small part of conductive threads were cut and a tiny hole was etched out at the feeding position from the ground plane, the conductive part was completely removed until the PDMS layer can be seen as shown in Figure 4.10(a). Besides that a thin rubber tape was also used to cover the ground-sleeve, thus helps center pin avoid touching the thread as depicted in Figure 4.10(b).



(a)



(b)

Figure 4.10 (a) Etching hole on ground plane, (b) Connectors with rubber tape

Antenna design 1 – microstrip-fed rectangular patch antenna was constructed and applied embroidered structure A, B and C as shown in Figure 4.1. The fabricated antennas were identified as 1A, 1B and 1C. In order to make a better

comparison and validation on research concept of different embroidered antenna structures on PDMS substrate with identical embroidery properties, antenna design 2 and 3 were further embroidered with structure A and B since they have identical embroidery properties to construct two more set of antennas 2A, 2B, 3A and 3B. All the seven antennas are put into measurement as reported in following sections.

4.3 Results and Discussion

4.3.1 Patch Resistance

The amount of conductive thread used in embroidery was obtained by measuring the thread cone on balance station before and after embroidery process. The resistance of embroidered patch layers was measured using Fluke PM 6034 by choosing the same reference point of measurement X and Y as shown in Figure 4.2, 4.6, 4.8. Figure 3.12 in Section 3.2.4 shows the measurement set-up for patch resistance before conductive layers were laminated on PDMS substrate. The measured resistance of embroidered patch layers was thus obtained and demonstrated in Table 4.4. According to the definition from thread manufacturer, the lineal resistance is the resistance between any two points on a straight line of a conductive thread. With Shieldex 40, the lineal resistance is 800,000 Ohm/m and the thread weight is 27,692.3 m/kg [51]. Deriving from the specification provided by manufacture in Table 3.1 and the obtained amount of conductive thread used in embroidery, the total value of lineal resistance of a conductive embroidered patch can be calculated. Table 4.4 shows the embroidery properties and the measured resistance characteristics of aforementioned seven antennas.

Table 4.4 Characteristic of conductive patch layers

Antenna	Stitch spacing (mm)	Stitch number	Weight of conductive patch (g)	Lineal resistance (Kohm)	Measured resistance (Ohm)
1A	0.4	2365	0.684	15,153.22	28.363
1B	0.4	2365	0.684	15,153.22	28.547
1C	0.4	2365	0.342	757,606	65.259
2A	0.4	2165	0.452	10,013.53	29.830
2B	0.4	2165	0.452	10,013.53	30.153
3A	0.4	2098	0.574	12,716.30	26.102
3B	0.4	2098	0.574	12,716.30	26.549
Ground	0.4	7725	2.226	49,314.44	53.658

Each aforementioned antenna design was embroidered with different patch structures (A, B and C) as shown in Figure 4.1. The same setting of stitch spacing (0.4 mm) on Embird Studio embroidery software was applied for all embroidered structures. Table 4.4 shows that the generated stitch number for each embroidered patch structure is identical corresponding to its antenna design (1, 2 and 3). The embroidery process was conducted precisely and hence the amount of conductive thread used in each embroidered patch is also identical among its set of design. The measured resistance result of each antenna design from the same reference points (X and Y) in Table 4.4 agrees with its lineal resistance. These antennas have the same amount of conductive thread regardless their difference in structuring except for antenna 1C which has higher resistance due to its poor structure with lowest amount of conductive thread. As a result, among each set of design, antenna (1A and 1B), (2A and 2B), (3A and 3B) have identical embroidered properties (stitch spacing, stich number, conductive thread amount) and similar electrical characteristics in manufacturing information and measured results. These conductive patch layers were then laminated on half-cured PDMS and integrated on a same 2-sided ground plane by using fresh PDMS as adhesive to complete a fully embroidery

antenna on polymer substrate. The processes follow the method introduced in Section 3.2.2. The conductive ground plane was also embroidered with a moderate setting of 0.4 mm stitch spacing and using same type of conductive thread. RF performance of these antennas will be measured and analyzed in term of reflection coefficients, radiation patterns and gain results in the following sections.

4.3.2 Reflection Coefficient

According to [7], return loss is the ratio between the power reflected back to the source and the transmitted power incident on the antenna. Therefore the smaller this ratio achieves the better the antenna radiates. Antenna reflection coefficient is measured in decibel (dB) with negative value of return loss. Equation (2.2) in Section 2.1.2 describes the formula to calculate reflection coefficient. The signal generator and network analyzer were set to operate from 0.01 to 10 GHz, covering the designed resonant frequency. Before measurement, the system calibration is performed to characterize the systematic errors and eliminate the effects from unexpected sources as demonstrated in Section 3.2.4. Figure 3.7 shows the schematic measurement set-up for reflection coefficient and Figure 3.8 shows the photograph of its measurement. Once the calibration process is finished, the antenna under test is connected to directional bridge (point X in Figure 3.7) to measure the reflection coefficient.

Figure 4.11 illustrates the reflection coefficient results of the three antenna structures of design 1 – microstrip-fed rectangular patch antenna (1A, 1B and 1C).

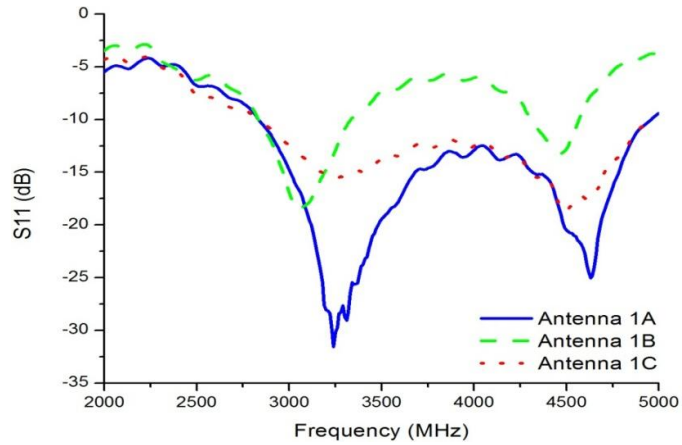


Figure 4.11 Measured reflection coefficient result of microstrip-fed rectangular patch antenna in different structures

According to equation (2.2), the formula of reflection coefficient, S11 value with -10 dB is achieved when the reflected power is only 10% compared to the transmitted power incident on the antenna, and thus the ratio between reflected power and incident power is 0.1. A low-loss antenna can be considered when it has 90% of incident power can be transmitted successfully [6]. Therefore, -10 dB threshold value of reflection coefficient is considered for reference level to determine the low-loss antenna performance. Figure 4.11 shows that the first resonant frequency of antenna 1A is at 3.238 GHz. The reflection coefficient result of this operating frequency can reach up to -25.442 dB together with 2.11 GHz wideband achievement (from 2.84 to 4.95 GHz), about 54% according to the center frequency at 3.895 GHz when taking -10 dB as reference level. In comparison with antenna 1A, the first resonant frequency of antenna 1B is at 3.05 GHz, it has lower reflection coefficient result with -18.565 dB while antenna 1C has -15.598 dB reflection coefficient result at its 3.25 GHz operating frequency. Although with the same amount of conductive thread and embroidery characteristic shown in Table 4.4, the antenna 1B, which has the thickest non-conductive surface facing the substrate causes less charges

concentration on the bottom of the conductive patch and increases loss. This is contrary to the operating mechanism of microstrip patch antenna which is described in Section 4.2.2 and thus the reflection coefficient is poorer than the normal two-sided embroidery, antenna 1A. The poor reflection coefficient result of antenna 1C is due to its lowest conductivity layer (65.259Ω) and the non-conductive layer facing downward the substrate. The measured operating frequency of antenna 1A is at 3.23 GHz which is about 32 % higher than the theoretical calculation (2.45 GHz) and simulation (2.35 GHz), although the antenna was fabricated with the same structural parameters in Table 4.1. This deviation is due to the conductive thread surface is not a continuous solid as estimated theoretically and the conductive material is embroidered from silver thread which is not perfect conductor. In 2011, Zheyu Wang *et al.* [44] introduced an embroidered transmission line on PDMS substrate. A copper model was also simulated for reference. The result shows that the embroidered transmission line on PDMS substrate has measured operating frequency 80% higher than the simulated copper model. Therefore, this research work has shown a better improvement on the fabrication of embroidery antenna on PDMS substrate and optimized the difference in operating frequency between measured and simulated results compared to other researcher. Moreover, the effect of different structures of embroidery patch antenna on polymer substrate with identical embroidery properties was also analyzed and demonstrated.

For further comparison and validation of research concept, two more antenna designs were fabricated and tested. The measured reflection coefficient result of microstrip-fed polygon patch antenna (antenna 2A and 2B) is illustrated in Figure 4.12.

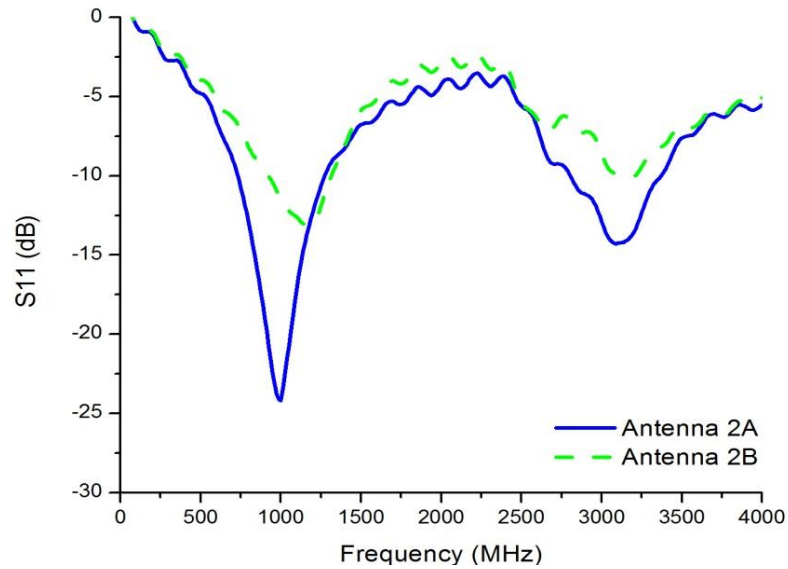


Figure 4.12 Measured reflection coefficient result of microstrip-fed polygon patch antenna in different structures

The results show that antenna 2A with normal two-sided embroidered patch has better reflection coefficient than double one-sided embroidery, antenna 2B at both operating frequency. Although both of them have identical embroidered properties and similar electrical characteristic as shown in Table 4.4, the first resonant frequency of antenna 2A is at 1 GHz with S11 result of -24.195 dB. Meanwhile, the reflection coefficient result of antenna 2B is -13.143 at its first resonant frequency, 1.17 GHz. The bandwidth of antenna 2A and 2B at its first operating frequency is 525 MHz and 388 MHz respectively. When the conductive embroidered layer facing against the substrate, antenna 2A has more charges concentration at the bottom of the patch as mentioned in Section 4.2.2. Higher attractive mechanism with lower dielectric loss is achieved at its operating frequency and thus it gives better reflection coefficient result than antenna 2B. The changing in feeding method was also investigated to validate the research concept of embroidery patch antenna on polymer substrate with identical embroidery properties. A SMA feeding was applied to polygon patch

antenna. The measured reflection coefficient results of polygon patch antenna with SMA feeding is presented in Figure 4.13.

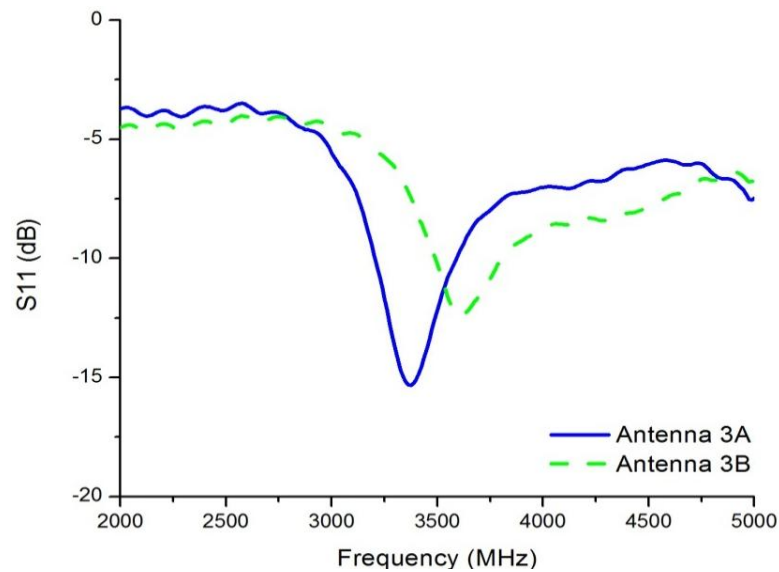


Figure 4.13 Measured reflection coefficient result of SMA-fed polygon patch antenna in different structures

The measured result in Figure 4.13 again shows the effect of embroidered structure of microstrip patch layer represented in Figure 4.1. At the antenna operating frequency, the reflection coefficient result of antenna 3A and 3B is -15.329 dB and -12.407 dB respectively. Antenna 3A with normal two-sided embroidery has better reflection coefficient result than antenna 3B with double one-sided embroidery although both of them have identical embroidered properties and similar electrical characteristic as shown in Table 4.4. Antenna 3B has non-conductive layer facing against the substrate which causes less charges concentration on the bottom of the conductive patch and increases loss. This is contrary to the operating mechanism of microstrip patch antenna which is described in Section 4.2.2 and prevents the charges travel to the ground plane. From the aforementioned measured results, Table 4.5 describes the reflection coefficient performance of three set of antenna designs.

Table 4.5 Measured reflection coefficient comparison between three antenna designs with different structures

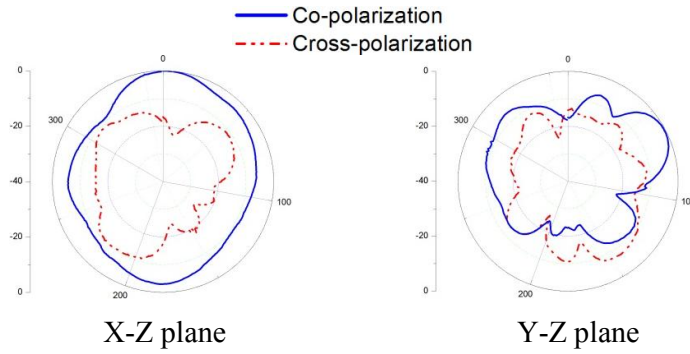
Antenna	1 st		2 nd	
	Resonant frequency (MHz)	Reflection coefficient magnitude (dB)	Resonant frequency (MHz)	Reflection coefficient magnitude (dB)
1A	3238	-25.442	4638	-25.036
1B	3050	-18.565	4469	-13.203
1C	3250	-15.598	4488	-18.73
2A	1000	-24.195	3088	-14.307
2B	1175	-13.143	3188	-10.1
3A	3375	-15.329	-	-
3B	3613	-12.407	-	-

Table 4.5 shows that three pairs of antenna likely have better radiation at the first operating frequency. Antennas with structure A, normal two-sided embroidery always have better reflection coefficient results than structure B, double one-sided embroidery regardless these two structures have identical embroidery properties and electrical characteristic as shown in Figure 4.1 and Table 4.4. According to the discussion in Section 4.2.2, antenna which has the non-conductive patch layer facing against the substrate causes less charges concentration on the bottom of the conductive patch, reduces the attractive mechanism with the ground plane and increases loss. This is contrary to the operating mechanism of microstrip patch antenna and thus the reflection coefficient is poorer than the normal two-sided embroidery. Therefore, Non-conductive surface against the substrate will increase dielectric loss and lead to poor reflection coefficient regardless identical embroidery characteristics and similar measured patch resistance results. The measured operating frequency of normal two-sided embroidery microstrip-fed rectangular patch antenna is about 32 % higher than its theoretical calculation and simulation, although the antenna was fabricated with the same structural parameters in Table 4.1. This deviation

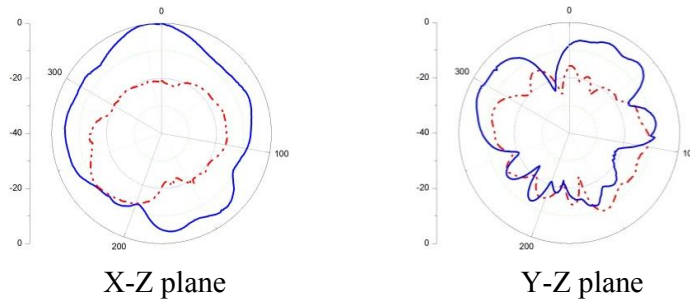
is due to the conductive thread surface is not a continuous solid as estimated theoretically and the conductive material is embroidered from silver thread which is not perfect conductor. However, this research work has shown a better improvement on the fabrication of embroidery antenna on PDMS substrate and optimized the difference in operating frequency between measured and simulated results compared to other researcher in [44]. Moreover, the effect of different structures of embroidery patch antenna on polymer substrate with identical embroidery properties was also analyzed and demonstrated.

4.3.3 Radiation Patterns

An antenna radiation pattern is defined as “a graphical representation of the radiation properties of the antenna as a function of space coordinates.” [6]. the signal generator and network analyzer were set to operate from 0.01 to 10 GHz, covering the designed resonant frequency. Before measurement, the system calibration is performed to characterize the systematic errors and eliminate the effects from unexpected sources as demonstrated in Section 3.2.4. Figure 3.8 shows the schematic measurement set-up for radiation pattern and Figure 3.10 shows the photograph of its measurement. Once the calibration process is finished, the test antenna is connected to point X as shown in Figure 3.8 and mounted over a tripod on a computerized positioner system. Meanwhile, a standard pyramidal horn is used as the transmitting antenna and connected to point Y. A software is programmed to rotate the positioner for 360 degree while the measurement result is taken and recorded during each degree. The measured far-field radiation patterns of all proposed antennas at its corresponding resonant frequencies are normalized and illustrated in Figure 4.14 to Figure 4.20.

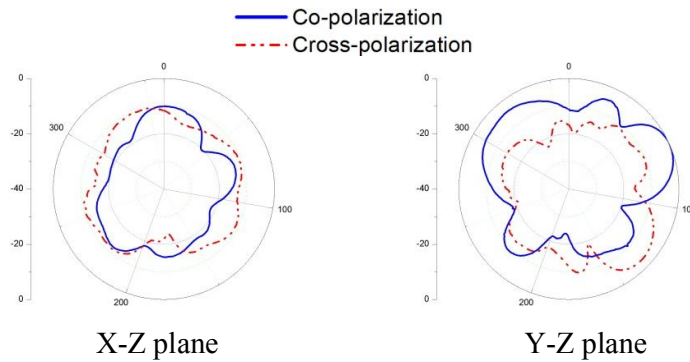


(a) 3.23 GHz

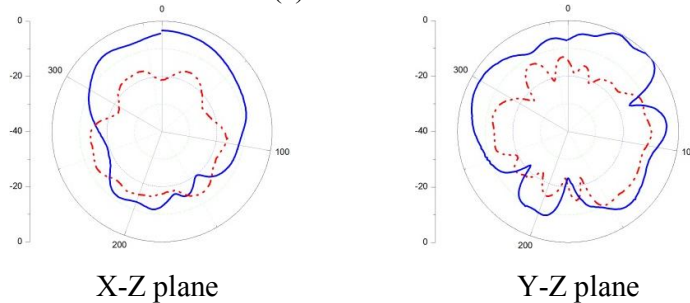


(b) 4.63 GHz

Figure 4.14 Normalized measured radiation patterns of antenna 1A at 3.23 and 4.63 GHz



(a) 3.05 GHz



(b) 4.46 GHz

Figure 4.15 Normalized measured radiation patterns of antenna 1B at 3.05 and 4.46 GHz

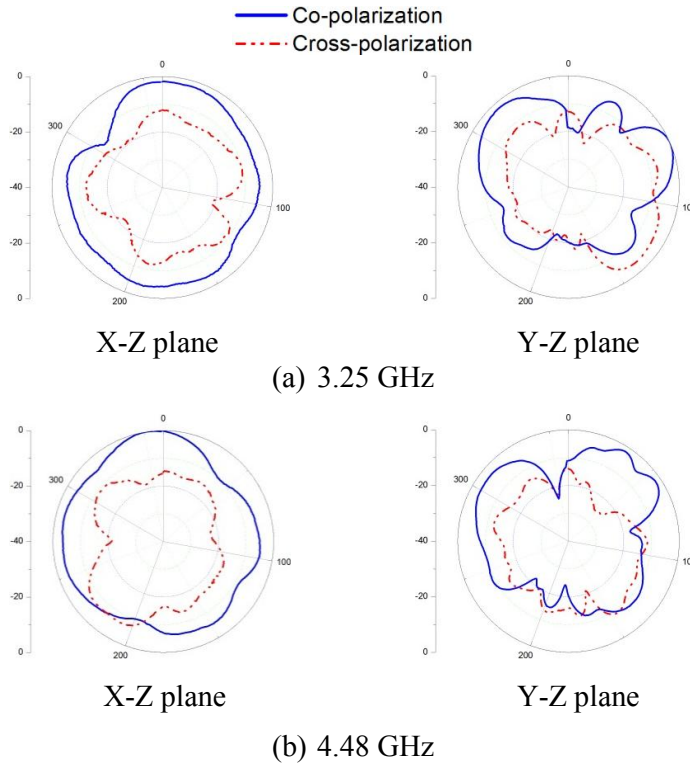


Figure 4.16 Normalized measured radiation patterns of antenna 1C at 3.25 and 4.48 GHz

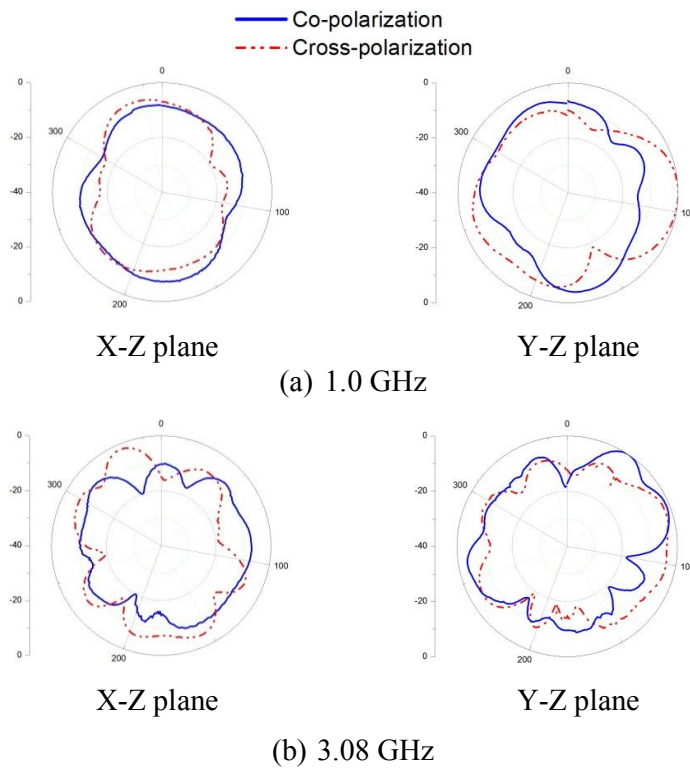


Figure 4.17 Normalized measured radiation patterns of antenna 2A at 1.0 and 3.08 GHz

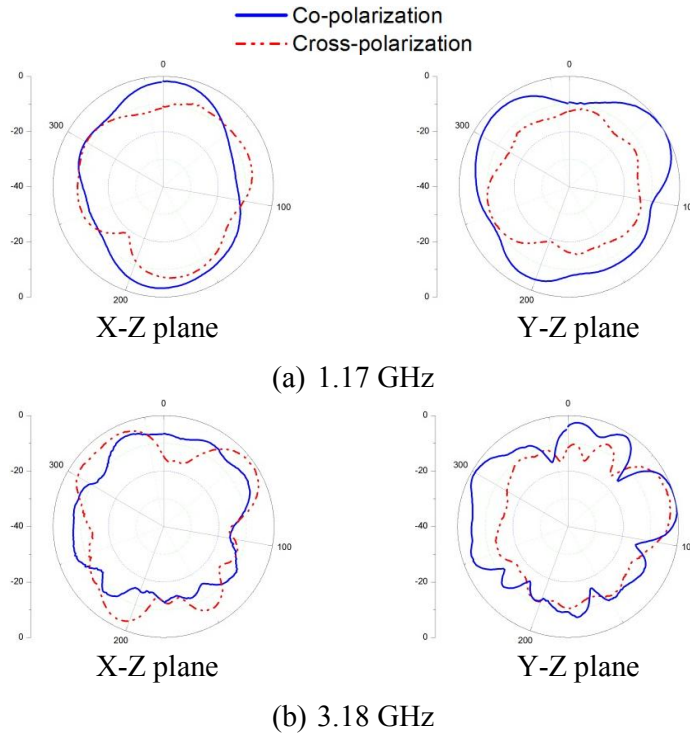


Figure 4.18 Normalized measured radiation patterns of antenna 2B at 1.17 and 3.18 GHz

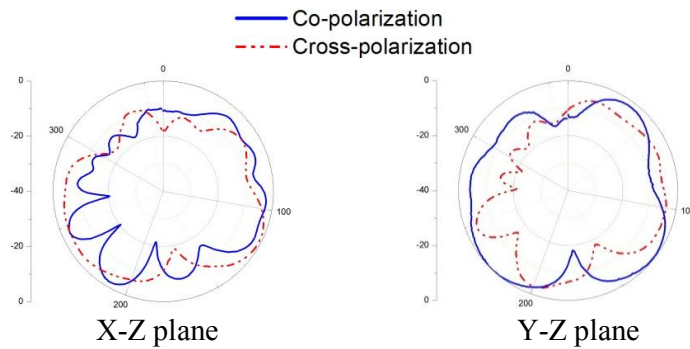


Figure 4.19 Normalized measured radiation patterns of antenna 3A at 3.37 GHz

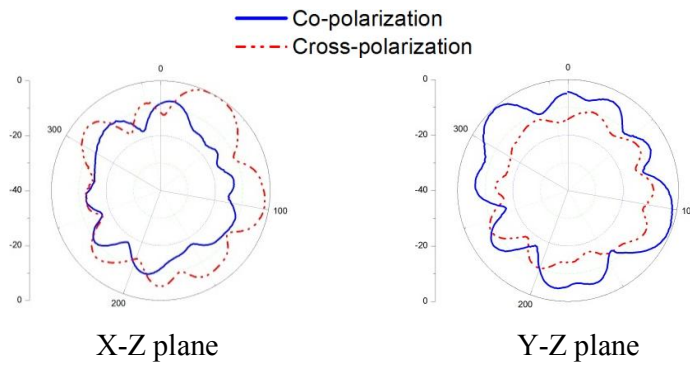


Figure 4.20 Normalized measured radiation patterns of antenna 3B at 3.61 GHz

The measured radiation pattern result in Figure 4.14 to 4.20 illustrates that on the x-z plane, the patch antennas with microstrip feeding (design 1 and 2) have strongest radiation at its origin angle, and this completely agrees with the patch antenna radiation characteristic in [6]. Meanwhile, the radiation patterns on the y-z plane tend to be stronger at approximately 90° from its origin. This is due to the embroidery antenna body is much less conductive and with high material loss compared to bulk metal antenna except for the feeding point which has silver epoxy applied on SMA connector. Therefore, during the turning process while measuring y-z plane, the radiated power reaches its higher level at the feeding faces to the transmitting antenna. Figure 4.19 and 4.20 depict that there is not much difference between x-z plane and y-z plane since the antenna with design 3 is fed from the ground plane and the feeding point is turned around in both cases during measurement.

All fabricated embroidery antennas were measured in a semi-rectangular anechoic chamber available at the university. The chamber is designed to minimize electromagnetic interference and simulate free-space conditions to maximize the volume of the quiet zone [6]. The simulated radiation pattern which is illustrated in Figure 4.4 shows smooth pattern drawing without interference effect. However, due to the imperfect condition of the chamber having walls that are not fully covered with RF absorbers, the measured radiation patterns indicate with slightly deviations and fluctuations in pattern drawing which are represented in Figure 4.14 to 4.20.

The simulated and measured radiation pattern show the representation of back-lobe (angles from 180° to 360°) due to the finite ground plane effect. It has been assumed in the analysis and design of patch antenna that the size of ground

plane is theoretically infinite. The large ground plane can eliminate the radiation back-lobe and diminish the ripples in the main pattern [6]. The effect of a finite ground plane on radiation fields has been studied by Huang in [63]. The research shows that if the size of the ground plane is increased, the ripples in the main pattern diminish and a finite ground plane gives rise to radiation in the backward direction. In actual usage only a finite size ground plane can be implemented to reduce the antenna size and the ground plane extension. However, finite ground plane give rise to diffraction of radiation from the ground plane resulting in changes in radiation pattern and increase the ripples in the radiation pattern [63]. On the above basis, the radiation patterns in Figure 4.14 to 4.20 show the effect of small ground plane and increase diffraction of radiation leading to the rise ripples beside the main beam especially on the patch antennas with SMA feeding which has a hole was cut out from the ground plane and the substrate.

The polarizations of all patch antennas were also analyzed and represented in Figure 4.14 to 4.20. The measured radiation patterns illustrate that most antennas have strong level in cross-polarization compared to co-polarization. According to [63], the cross-polarized component of patch antenna is increased with the resonant frequency and substrate thickness. Meanwhile, the co-polarization radiation is not affected by these parameters. During antenna fabrication process mentioned in Section 3.2.2, the embroidered conductive layers were laminated on half-cured PDMS substrate. These layers were unavoidable sunk slightly into the PDMS and affect to the substrate thickness. Besides that, the imperfect balance of PDMS mold during curing has also contributed to this defection. As a result, the cross-polarization radiation level is quite high. However, it is clearly noticed that the embroidered structure does

not affect the radiation pattern since the shape of patterns have not changed and this agrees with the patch antenna theory mentioned in [6]. On the above basis, there is a good match between theoretically far-field radiation pattern characteristics of patch antenna and the measured results.

4.3.4 On-axis Gain

Depending on the availability of standard-gain horn antenna, the on-axis gain of proposed patch antennas were able to be measured from 1.7 GHz to 18 GHz range by using gain-transfer method mentioned in Section 3.2.4. Table 4.6 shows the measured on-axis gain of each antenna at its resonant frequency.

Table 4.6 Measured on-axis gain of proposed antennas

Antenna	Resonant frequency (MHz)	S11 (dB)	On-axis gain (dB)
1A	3238	-25.442	-0.172
	4638	-25.036	1.866
1B	3050	-18.565	-12.975
	4469	-13.203	-3.936
1C	3250	-15.598	-4.654
	4488	-18.73	1.349
2A	3088	-14.307	-13.463
2B	3188	-10.1	-13.869
3A	3375	-15.329	-11.051
3B	3613	-12.407	-13.457

Among each antenna design (1, 2 and 3), structure A embroidered antenna are always have higher gain than structure B embroidered antenna regardless their identical embroidery properties and similar electrical characteristics. This is because of structure A has most of its electronics charges concentrate at the bottom side which facing against the substrate and reduce the dielectric loss during radiation.

The results of microstrip-fed rectangular patch antenna depict that antenna 1B has the lowest gain at its first and second resonant frequency with -12.975 dB, -3.936 dB respectively. This is due to antenna 1B has the thickest non-

conductive surface facing against the substrate causes most dielectric loss and the gain is lower than antenna 1C which also has single non-conductive layer facing against the substrate. Microstrip-fed polygon patch antenna and SMA-fed polygon patch antenna also have better gain results in its single two-sided embroidery antennas (structure A) than double one-sided embroidery antenna (structure B).

According to the discussion in Section 4.2.2, non-conductive layer facing against the substrate will be contrary to the attractive mechanism of the charges at the bottom of the patch and the ground plane. This will lead to increase loss and thus reduce antenna gain. The results in Table 4.6 convince that the thicker the non-conductive layer facing the substrate, the lower the gain of the antenna can radiate.

4.4 Summary

With identical stitch density, stitch number and conductive thread amount, single two-sided embroidery antenna structure gives similar conductivity as double one-sided embroidery antenna structure. However, two-sided embroidery antenna performs better in terms of reflection coefficient and on-axis gain. This is due to majority charges concentrate at the bottom of the patch and non-conductive layer facing downward against the substrate will give poorer reflection coefficient and gain results regardless of its identical conductivity surface. Radiation patterns were also measured and analyzed, the imperfect fabrication process during lamination of embroidered layer on half-cured PDMS and small ground plane have made effects on the substrate thickness and cause appearance of back-lobe as well as incensement of ripples and cross-polarization level. However, the research has shown the feasibility of

new class of embroidery antenna on PDMS substrate. Moreover, through different antenna designs and feeding techniques, the research has identified the effects of embroidered structure while the antennas have identical embroidered properties and similar electrical characteristics.

The next chapter will introduce a new path way to enhance the conductivity of embroidered patch layers of the proposed antennas. Dyeing method with conductive nanopowders and the effect on antennas performance will be investigated and analyzed.

CHAPTER 5

Embroidery Patch Antennas Dyed with Nanopowders on Polymer Substrate

5.1 Introduction

Previous chapter shows the feasibility of embroidery patch antenna on PDMS substrate and the effects of embroidered structure while the antennas have identical embroidered properties and similar electrical characteristics. Since the embroidered conductive layers take important effects on antenna performance, the conductivity of radiated layers is a considerable parameter which should be investigated. Researches showed that conductivity of embroidered layers can be improved by selecting high conductive thread with more metal concentration [49] or considering several embroidered parameters such as stitch direction, spacing between stitches, stitch density, stitch type [23]-[28]. However, these methods have the distinctive disadvantage of increasing stiffness and reducing elasticity of embroidered layers. During the embroidery process, the conductive thread with high metal concentration can cause excess heat due to the strong friction and damage the needle [50]. For thousands of years, humans have been decorating clothing through immersion of fabrics in liquid dyes [65]. In 2010, Yakup Bayram *et al.* dyed commodity cotton textile with single wall carbon nanotube (SWNT) solution after dispersion and coated with Ag and Au to create conductive textile for RF application [66]. As a result of this constraint, this chapter researches on enhancing the conductivity of embroidered antennas on PDMS while avoid aforementioned issues by dyeing technique with conductive nanopowder solutions. Antenna patch resistance can

be reduced by combining the antenna conductive layer with exceptional properties of graphene or metal oxide (ZnO, CuO and Al₂O₃) all of which are in nanostructure powder form. Graphene is a basic building block for graphitic materials of all other dimensionalities [67]. It has attracted significant attention as a result of its outstanding electronic, mechanical and chemical properties [68]. Meanwhile, ZnO, CuO and Al₂O₃ are important metal oxide nanostructure which have unique advantages in electronic devices, low processing cost, durability and strong energy [69]. This liquid route method provides a useful pathway for incorporating nanopowder into porous, light and flexible embroidered layers while popular spin coating or vacuum coating method cannot achieve.

5.2 Dyeing Solution Preparation

The dyeing technique in Section 5.2 and 5.3 includes nanopowder dispersion and immersion process was introduced in [70], [71]. Graphene, ZnO, CuO and Al₂O₃ nanopowders were dispersed in ethanol solvent to prepare as dyeing solutions. According to [68], graphene achieves a maximum concentration of 0.05 mg/mL in aqueous solution containing 70 vol. % ethanol. The concentration of ZnO, CuO, Al₂O₃ used in ethanol solvent is 0.5, 0.55 and 0.35 mg/mL respectively. Figure 5.1 shows the dyeing solution preparation process. Figure 5.1 (a) and (b) show the relevant amount of nanopowder with its corresponding ethanol volume were poured into a conical flask. The solutions were then utilized ultrasonic irradiation in sonicating bath for two hours to obtain homogeneous dispersion, Figure 5.1 (c). Finally, homogeneous dyeing solution is achieved as shown in Figure 5.1 (d).

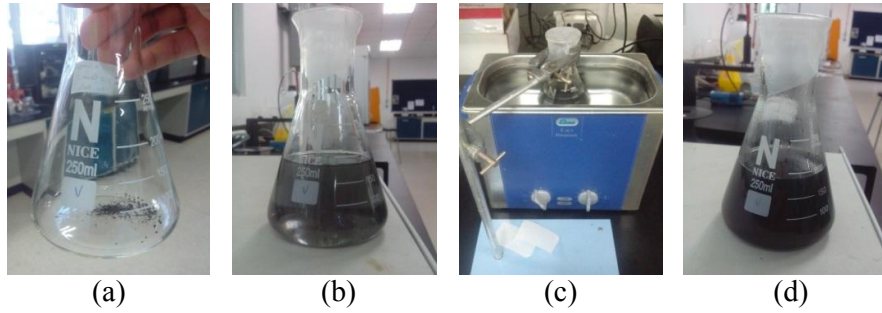


Figure 5.1 Dyeing solution preparation process

The photograph of graphene, ZnO, CuO and Al₂O₃ dyeing solution before and after sonicating is depicted in Figure 5.2.

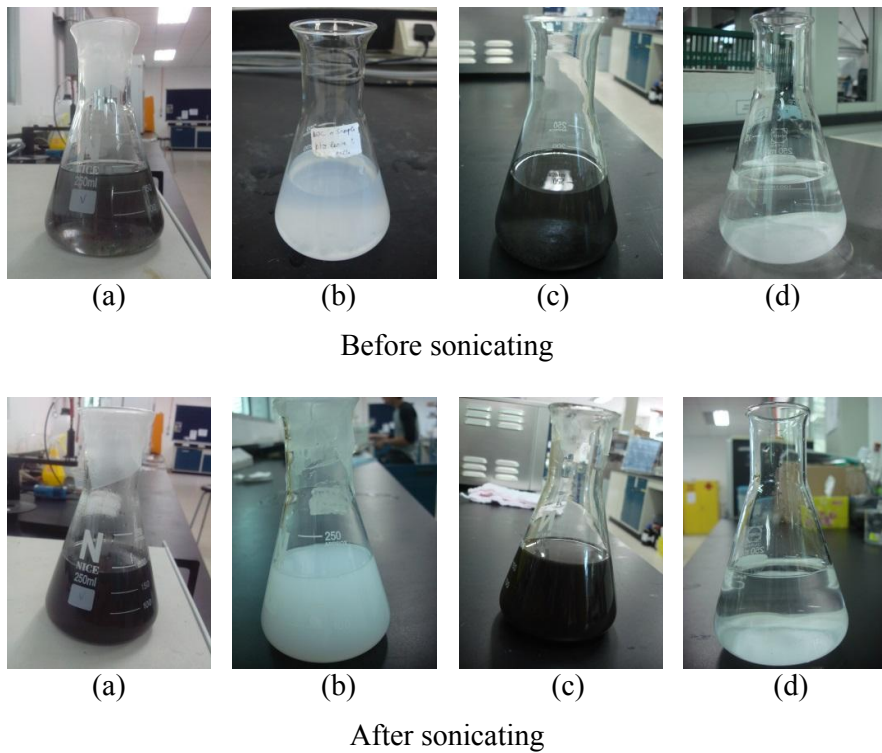


Figure 5.2 Photograph of dyeing solution before and after sonicating process (a) Graphene, (b) ZnO, (c) CuO, (d) Al₂O₃

Figure 5.2 illustrates the comparison between dyeing solutions before and after sonicating process. All dyeing solutions were utilized ultrasonic irradiation to obtain homogeneous dispersion. Figure 5.2 (a), (b) and (c) show that graphene, ZnO and CuO solution become denser and darker compared to its original solution before dyeing except for Al₂O₃ solution since its nanopowder is hydrophobic [72] and cannot be dispersed in ethanol solvent. Therefore, only

graphene, ZnO and CuO dyeing solution are eligible to dye for embroidered patch antenna.

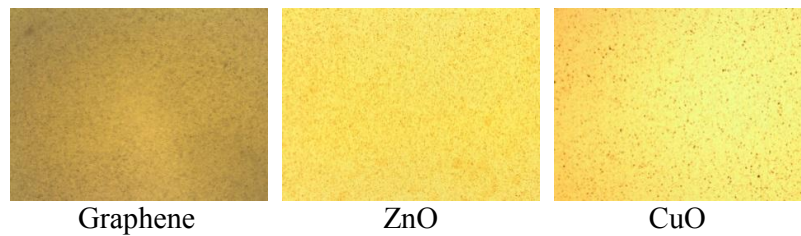


Figure 5.3 Microscope zoom 4x view of dyeing solution

Figure 5.3 shows the microscope zoom 4x view of graphene, ZnO and CuO dyeing solutions after sonicating process. Homogeneous dispersion was achieved as nanoparticles were well distributed in ethanol solvent.

5.3 Embroidered Patch Resistance

The design of embroidered microstrip-fed rectangular patch antenna was introduced in Section 4.2.2. The embroidered antenna structure was followed antenna design 1A in Table 4.4 with 0.4 mm stitch spacing. Figure 4.2 shows the front view of the microstrip-fed rectangular patch antenna with two points X and Y are the references points for measuring the patch resistance. The measurement set-up is demonstrated in Figure 3.12 which shows that Fluke PM6304 was used to determine the resistance of the patch layer by choosing the same reference points X and Y. Before dyeing with nanopowder solutions, the measured resistance of embroidered microstrip-fed rectangular patch layer is 28.363 Ohm originally. The embroidered patch was dipped in prepared dyeing solutions and then dried for measuring the resistance after each time of dyeing process is completed. The resistance variation of embroidered patch layer is recorded accordingly and illustrated in Figure 5.6. Details of dyeing process and measured resistance effect are described as follows.

The embroidered patch layers were dipped 30 seconds in prepared dyed dispersions then dried for 20 minutes at 70⁰C. This dyeing process was repeated five times for graphene and 11 times for ZnO and CuO dyeing solution to possess the resistance effect in Table 5.6. Figure 5.4 shows the microscope zoom 4x view of different dyed embroidered patches with nanopowder solutions compared with original patch without dyeing under same microscope setting condition.

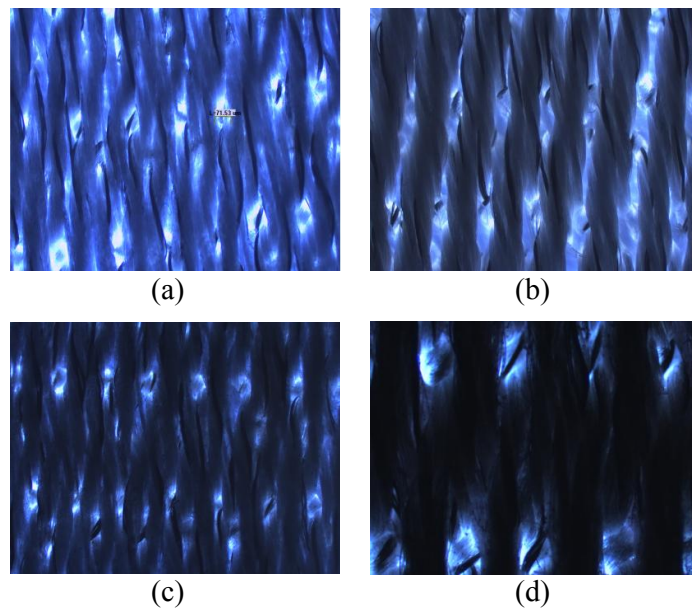
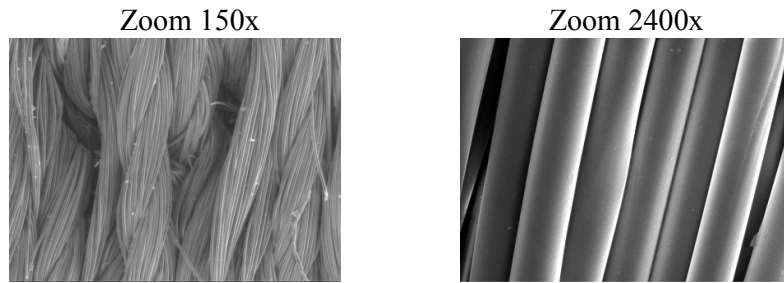
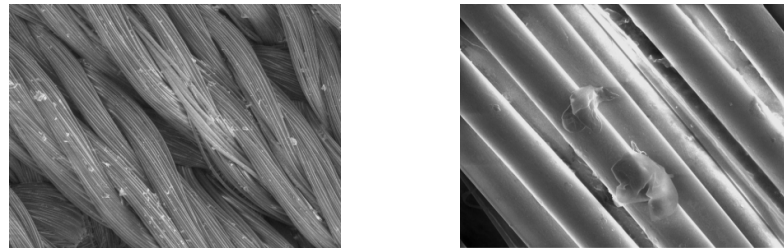


Figure 5.4 Microscope zoom 4x view of dyed embroidered antenna patch (a) origin without dyeing, (b) ZnO, (c) graphene, (d) CuO

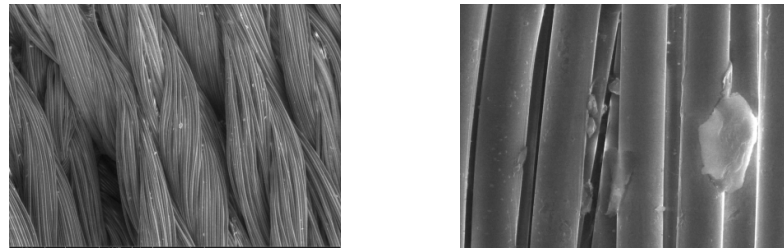
The changing color in Figure 5.4 indicates that graphene and metal nanopowders were deposited on embroidered surfaces. The SEM images of all proposed dyed embroidered patches under zoom 150x and 2400x are illustrated in Figure 5.5.



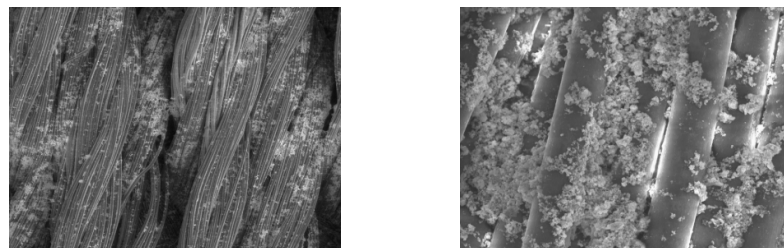
(a) Origin without dyeing



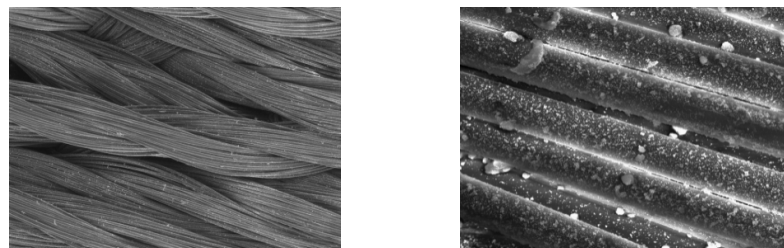
(b) 5 times dyeing with graphene



(c) 24 hours dyeing with graphene



(d) 11 times dyeing with CuO



(e) 11 times dyeing with ZnO

Figure 5.5 SEM images of proposed embroidered patches after dyeing effect

Figure 5.5 (b) and (c) show that graphene nanopowder has been deposited on dyed surfaces compared to the origin without dyeing in Figure 5.5 (a). However, the graphene deposited amount is much less than the amount of CuO and ZnO dyed surfaces in Figure 5.5 (d), (e). The measured results of embroidered microstrip-fed rectangular patch antenna were presented as antenna 1A with original patch resistance is 28.363 Ohm. Figure 5.6 illustrates the measured resistance results of embroidered patch layers dyed with graphene, ZnO, CuO solutions after multiple repeated dyeing processes.

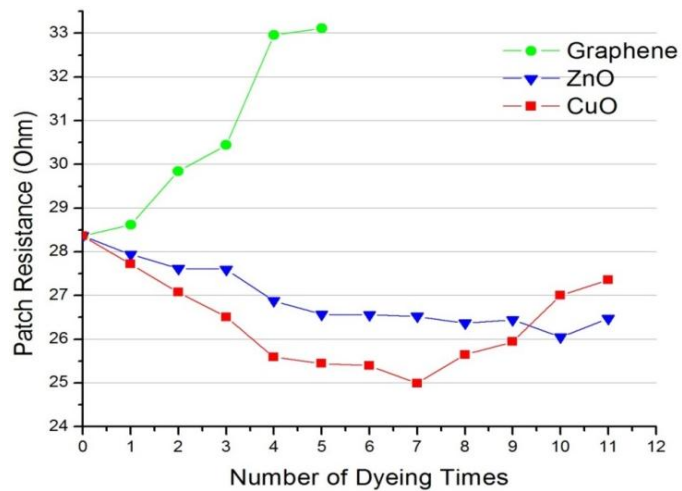


Figure 5.6 Resistances of graphene, ZnO and CuO dyed patches

The result shows that ethanol solvent reacted with silver thread and this caused lost in conductivity. Graphene dyed patch shows the tendency to increase its resistivity and graphene solution is therefore not strong enough to enhance the antenna patch conductivity. Due to the increase of resistance, graphene dyeing process was stopped after five times immersion. The embroidered patch layer was further dipped 24 hours in graphene solution. However, the conductive threads started to be detached from embroidered layer after long dipping time in solution and the conductivity raises up to 37.7 Ohm.

Figure 5.7 shows the microscope zoom 4x view of embroidered patch layer before and after 24 hours immersion in graphene solution.

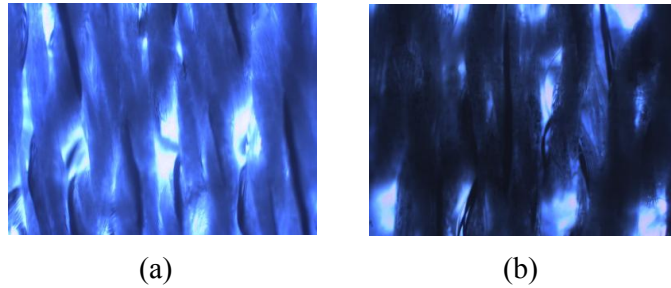


Figure 5.7 Microscope zoom 4x view of embroidered antenna patch (a) before immersion, (b) after 24 hours graphene immersion

In contrast with graphene dyeing solution, ZnO and CuO dispersion solutions contribute to the increase of conductivity up to 8.14% after 10 times dyeing for ZnO and 11.87% after seven times dyeing for CuO solution. The ZnO and CuO dyed antenna patches seemed to reach its limitation when the lowest patch resistance achieves at 26 and 25 Ohm respectively. In 2010, Yakup Bayram *et al.* [66] dyed commodity cotton textile with single wall carbon nanotube (SWNT) solution after dispersion. This process was repeated 10 times then Au was sputtered for 200 seconds to further reduce the resistance. As a result, the textile resistance was enhanced from 10 k Ω originally to 10 Ω after dyeing process and Au particles integration. This research work has improved the conductivity of the textile but compromised flexible nature of the E-textile as well as caused extra cost [66].

5.4 Embroidery Patch Antennas Dyed with Nanopowder on PDMS substrate

Two embroidered patch antennas were fabricated by applying dyeing technique in CuO and ZnO solutions with 7 and 10 times immersion process respectively to achieve its best resistance. The nanopowder dyed patches were laminated and integrated on PDMS substrate followed by a two sided ground

plane. The antenna fabrication process was introduced in Chapter 4 and the photograph of ZnO as well as CuO dyed antennas are depicted in Figure 5.8.

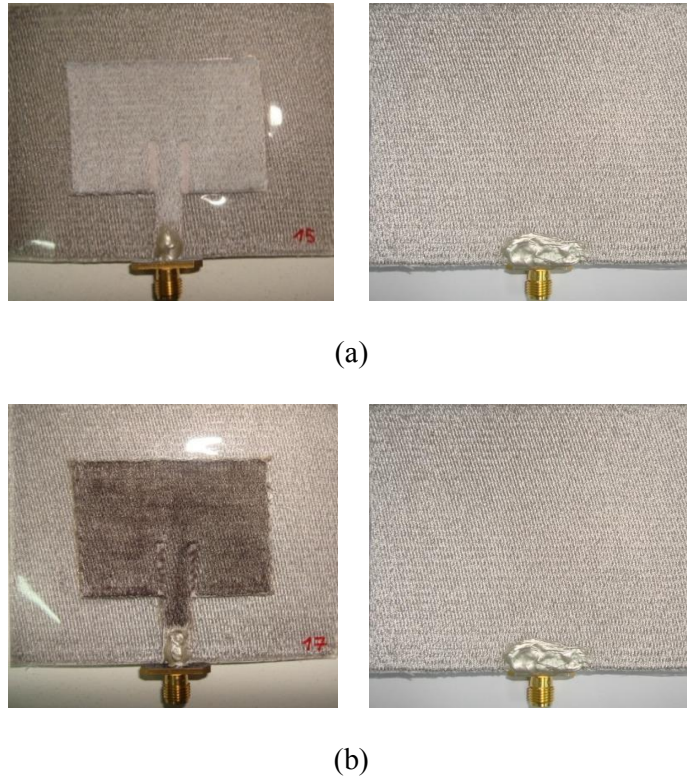


Figure 5.8 Photograph of antenna prototype with front and back view (a) dyed with ZnO solution, (b) dyed with CuO solution

RF performance of these proposed antennas in term of reflection coefficients, radiation patterns and gain are introduced in the following sections.

a) Reflection coefficient

Figure 5.9 shows the measured reflection coefficient results of ZnO and CuO dyed antenna. The results were analyzed in Table 5.1 compared with origin without dyeing version mentioned in Section 4.3.2.

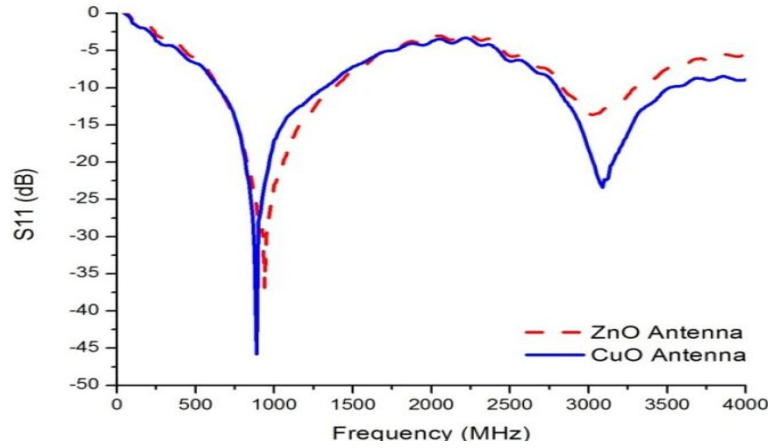


Figure 5.9 Measured reflection coefficient results of dyed embroidered patch antennas on PDMS substrate

Table 5.1 Reflection coefficient comparisons between original and dyed patch antennas

Antenna	Patch resistance (Ohm)	1 st		2 nd	
		Resonant frequency (MHz)	Reflection coefficient magnitude (dB)	Resonant frequency (MHz)	Reflection coefficient magnitude (dB)
Origin without dyeing	28.363	3238	-25.442	4638	-25.036
Dyed with ZnO	26.053	938	-36.874	3025	-13.648
Dyed with CuO	24.994	888	-45.817	3088	-23.426

The measured results in Table 5.1 show that higher conductive embroidered patch antenna gives better reflection coefficient level. Embroidery patch antenna on PDMS substrate without dyeing has patch resistance as 28.363 Ohm and its first resonant frequency at 3238 MHz with -25.442 dB. After dyeing, ZnO and CuO nanopowder were deposited respectively on embroidered surfaces. The process helps to improve the conductivity and reflection coefficient level improves to -36.874 dB and -45.817 dB respectively. However, the immersion process and the deposition of nanopowder have shifted the first resonant frequency down to 938 MHz for ZnO dyed antenna and 888 MHz for CuO dyed antenna compared to antenna without dyeing. Dyeing embroidery

patch antenna with conductive nanopowder solution improves the conductivity of embroidered patch layer as well as the antenna performance in term of reflection coefficient level.

b) Radiation patterns

The measured far-field radiation patterns of two antennas at its corresponding resonant frequencies are normalized and illustrated in Figure 5.10, 5.11.

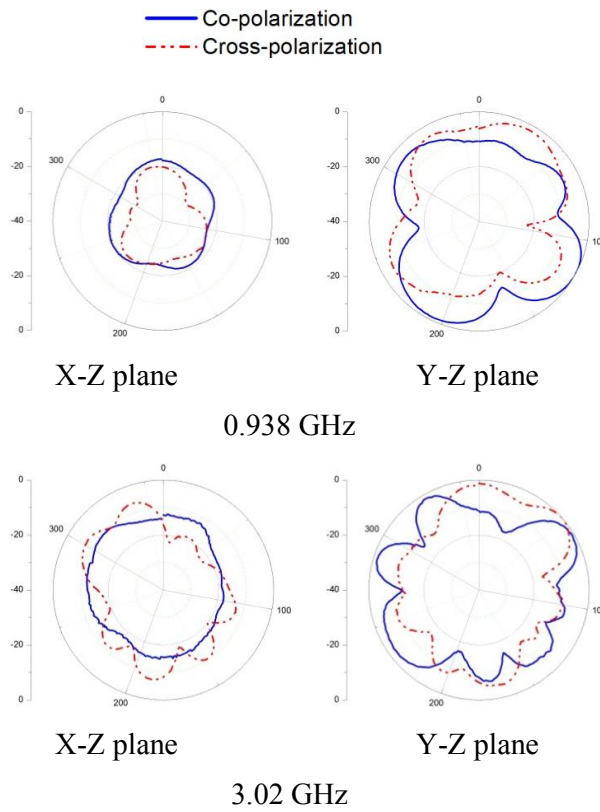
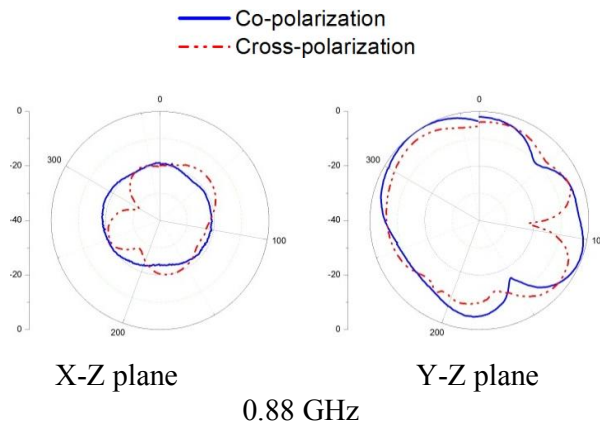


Figure 5.10 Normalized measured radiation patterns of ZnO dyed antenna



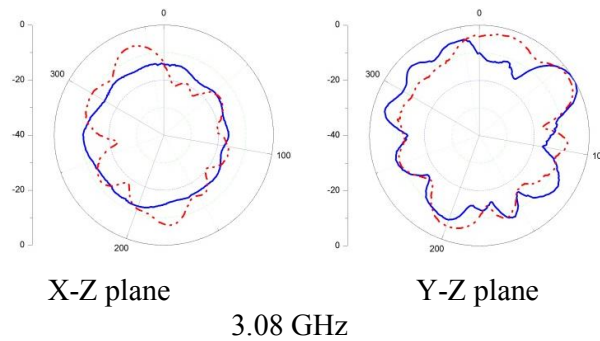


Figure 5.11 Normalized measured radiation patterns of CuO dyed antenna

The measured radiation pattern results illustrate that on the x-z plane, the patch antennas have strongest radiation at its origin angle. Meanwhile, the radiation patterns on the y-z plane are tending to be stronger approximately 90° from its origin. This is because the embroidery antenna body is much less conductive and with high material loss compared to bulk metal antenna except for the feeding point which has silver epoxy applied on SMA connector. Therefore, during turning process on y-z plane, the radiated power reaches its higher level at the feeding faces to the transmitting antenna. The effect of small ground plane increases diffraction of radiation leading to the rise ripples [6]. Most antennas cross-polarization level is strong compared to co-polarization level due to its imperfect substrate thickness [63]. In fabrication process, conductive layers were unavoidable sunk slightly into the PDMS and the contribution of unbalance of PDMS mold during curing. Figure 5.10, 5.11 indicate that dyed embroidery patch antenna with nanopowder has lower radiation on the x-z plane compared to antenna without dyeing in Figure 4.13 because of the immersion process of embroidered patch in nanopowder dyeing solution.

c) On-axis Gain

Table 5.2 Measured On-axis gain of proposed antennas

Antenna	Resonant frequency (MHz)	S11 (dB)	On-axis gain (dB)
1A	3238	-25.442	-0.172
	4638	-25.036	1.866
ZnO	3025	-13.648	-14.399
CuO	3088	-23.426	-15.4

Table 5.2 shows the measured on-axis gains of proposed patch antennas by using gain-transfer method. The effect of dyeing process has reduced the gain of original antenna at its operating frequency range due to the nanopowder deposited on radiating surfaces and the reaction of ethanol with silver thread.

5.5 Summary

In this chapter, a new method to improve the conductivity of embroidery patch antenna is introduced. With dyeing method, ZnO and CuO dispersion solutions have improved the conductive characteristic of embroidered patch antenna and the level of reflection coefficient result. Although nanopowder is deposited, the graphene dyed patch raises up sheet resistance because of existing process of ethanol and silver thread reaction.

CHAPTER 6

Conclusion and Future Work

The major objectives of this research effort were to conduct investigations relating to embroidery patch antenna on PDMS substrate.

In the context of antenna fabrication, single two-sided embroidery antenna structure gives similar conductivity as double one-sided embroidery antenna structure with identical embroidery properties. However, two-sided embroidery antenna performs better in terms of reflection coefficient and on-axis gain. This is due to majority charges concentrate at the bottom of the patch and non-conductive layer facing downward against the substrate will give poorer reflection coefficient and gain results regardless of its identical conductivity surface. Through different antenna designs and feeding techniques, the research has identified the effects of embroidered structure while the antennas have identical embroidered properties and similar electrical characteristics.

Considering the conductivity of embroidered patch layer, a new path way to enhance the conductivity of embroidered layer by dyeing method was introduced. ZnO and CuO dispersion solutions have improved the conductive characteristic of embroidered patch antenna and the level of reflection coefficient result. Although nanopowder is deposited, the graphene dyed patch raises up sheet resistance because of existing process of ethanol and silver thread reaction.

As noticed from this work, the imperfect fabrication process during lamination of embroidered layer on half-cured PDMS and unbalance surface of the mold during curing time have made effects on the substrate thickness and

cause appearance of back-lobe, incensement of ripples and cross-polarization level. Moreover, discontinuous surface and poor conductivity of embroidered patch layer also cause shift in resonant frequency. Yet another possible future work of interest could be researching on a method to fabricate embroidery antenna on PDMS, and control the substrate thickness precisely. Moreover, a study of resonant frequency of this type of antenna should be invested as well. Although the ZnO and CuO dyeing solution of conductive nanopowder can help to reduce the patch resistance, a better material or coating method can be possibly research since embroidery surfaces suffer from this liquid route method and the resistance reducing is not so remarkable.

References

- [1] B. Gupta, S. Sankaralingam and S. Dhar, "Development of wearable and implantable antenna in the last decade: a review," *Microwave Symposium (MMS)*, 2010 Mediterranean, pp. 251-267, August 2010.
- [2] K. V. S. Rao, P. V. Nikitin and S. F. Lam, "Antenna design for UHF RFID tags: a review and a practical application," *IEEE Transactions on Antennas and Propagation*, vol. 53, pp. 3870-3876, December 2005.
- [3] M. Marroncelli, D. Trinchero, V. Lakafosis and M. M. Tentzeris, "Concealable, low-cost paper-printed antennas for WISP-based RFIDs," *IEEE International Conference on RFID*, pp. 6-10, April 2011.
- [4] J. Melby, "JTRS and the evolution toward software-defined radio," *Proceedings of Military Communications Conference (MILCOM)*, vol. 2, pp. 1286-1290, October 2002.
- [5] K. Koski, A. Vena, L. Sydanheimo, L. Ukkonen and Y. Rahmat-Samii, "Design and implementation of electrotexile ground planes for wearable UHF RFID patch tag antennas," *IEEE Antennas and Wireless Propagation Letters*, vol. 12, pp. 964-967, August 2013.
- [6] C. A. Balanis, *Antenna theory analysis and design*, 3rd ed, John Wiley & Sons, New Jersey, 2005.
- [7] T. S. Bird, "Definition and misuse of return loss," *IEEE Antennas and Propagation Magazine*, vol. 51, no. 2, pp. 166-167, April 2009.
- [8] "IEEE standard definitions of terms for antennas," IEEE std. 145, March 1993.
- [9] S. Sankaralingam, S. Dasgupta, S. S. Roy, K. Mohanty and B. Gupta, "A fully fabric wearable antenna for HiperLAN/2 applications," *2011 Annual IEEE India Conference (INDICON)*, pp. 1-5, December 2011.
- [10] P. J. Massey, "Mobile phone fabric antennas integrated within clothing," *Eleventh International Conference on Antennas and Propagation*, vol. 1, pp. 344-347, 2001.
- [11] P. Salonen and L. Hurme, "A novel fabric WLAN antenna for wearable applications," *IEEE Antenna and Propagation Society International Symposium*, vol. 2, pp. 700-703, June 2003.
- [12] P. Salonen, Y. Rahmat-Samii, H. Hurme and M. Kivikoski, "Effect of conductive material on wearable antenna performance: a case study of WLAN

antennas,” *IEEE Antennas and Propagation Society International Symposium*, vol. 1, pp. 455-458, June 2004.

[13] Yuehui Ouyang, E. Karayianni and W. J. Chappell, “Effect of fabric patterns on electrotile patch antennas,” *IEEE Antennas and Propagation Society International Symposium*, vol. 2B, pp. 246-249, July 2005.

[14] A. Tronquo, H. Rogier, C. Hertleer and L. Van Langenhove, “Robust planar textile antenna for wireless body LANs operating in 2.45GHz ISM band,” *Electronics Letter*, vol. 42, pp. 142-143, February 2006.

[15] J. Lilja, P. Salonen and P. de Maagt, “Characterization of conductive textile materials for software antenna,” *IEEE Antennas and Propagation Society International Symposium (APSURSI)*, pp. 1-4, June 2009.

[16] S. Sankaralingam and B. Gupta, “Development of textile antennas for body wearable applications and investigations on their performance under bent conditions,” *PIER Progress in Electromagnetics Research B*, vol. 22, pp. 53-71, 2010.

[17] Ling Xu and J. L. Li, “A dualband microstrip antenna for wearable application,” *10th International Symposium on Antennas, Propagation & EM Theory (ISAPE)*, pp. 109-112, October 2012.

[18] “IEEE recommended practice for determining the peak spatial-average specific absorption rate (SAR) in the human head from wireless communication devices: measurement techniques,” *IEEE std. 1528-2013*, pp. 1-246, September 2013.

[19] G. George, N. R. D. Thiripurasundari, R. Poonkuzhali and Z. C. Alex, “Design of meander line wearable antenna,” *IEEE Conference on Information & Communication Technologies (ICT)*, pp. 1190-1193, April 2013.

[20] N. Chahat, M. Zhadobov and R. Sauleau, “Wearable textile patch antenna for BAN at 60 GHz,” *7th European Conference on Antennas and Propagation (EuCAP)*, pp. 217-219, April 2013.

[21] W. G. Whittow, A. Chauraya, J. C. Vardaxoglou and Yi Li, “Inkjet-printed microstrip patch antennas realized on textile for wearable applications,” *IEEE Antennas and Wireless Propagation Letter*, vol. 13, pp. 71-74, January 2014.

[22] Loc Ngo Quang Bao, Pei Cheng Ooi and Jit Kai Chin, “The effect of different structures of embroidery patch antenna on polymer substrate with identical embroidery properties,” *IEEE Antennas and Propagation Society International Symposium (APSURSI)*, July 2014.

[23] A. Chauraya, Shiyu Zhang, W. Whittow and T. Acti, “Addressing the challenges of fabricating microwave antennas using conductive threads,” *6th*

European Conference on Antennas and Propagation (EUCAP), pp. 1365-1367, March 2012.

[24] Shiyu Zhang, A. chauraya, W. Whittow, R. Seager, T. Acti, T. Dias, Y. Vardaxoglou, "Embroidered wearable antennas using conductive threads with different stitch spacings," *Loughborough Anntennas and Propagation Conference (LAPC)*, pp. 1-4, November 2012.

[25] E. Moradi, K. Koski, L. Ukkonen, Y. Rahmat-Samii, T. Bjorninen and L. Sydanheimo, "Embroidered RFID tags in body-centric communication," *Internation Workshop on Antenna Technology (IWAT)*, pp. 367-370, March 2013.

[26] R. Seager, S. Zhang, A. Chauraya, W. Whittow, Y. Vardaxoglou, T. Acti and T. Dias, "Effect of the fabrication parameters on the performance of embroidered antennas," *IET Microwaves, Antennas & Propagation*, vol. 7, pp. 1174-1181, November 2013.

[27] Lanlin Zhang, Zheyu Wang, D. Psychoudakis and J. L. Volakis, "E-fiber electronics for body-worn devices," *6th European Conference on Antennas and Propagation (EUCAP)*, pp. 760-761, March 2012.

[28] J. S. Roh, Y. S. Chi, J. H. Lee and Youndo Tak, "Embroidered wearable multiresonant folded dipole antenna for FM reception," *IEEE Antennas and Wireless Propagation Letters*, vol. 9, pp. 803-806, August 2010.

[29] S. Ahmad, N. S. Saidin and C. M. C. Isa, "Development of embroidered Sierpinski carpet antenna," *IEEE Asia-Pacific Conference on Applied Electromagnetics (APACE)*, pp. 123-127, December 2012.

[30] M. A. R. Osman, M. K. Abd Rahim, N. A. Samsuri, H. A. M. Salim and M. F. Ali, "Embroidered fully textile wearable antenna for medical monitoring applications," *PIER Progress in Electromagnetics Research*, vol. 117, pp. 321-337, 2011.

[31] T. Kaufmann, I. fumeaux and C. Fumeaux, "Comparison of fabric and embroidered dipole antennas," *7th European Conference on Antennas and Propagation (EuCAP)*, pp. 3252-3255, April 2013.

[32] Zheyu Wang, Lanlin Zhang, D. Psychoudakis and J. L. Volakis, "Flexible textile antennas for body-worn communication," *IEEE International Workshop on Antenna Technology (iWAT)*, pp. 205-208, March 2012.

[33] Zheyu Wang, Lanlin Zhang, D. Psychoudakis and J. L. Volakis, "GSM and Wi-Fi textile antenna for high data rate communications," *IEEE Antennas and Propagation Society International Symposium (APSURSI)*, pp. 1-2, July 2012.

- [34] K. Koski, E. Moradi, A. A. Babar, T. Bjorninen, L. Sydanheimo, L. Ukkonen, Y. Rahmat-Samii, "Durability of embroidered antennas in wireless body-centric healthcare applications," *7th European Conference on Antennas and Propagation (EuCAP)*, pp. 565-569, April 2013.
- [35] M. Toivonen, K. Koski, E. Moradi and A. A. Babar, "Washing durability of embroidered polymer coated RFID tags," *IEEE Antennas and Propagation Society International Symposium (APSURSI)*, pp. 1490-1491, July 2013.
- [36] M. E. de Cos and F. Las-Heras, "Polypropylene-Based dual-band CPW-fed monopole antenna," *IEEE Antennas and Propagation Magazine*, vol. 55, pp. 264-273, August 2013.
- [37] Haiwen Liu, Shuangshuang Zhu, Pin Wen, Xiang Xiao, Wenquan Che, Xuehui Guan, "Flexible CPW-fed fishtail-shaped antenna for dual-band applications," *IEEE Antennas and Wireless Propagation Letter*, vol. 13, pp. 1536-1225, April 2014.
- [38] A. C. Durgun, C. A. Balanis, C. R. Birtcher and D. R. Allee, "Design, simulation, fabrication and testing of flexible bow-tie antennas," *IEEE Transactions on Antennas and Propagation*, vol. 59, pp. 4425-4435, December 2011.
- [39] S. Nikolaou, G. E. Ponchak, J. Papapolymerou and M. M. Tentzeris, "Conformal double exponentially tapered slot antenna (DE TSA) on LCP for UWB applications," *IEEE Transactions on Antennas and Propagation*, vol. 54, pp. 1663-1669, June 2006.
- [40] S. Y. Y. Leung and D. C. C. Lam, "Performance of printed polymer-based RFID antenna on curvilinear surface," *IEEE Transactions on Electronics Packaging Manufacturing*, vol. 30, pp. 200-205, July 2007.
- [41] C. P. Lin, C. H. Chang, Y. T. Cheng and C. F. Jou, "Development of a flexible SU-8/PDMS-based antenna," *IEEE Antennas and Wireless Propagation Letters*, vol. 10, pp. 1108-1111, October 2011.
- [42] Jovanche Trajkovikj, Jean Francois Zurcher and Anja K. Skrivervik, "PDMS, a robust casing for flexible W-BAN antennas," *IEEE Antennas and Propagation magazine*, vol. 55, pp. 287-297, October 2013.
- [43] R. A. Liyakath, A. Takshi and G. Mumcu, "Multilayer stretchable conductors on polymer substrates for conformal and reconfigurable antennas," *IEEE Antennas and Wireless Propagation Letters*, vol. 12, pp. 603-606, April 2013.
- [44] Zheyu Wang, Lanlin Zhang, Y. Bayram, J. L. Volakis, "Multilayer printing of embroidered RF circuits on polymer composites," *IEEE*

International Symposium on Antennas and Propagation (APSURSI), pp. 278-281, July 2011.

[45] S. Koulouridis, G. Kiziltas, Yijun Zhou, D. J. Hansfor and J. L. Volakis, "Polymer-Ceramic composites for microwave applications: fabrication and performance assessment," *IEEE Transactions on Microwave Theory and Techniques*, vol. 54, pp. 4202-4208, December 2006.

[46] J. L. Volakis, Lanlin Zhang, Zheyu Wang and Y. Bayram, "Embroidered flexible RF electronics," *IEEE International Workshop on Antenna Technology (iWAT)*, pp. 8-11, March 2012.

[47] Zheyu Wang, Lanlin Zhang, Y. Bayram and J. L. Volakis, "Embroidered conductive fibers on polymer composite for conformal antennas," *IEEE Transactions on Antennas and Propagation*, vol. 60, pp. 4141-4147, September 2012.

[48] Zheyu Wang, L. Z. Lee and J. L. Volakis, "A 10:1 bandwidth textile-based conformal spiral antenna with integrated planar balun," *IEEE Antennas and Propagation Society International Symposium (APSURSI)*, pp. 220-221, July 2013.

[49] Yuehui Ouyang and W. J. Chappell, "High frequency properties of electro-textile for wearable antenna applications," *IEEE Transactions on Antennas and Propagation*, vol. 56, pp. 381-389, February 2008.

[50] T. Acti, Shiyu Zhang, A. Chauraya, W. Whittow, R. Seager, T. Dias and Y. Vardaxoglou, "High performance flexible fabric electronics for megahertz frequency communications," *IEEE Loughborough Antennas and Propagation conference (LAPC)*, pp. 1-4, November 2011.

[51] Conductive Sewing Thread, Technical Data Sheet, Shieldex, Statex, 2010.

[52] E. Moradi, T. Bjorninen, L. Ukkonen and Y. Rahmat Samii, "Effects of sewing pattern on the performance of embroidered dipole-type RFID tag antennas," *IEEE Antennas and Wireless Propagation Letters*, vol. 11, pp. 1482-1485, December 2012.

[53] Sylgard 184 Silicone Elastomer, Product Information, Dow Corning, 2014.

[54] Lanlin Zhang, Zheyu Wang and J. L. Volakis, "Textile antennas and sensors for body-worn applications," *IEEE Antennas and Wireless Propagation Letters*, vol. 11, pp. 1690-1693, January 2013.

[55] User's Manual, CST Microwave Studio, 2006.

[56] Agilent 8757D Scalar Network Analyzers, Configuration Guide, 2006.

- [57] Agilent E8257D PSG Microwave Analog Signal Generator, Data Sheet, 2012.
- [58] Agilent 83000A Series Microwave System Amplifiers, Product Overview, 2002.
- [59] Agilent Technologies 85027 A/B/C Directional Bridge, Operation and Service manual, 2007.
- [60] Agilent Technologies 11667B Power Splitter, Operating and Service Manual, 2004.
- [61] Agilent Technologies 85025A/B/D/E Detectors, User's and Service Guide, 2007.
- [62] "IEEE standard test procedure for antennas," IEEE std. 149-1979, December 2008.
- [63] R. Garg, P. Bhartia, Inder Bahl and A. Ittipiboon, *Microstrip antenna design handbook*, Artech House, 2001.
- [64] "Dielectric Loss", Wikipedia, the free encyclopedia, <https://en.wikipedia.org/wiki/Dielectric_loss>, 2015 (accessed 17 September 2015).
- [65] R. S. Horsfall and L. G. Lawrie, *The dyeing of textile fibres*, 2nd ed, Chapman & hall ltd, London, 1946.
- [66] Y. Bayram, Yijun Zhou, Bong Sup Shim, Shimei Xu, Jian Zhu, N. A. Kotov and J. L. Volakis, "E-textile conductors and polymer composites for conformal lightweight antennas," *IEEE Transactions on Antenna and Propagation*, vol. 58, pp. 2732-2736, May 2010.
- [67] A. K. Geim and K. S. Novoselov, "The rise of graphene," *Nature materials* 6, pp. 183-191, 2007.
- [68] Wei-Wei Liu, Bao-Yu Xia, Xiao-Xia Wang and Jian-Nong Wang, "Exfoliation and dispersion of graphene in ethanol-water mixtures," *Frontiers of Materials Science*, vol. 6, Issue 2, p. 176-182, June 2012.
- [69] Ahmad Umar, *Metal oxide nanostructures and their applications*, Amer Scientific Pub, October 2009.
- [70] M. in het Panhuis, J. Wu, S. A. Asharaf and G. G. Wallace, "Conducting textile from single-walled carbon nanotubes," *Synth. Met.*, vol. 157, no. 8-9, pp. 358-362, 2007.

[71] Y. Liu, J. Tang, R. Wang, H. Lu, L. Li, Y. Kong, K. Oi and J. H. Xin, “Artificial lotus leaf structures from assembling carbon nanotubes and their applications in hydrophobic textile,” 17th ed, pp. 1071-1078, 2007.

[72] “Aluminium Oxide”, *Wikipedia, The Free Encyclopedia*, <http://en.wikipedia.org/wiki/Aluminium_oxide>, December 2014 (accessed 12 January 2015).

Appendices

Four following papers are attached as appendices for reference:

[1] Loc Ngo Quang Bao, Pei Cheng Ooi and Jit Kai Chin, “The effect of different structures of embroidery patch antenna on polymer substrate with identical embroidery properties,” *IEEE International Symposium on Antennas and Propagation and USNC-URSI Radio Science Meeting (APSURSI)*, Memphis, Tennessee, USA, pp. 840-841, July 2014.

[2] Loc Ngo Quang Bao, Pei Cheng Ooi, Jit Kai Chin and Chuan Chin Pu, “Investigation of embroidery conductive layer dyed with graphene and ZnO,” presented in *19th International Symposium on Antennas and Propagation (ISAP)*, Taiwan, pp. 515-516, December 2014.

[3] Loc Ngo Quang Bao, Pei Cheng Ooi, Jit Kai Chin and Chuan Chin Pu, “Embroidery Patch Antennas on Polymer Substrate with Identical Embroidery Properties,” submitted to the *IEEE Transaction on Antennas and Propagation*.

[4] Loc Ngo Quang Bao, Pei Cheng Ooi, Jit Kai Chin and Chuan Chin Pu, “Embroidery Patch Antennas Dyed with Nanopowders on Polymer Substrate,” submitted to the *IEEE Transaction on Antennas and Propagation*.

The Effect of Different Structures of Embroidery Patch Antenna on Polymer Substrate with Identical Embroidery Properties

Loc Ngo Quang Bao, Pei Cheng Ooi, Jit Kai Chin
 The University of Nottingham Malaysia Campus
 Jalan Broga, Semenyih, Selangor Darul Ehsan, Malaysia
ngoquangbaoloc@gmail.com, Belle.Ooi@nottingham.edu.my

Abstract—This paper presents a novel class embroidery patch antenna on polymer composite — polydimethylsiloxane (PDMS). By lamination and polymer integration, different structures of fully embroidered polymer patch antenna with ground plane have been designed, fabricated and tested. Analysis of the effect of conductive patch weight, conductive characteristics using different embroidery structure on antenna performance has been carried out. The measured results show that although double embroidered layer on one side of fabric has similar conductivity and identical embroidery properties as two-sided embroidery, the antenna performs better using two-sided embroidery structure.

Index terms—embroidery antenna, polymer antenna, patch antenna.

I. INTRODUCTION

Wearable antenna with garment integration becomes essential nowadays in many applications such as in medical field, military development, mineworker tracking and environment monitoring. These antennas need not only possess good RF performance characteristics but also mechanical structure which adaptable to conformity and durability [1-3].

Embroidery antenna is potential candidate that meets the requirements. Furthermore, computerized sewing machine can be used to fabricate textile antennas quickly and on a mass manufacturing scale, highly flexible to change the design at minimal costs and time. Conductivity of embroidered layers can be improved by selecting high conductive thread, increasing stitch density and stitch type. The antenna performance can also be enhanced by considering stitch density, stitch direction and spacing between stitches [4]. Numerous researches on embroidery antenna with different types of conductive threads were introduced in [5-7].

Polymer is becoming an important material used for microwave and electronic applications. PDMS is the most widely used silicone-based organic polymer and is well-known for its advantage properties including nonflammable, water resistant, room temperature fabrication, low lost and adjustable dielectric constant by adding ceramic powder [8]. To increase embroidery antenna durability, reinforcement, miniature and low lost dielectric, PDMS substrate was introduced in [3], [9].

This paper presents different structures of fully embroidered patch antenna on PDMS substrate. The structures vary with the patch weight and conductive characteristics. Antenna performance analysis has been carried out on the different structures.

II. ANTENNA DESIGN AND CHARACTERIZATION

Fig. 1(a) shows the front view of the antenna structure and Fig. 1(b) is the photograph of the antenna prototype. The antenna parameters are illustrated in Table I.

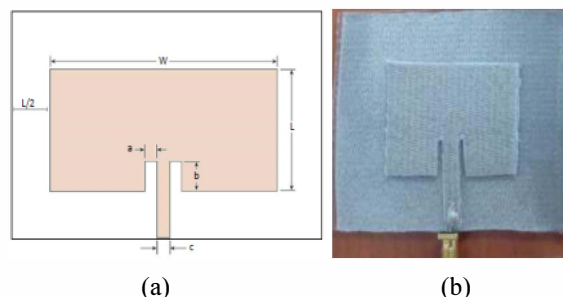


Fig 1. (a) Antenna structure, (b) Photograph of prototype.

TABLE I. PARAMETERS OF THE ANTENNA

Parameter	Value
W	43.29225 mm
L	34.6135 mm
a	2 mm
b	13 mm
c	5 mm
Substrate thickness	2 mm
Dielectric constant (ϵ_r)	3

A. Embroidered Conductive Layers

The conductive layers have been embroidered by using Shieldex 40-22/7 +110 PET 3 ply. The thread lineal resistance is 800 Kohm/m and the weight is 27,692.3m/kg. The conductive thread was embroidered on very thin cotton fabric with 0.25 mm thickness. The minimal thickness of the fabric minimizes its effect on the antenna performance and its losses are very small compared to the losses of the sewing thread [7]. Three different patch layers (A, B and C) and hence different structures have been embroidered differently using conductive thread and normal thread from bobbin, as shown in Fig. 2. All

three structures are having the same two-sided ground plane. The amount of conductive thread used was obtained by balance station before and after embroidery. The resistance of patch layer was measured using Fluke PM 6304 by choosing the same reference point of measurement.

2-sided embroidery patch	1-sided embroidery patch	1-sided embroidery patch
PDMS substrate	1-sided embroidery patch	Non conductive side
2-sided embroidery ground	Non conductive layer	PDMS substrate
Antenna A	Non conductive layer	Antenna C
	PDMS substrate	
	2-sided embroidery ground	
Antenna B		

Fig 2. Three different structures of the antenna A, B and C

TABLE II. CHARACTERISTICS OF THE CONDUCTIVE LAYERS

Antenna	Patch A	Patch B	Patch C	Ground
Stitch density (mm)	0.4	0.4	0.4	0.4
Stitch number	2365	2365	2365	7725
Weight of conductive patch (g)	0.684	0.684	0.342	2.226
Lineal resistance (Kohm)	15,153.226	15,153.226	757,606	49,314.44
Measured patch resistance (Ohm)	28.363	28.547	65.259	53.658

Table II shows the embroidery structure properties and conductive characteristics of the three antennas (A, B and C).

The measured results in Table II show that although antennas A and B are two different embroidery structures, they have similar conductivity, identical stitch number, stitch density and conductive thread amount.

B. Polymer Lamination and Integration

Three antennas have been laminated on half-cured PDMS and multi layers integration has been applied with fresh PDMS as glue. After that, the antennas have been left to be fully cured. The processes follow the method introduced in [3], [9].

III. ANTENNA PERFORMANCE

Fig. 4 illustrates the reflection coefficient results of the three antenna structures. The operating frequency of antenna A is from 2.84 GHz to 4.95 GHz for a reflection coefficient of better than -10 dB. Wide bandwidth of 54% is thus achieved. Although with the same amount of conductive thread and embroidery characteristic, the antenna B, which has the thickest non-conductive surface facing the substrate causes most dielectric loss and thus the reflection coefficient is poorer than the normal two-sided embroidery, antenna A. This is due to antenna A has most of its electronic charges at the bottom side which facing the substrate. According to [10], the conductive layers of microstrip patch antenna should be faced downward against the substrate since substrate layer is thin and most of electronic charges concentrate on the bottom of the patch. The poor reflection coefficient result of antenna C was due to its lowest conductivity layer and the non-conductive layer facing downward the substrate.

The resonant frequency is different from theoretical calculation due to the conductive thread surface is not a continuous solid as estimated theoretically.

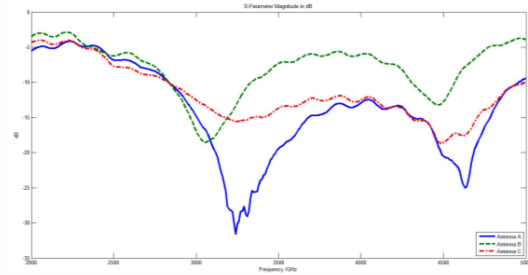


Fig 4. Reflection coefficient versus frequency

IV. CONCLUSION

With identical stitch density, stitch number and conductive thread amount, single two-sided embroidery antenna structure gives similar conductivity as two one-sided embroidery antenna structure. However, two-sided embroidery antenna performs better in terms of reflection coefficient. This is due to majority charges concentrate at the bottom of the patch and non-conductive layer facing downward against the substrate will give poorer reflection coefficient regardless of its identical conductivity surface.

ACKNOWLEDGEMENT

This research has been supported by Malaysia Government, Ministry of Science, Technology and Innovation (MOSTI), with project no 06-02-12-SF0213.

REFERENCES

- [1] M. A. R. Osman, M. K. Abd Rahim, N. A. Samsur, H. A. M. Salim, and M. F. Ali, "Embroidered fully textile wearable antenna for medical monitoring applications," *Progress In Electromagnetics Research*, vol. 117, pp. 321–337, 2011.
- [2] L. Vallozzi, W. Vandendriessche, H. Rogier, C. Hertleer, and M. L. Scarpell, "Wearable textile GPS antenna for integration in protective garments," *Antennas and Propagation (EuCAP)*, 2010 4th European Conference, pp. 1–4, April 2010.
- [3] Zheyu Wang, Lanlin Zhang, Y. Bayram, and J. L. Volakis, "Multilayer printing of embroidered RF circuit on polymer composites," *Antennas and Propagation (APSURSI)*, pp. 278–281, July 2011.
- [4] A. Chauraya, Shiyu Zhang, W. Whittow, T. Acti, R. Seager, T. Dias, and Y. C. Varadaxoglou, "Addressing the challenges of fabricating microwave antennas using conductive threads," *Antennas and Propagation (EUCAP)*, 2012 6th European Conference, pp. 1365–1367, March 2012.
- [5] R. Jung-Sim, C. Yong-Seung, L. Jae-Hee, T. Youndo, N. Sangwook, and K. Tae Jin, "Embroidered wearable multiresonant folded dipole antenna for FM reception," *Antennas and Wireless Propagation Letters*, vol.9, pp. 803–806, August 2010.
- [6] T. Maleszka and P. Kabacik, "Bandwidth properties of embroidered loop antenna for wearable applications," *Wireless Technology Conference (EuWIT)*, 2010 European Conference, pp. 89–92, Sept 2010.
- [7] E. Moradi, T. Bjorninen, L. Ukkonen, and Y. Rahmat-Samii, "Effects of sewing pattern on the performance of embroidered dipole-type RFID tag antennas" *Antennas and Wireless Propagation Letters*, vol. 11, pp. 1482–1485.
- [8] S. Koulouridis, G.Kiziltas, Yijun Zhou, D. J. Hansford, and J. L. Volakis, "Polymer-Ceramic composites for microwave applications: fabrication and performance assessment," *Microwave Theory and Techniques*, vol. 54, pp. 4202–4208, Dec 2006.
- [9] Lanlin Zhang, Zheyu Wang, and J. L. Volakis, "Textile antennas and sensors for body-worn applications," *Antennas and Wireless Propagation Letters*, vol. 11, pp. 1690–1693, Jan 2013.
- [10] Yuehui Ouyang, W. J. Chappell, "High frequency properties of electro-textiles for wearable antenna applications," *IEEE Transaction on Antennas and Propagation*, vol. 56, iss. 2, pp. 381–389, Feb 2008.

Investigation of Embroidery Conductive Layer Dyed with Graphene and ZnO

Loc Ngo Quang Bao¹, Pei Cheng Ooi¹, Jit Kai Chin¹, Chuan Chin Pu²

¹The University of Nottingham, Malaysia Campus, Jalan Broga, Semenyih, 43500 Selangor Darul Ehsan, Malaysia

²Sunway University, Jalan Universiti, Bandar Sunway, Petaling Jaya, 46150 Selangor Darul Ehsan, Malaysia

Abstract - This paper presents a method to improve the conductivity of embroidered patch antenna by using graphene and zinc oxide (ZnO) nanopowder. By dispersion and immersion of graphene and ZnO, the embroidered conductive patch layers have been designed, fabricated and tested. Analysis of the effect of graphene and ZnO solution on patch resistance has been carried out. The measured results show that the conductivity performs better with ZnO dyed embroidered patch layer. In contrast, graphene improves the sheet resistance while ethanol solvent reacts with silver thread.

Index Terms — embroidery antenna, patch antenna, graphene, zinc oxide.

I. INTRODUCTION

Wearable antenna with garment integration becomes essential nowadays in many applications such as in medical field, military development, mineworker tracking and environment monitoring. These antennas need not only possess good RF performance characteristics but also mechanical structure which is adaptable to conformity and durability [1]-[3]. The wearable antenna needs to be hidden and low profile. Therefore, patch antenna with microstrip feeding is suitable for any wearable application [4].

Embroidery patch antenna is a potential candidate that meets the requirements. Furthermore, computerized sewing machine can be used to fabricate textile antennas quickly and on mass manufacturing scales, highly flexible to change the design at minimal costs and time. Researches show that conductivity of embroidered layers can be improved by selecting high conductive thread with more metal concentration, considering stitch direction and spacing between stitches or increasing stitch density, stitch type [5]-[8]. However, these methods have the distinctive disadvantage of increasing stiffness and reducing elasticity. Higher thread friction could also generate excess heat at each of the contact points at high machine speeds and needles damages mainly due to the coarse nature of the conductive threads utilized [9]. As a result of this constraint, the conductivity can be improved by combining the antenna conductive layer with exceptional properties of ZnO or graphene, both of which are in nanostructure powder form.

Graphene is a basic building block for graphitic materials of all other dimensionalities [10]. It has attracted significant attention as a result of its outstanding electronic, mechanical and chemical properties [11]. Meanwhile, ZnO is an important metal oxide nanostructure which has unique

advantages in electronic devices, low processing cost, durability and strong energy [12].

This paper reports the initial stage to prepare the embroidery conductive layer for antenna through immersion. For thousands of years, humans have been decorating clothing through immersion of fabrics in liquid dyes [13]. This process provides a useful pathway for incorporating nanopowder into porous, light and flexible embroidered layers which popular spin coating or vacuum coating method cannot achieve.

II. PATCH DESIGN AND DYEING PROCEDURE

Fig. 1(a) shows the front view of the patch structure and Fig. 1(b) is the photograph of the patch prototype. The patch parameters are illustrated in Table I.

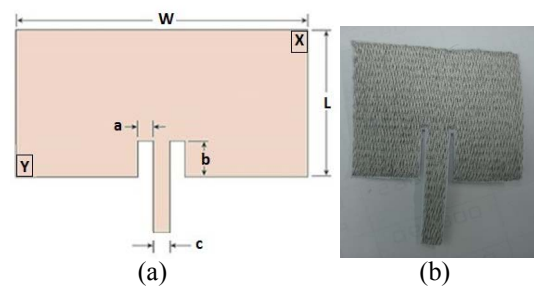


TABLE I
PARAMETERS OF CONDUCTIVE PATCH

Parameter	a	b	c	W	L
Value (mm)	2	13	5	49.2925	34.6135

A. Embroidered Conductive Layers

The conductive layers have been embroidered by using Shieldex 40-22/7 +110 PET 3ply. The thread lineal resistance is 800 Kohm/m. The conductive thread was embroidered with 2365 stitches and 0.4 mm density on very thin cotton fabric with 0.25 mm thickness. The minimal thickness of the fabric minimizes its effect on the antenna performance and its losses are very small compared to the losses of the sewing thread [14]. The resistances of patch layers were measured using Fluke PM 6304 by choosing the same reference points X, Y as shown in Fig. 1(a).

B. Dispersion and Dyeing Process

Graphene 8nm nanoflakes and 25nm ZnO nanopowder were prepared for dyed solution. According to [11], graphene was observed in the aqueous solution containing 70 vol. % ethanol with maximum concentration of 0.05 mg/mL. while concentration of ZnO in ethanol solvent is 0.5 mg/mL. The solutions were utilized ultrasonic irradiation in sonicating bath for two hours to obtain homogeneous dispersion. The embroidered patch layers were dipped 30 seconds in prepared dyed dispersions then dried for 20 minutes at 70°C. This dyeing process was repeated 5 times and 11 times for graphene, ZnO solution respectively to possess the resistance effect.

III. RESULTS AND DISCUSSIONS

Fig. 2 illustrates the measured resistance results of conductive embroidered antenna patch layer applied graphene and ZnO solution after multiple repeated dyeing process.

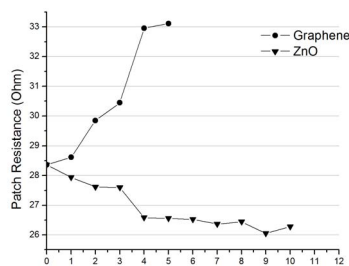


Fig. 2. Resistances of graphene and ZnO dyed antenna patches.

The result shows that ethanol solvent has reacted with silver thread and it causes lost in conductivity. As a result, graphene dyed patch shows the trend to increase in resistivity and graphene solution is therefore not strong enough to enhance the antenna patch conductivity. The graphene dyeing process was stopped after 5 times immersion. In contrast, ZnO dispersion solution helps to increase conductivity up to 7.3% after 10 times dyeing and the ZnO dyed antenna patch seemed to reach its limitation when the average patch resistance achieves at 26.4 Ohm.

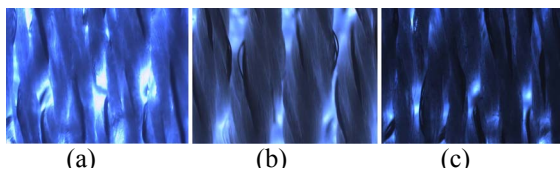


Fig. 3. Microscope zoom 4x view of dyed embroidered antenna patch (a) origin without immersion, (b) ZnO, (c) graphene.

Fig. 3 shows the microscope zoom 4x view of different dyed embroidered antenna patch with ZnO, graphene solutions compared with Fig. 3(a) without immersion under same microscope setting condition. The changing color in Fig. 3 (b), (c) indicates that graphene and ZnO nanopowder were deposited on embroidered surface and the longer time the dyeing process is, the more nanopowder will be placed and the wider gap between threads will be created.

IV. CONCLUSION

In this paper, a new method to improve the conductivity of embroidery patch antenna is introduced. With simple

dyeing method, ZnO dispersion solution has improved the conductive characteristic of embroidered patch antenna. Although nanopowder is deposited, the graphene dyed patch raises up sheet resistance because of existing process of ethanol and silver thread reaction. The ZnO dyed embroidered antenna patch will be further integrated with polymer substrate by lamination method to complete a novel class of embroidery antenna with high strength and performance [15].

ACKNOWLEDGEMENT

This research has been supported by Malaysia Government, Ministry of Science, Technology and Innovation (MOSTI), with project no 06-02-12-SF0213.

REFERENCES

- [1] M. A. R. Osman, M. K. Abd Rahim, N. A. Samsur, H. A. M. Salim, and M. F. Ali, "Embroidered fully textile wearable antenna for medical monitoring applications," *Progress In Electromagnetics Research*, vol. 117, pp. 321–337, 2011.
- [2] L. Vallozzi, W. Vandendriessche, H. Rogier, C. Hertleer, and M. L. Scarpell, "Wearable textile GPS antenna for integration in protective garments," *Antennas and Propagation (EuCAP)*, 4th European Conference, pp. 1–4, April 2010.
- [3] Zheyu Wang, Lanlin Zhang, Y. Bayram, and J. L. Volakis, "Multilayer printing of embroidered RF circuit on polymer composites," *Antennas and Propagation (APSURSI)*, pp. 278–281, July 2011.
- [4] S. Sankaralingam, S. Dasgupta, S. S. Roy, K. Monhanty, and B. Gupta, "A fully fabric wearable antenna for HiperLAN/2 applications," *India conference (INDICON)*, pp. 1–5, Dec 2011.
- [5] A. Chauraya, Shiyu Zhang, W. Whittow, T. Acti, R. Seager, T. Dias, and Y. C. Varadaxoglou, "Addressing the challenges of fabricating microwave antennas using conductive threads," *Antennas and Propagation (EuCAP)*, 6th European Conference, pp. 1365–1367, March 2012.
- [6] R. Jung-Sim, C. Yong-Seung, L. Jae-Hee, T. Youndo, N. Sangwook, and K. Tae Jin, "Embroidered wearable multiresonant folded dipole antenna for FM reception," *Antennas and Wireless Propagation Letters*, vol. 9, pp. 803–806, August 2010.
- [7] T. Maleszka and P. Kabacik, "Bandwidth properties of embroidered loop antenna for wearable applications," *Wireless Technology Conference (EuWIT)*, *European Conference*, pp. 89–92, Sept 2010.
- [8] Shiyu Zhang, A. Chauraya, W. Whittow, R. Seager, T. Acti, T. Dias, and Y. Vardaxoglou, "Embroidered wearable antennas using conductive threads with different stitch spacings," *Antennas and Propagation Conference (LAPC)*, pp. 1–4, 2012.
- [9] T. Acti, Shiyu Zhang, A. Chauraya, W. Whittow, R. Seager, T. Dias, and Y. Vardaxoglou, "High performance flexible fabric electronics for megahertz frequency communication," *Antennas and Propagation Conference (LAPC)*, pp. 1–4, 2011.
- [10] A. K. Geim and K. S. Novoselov, "The rise of graphene," *Nature materials* 6, pp. 183–191, 2007.
- [11] Wei-Wei Liu, Bao-Yu Xia, Xiao-Xia Wang, and Jian-Nong Wang, "Exfoliation and dispersion of graphene in ethanol-water mixtures," *Frontiers of Materials Science*, vol. 6, Issue 2, pp. 176–182, June 2012.
- [12] C. X. Xu, X. W. Sun, B. J. Chen, P. Shum, S. Li, and X. Hu, "Nanostructural zinc oxide and its electrical and optical properties," *J. Appl. Phys.* 95, 661, 2004.
- [13] R. S. Horsfall and L. G. Lawrie, *The dyeing of textile fibres*, 2nded, Chapman & hall ltd, London, 1946.
- [14] E. Moradi, T. Bjorninen, L. Ukkonen, and Y. Rahmat-Samii, "Effects of sewing pattern on the performance of embroidered dipole-type RFID tag antennas," *Antennas and Wireless Propagation Letters*, vol. 11, pp. 1482–1485, 2012.
- [15] L. Ngo Quang Bao, P. C. Ooi and J. K. Chin, "The Effect of Different Structures of Embroidery Patch Antenna on Polymer Substrate with Identical Embroidery Properties," in *Proceedings IEEE International Symposium on Antennas and Propagation and USNC-URSI Radio Science Meeting 2014*, Memphis, Tennessee, USA, 6-11 July 2014, pp. 840-841.

Embroidery Patch Antennas on Polymer Substrate with Identical Embroidery Properties

Loc Ngo Quang Bao, *Student Member, IEEE*, Pei Cheng Ooi, *Member, IEEE*, Jit Kai Chin, and Chuan Chin Pu

Abstract—This paper presents a novel class embroidery patch antennas on polymer composite — polydimethylsiloxane (PDMS). By lamination and polymer integration, different structures and feeding techniques of fully embroidered polymer patch antenna with ground plane have been designed, fabricated and tested. Analysis of the effect of conductive patch weight, conductive characteristics using different embroidery structure on antenna performance has been carried out. The measured results show that although double embroidered layer on one side of fabric has similar conductivity and identical embroidery properties with two-sided embroidery, the antenna performs better using two-sided embroidery structure in term of reflection coefficient and gain measurement.

Index terms—embroidery antenna, polymer antenna, patch antenna.

I. INTRODUCTION

Wearable antenna with garment integration becomes essential nowadays in many applications such as in medical field, military development, mineworker tracking and environment monitoring. These antennas need not only possess good RF performance characteristics but also mechanical structure which adaptable to conformity and durability [1-3].

Embroidery antenna is potential candidate that meets the requirements. Furthermore, computerized sewing machine can be used to fabricate textile antennas quickly and on a mass manufacturing scale, highly flexible to change the design at minimal costs and time. Conductivity of embroidered layers can be improved by selecting high conductive thread, increasing stitch density and stitch type. The antenna performance can also be enhanced by considering stitch density, stitch direction and spacing between stitches [4]. Numerous researches on embroidery antenna with different types of conductive threads were introduced in [5-7].

Polymer is becoming an important material used for microwave and electronic applications. PDMS is the most widely used silicone-based organic polymer and is well-known for its advantage properties including nonflammable, water resistant, room temperature fabrication, low loss and adjustable dielectric constant by adding ceramic powder [8]. To increase embroidery antenna durability, reinforcement, miniature and low loss dielectric, PDMS substrate was introduced in [3], [9].

This paper presents different structures of fully embroidered patch antenna on PDMS substrate. The structures vary with the patch design, feeding techniques, patch weight and conductive characteristics with identical embroidered and electrical properties. Antenna performance analysis in term of

reflection coefficient, radiation pattern and gain has been carried out.

II. ANTENNA DESIGN AND CHARACTERIZATION

Three different patch antenna designs include microstrip-fed rectangular patch (design 1), microstrip-fed polygon patch (design 2) and SMA-fed polygon patch (design 3) have been fabricated and tested. Fig. 1 shows the front view of the antenna designs and their photograph prototypes. The antenna parameters are illustrated in Table I.

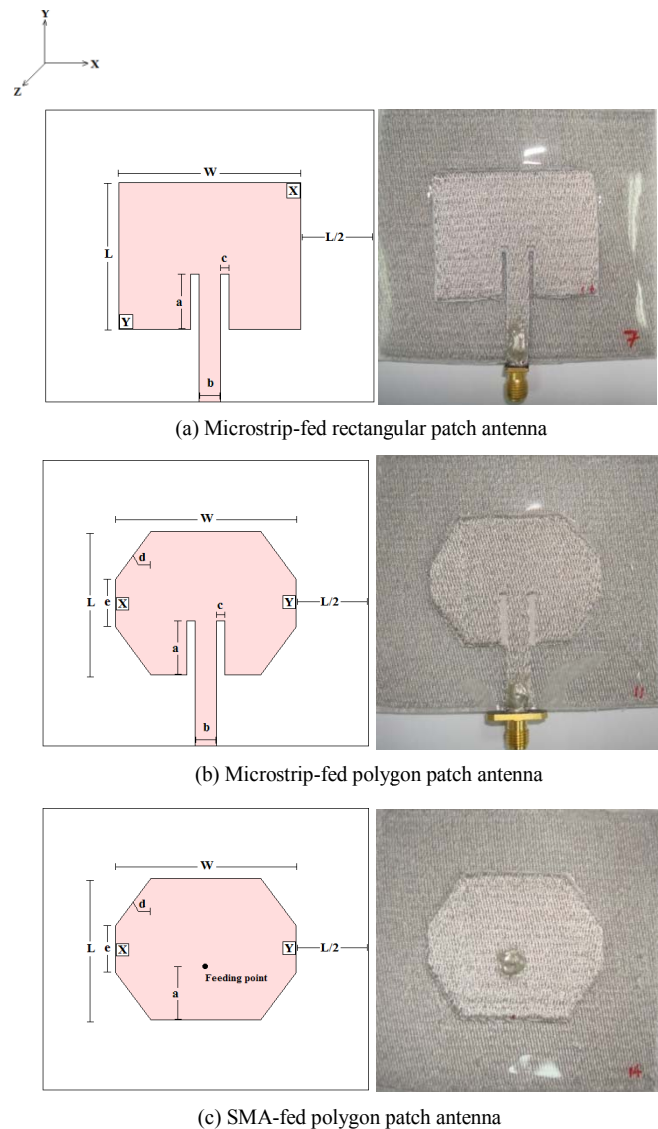


Fig 1. Antenna designs and photograph of prototypes.

TABLE I
PARAMETERS OF THE ANTENNA

Parameter	Value
W	43.29225 mm
L	34.6135 mm
a	13 mm
b	5 mm
c	2 mm
d	14.37 mm
e	11.53 mm
Substrate thickness	2 mm
Dielectric constant (ϵ_r)	3

A. Embroidered Conductive Layers

The conductive layers have been embroidered by using Shieldex 40-22/7 +110 PET 3 ply. The thread lineal resistance is 800 Kohm/m and the weight is 27,692.3m/kg. The conductive thread was embroidered on very thin cotton fabric with 0.25 mm thickness. The minimal thickness of the fabric minimizes its effect on the antenna performance and its losses are very small compared to the losses of the sewing thread [7]. Three different patch layers (A, B and C) and hence different structures have been embroidered differently using conductive thread and normal thread from bobbin, as shown in Fig. 2.

2-sided embroidery patch	1-sided embroidery patch	1-sided embroidery patch
PDMS substrate	1-sided embroidery patch	Non conductive side
2-sided embroidery ground	Non conductive layer	PDMS substrate
Structure A	Non conductive layer	2-sided embroidery ground
	PDMS substrate	Structure C
	2-sided embroidery ground	
	Structure B	

Fig 2. Three different embroidery structures.

Antenna design 1 was constructed using structure A, B and C, identified as antennas 1A, 1B and 1C. With different antenna designs and feeding techniques, designs 2 and 3 have been embroidered with structure A and B, identified as antennas 2A, 2B, 3A and 3B. All seven antennas are having the same two-sided ground plane. The amount of conductive thread used was obtained by balance station before and after embroidery. The resistance of patch layer was measured using Fluke PM 6304 by choosing the same reference points X and Y as shown in Fig. 1.

The measured resistance results of each antenna design using the same reference points in Table II agrees with their lineal resistance since they have the same amount of conductive thread regardless of their different structures except for antenna 1C which has higher resistance due to its poor structure with lowest amount of conductive thread. Among each set of design, as shown in Table II, antennas have identical embroidered properties and similar electrical characteristics.

TABLE II
CHARACTERISTICS OF THE CONDUCTIVE LAYERS

Antenna	Stitch spacing (mm)	Stitch number	Weight of conductive patch (g)	Lineal resistance (Kohm)	Measured resistance (Ohm)	
Set 1	1A	0.4	2365	0.684	15,153.22	28.363
	1B	0.4	2365	0.684	15,153.22	28.547
	1C	0.4	2365	0.342	757.606	65.259
Set	2A	0.4	2165	0.452	10,013.53	29.830

2	2B	0.4	2165	0.452	10,013.53	30.153
Set 3	3A	0.4	2098	0.574	12,716.30	26.102
	3B	0.4	2098	0.574	12,716.30	26.549
	Ground	0.4	7725	2.226	49,314.44	53.658

B. Polymer Lamination and Integration

These antennas were laminated on half-cured PDMS and multi layers integration has been applied with fresh PDMS as glue. After that, the antennas have been left to be fully cured. The processes follow the method introduced in [3], [9] and [10].

III. ANTENNA PERFORMANCE

Fig. 3(a) illustrates the reflection coefficient results of the three antennas 1A, 1B and 1C. The operating frequency of antenna A is from 2.84 GHz to 4.95 GHz for a reflection coefficient of better than -10 dB. Wide bandwidth of 54% is thus achieved. Although with the same amount of conductive thread and embroidery characteristic, the antenna 1B, which has the thickest non-conductive surface facing the substrate causes most dielectric loss and thus the reflection coefficient is poorer than the normal two-sided embroidery, antenna 1A. This is due to antenna A has most of its electronic charges at the bottom side which facing the substrate. The poor reflection coefficient result of antenna 1C was due to its lowest conductivity layer and the non-conductive layer facing downward the substrate.

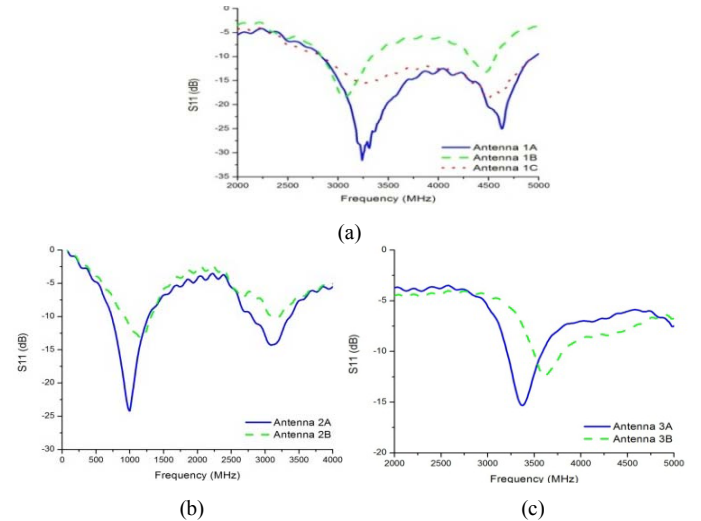


Fig 3. Measured reflection coefficient of different structures (a) Microstrip-fed rectangular patch, (b) Microstrip-fed polygon patch and (c) SMA-fed polygon patch antennas

Fig. 3(b), (c) shows that the feeding technique and antenna design do not affect the reflection coefficient results but the structure of embroidered patch layers. Antenna 2A and 3A with normal two-sided embroidery has better reflection coefficient result than antenna 2B and 3B respectively which have identical properties with double one-sided embroidery but the non-conductive layer faces again the substrate which causes dielectric loss and prevents the electronic charges travel to the ground. According to [11], the conductive layers of microstrip patch antenna should be faced downward against the substrate since substrate layer is thin and most of electronic charges concentrate on the bottom of the patch. The resonant frequency

is different from theoretical calculation due to the conductive thread surface is not a continuous solid as estimated theoretically.

The measured far-field radiation patterns of all antennas at its corresponding resonant frequencies are normalized and illustrated from Fig. 4 to Fig. 9.

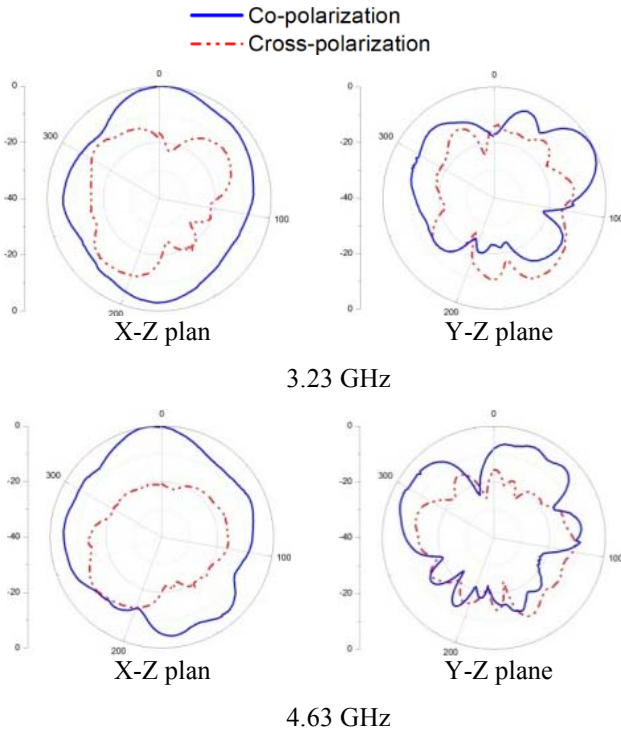


Fig. 4. Normalized measured radiation patterns of antenna 1A

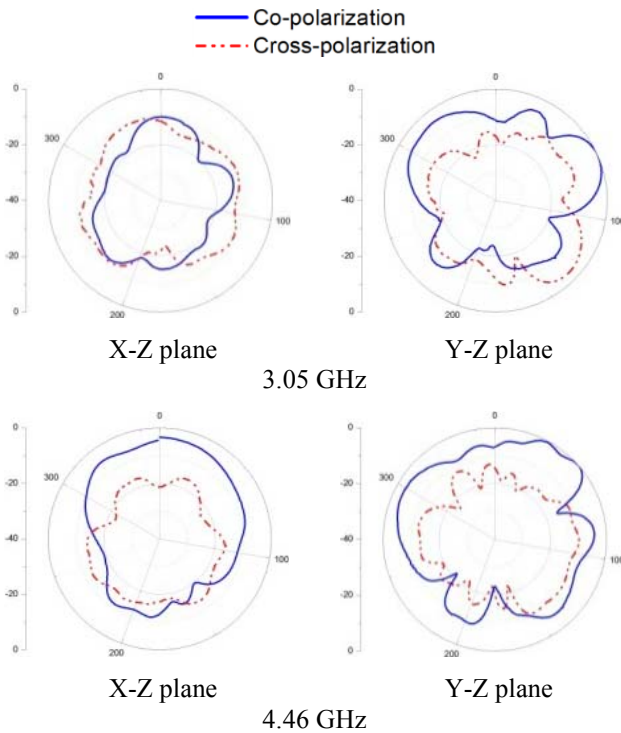


Fig. 5. Normalized measured radiation patterns of antenna 1B

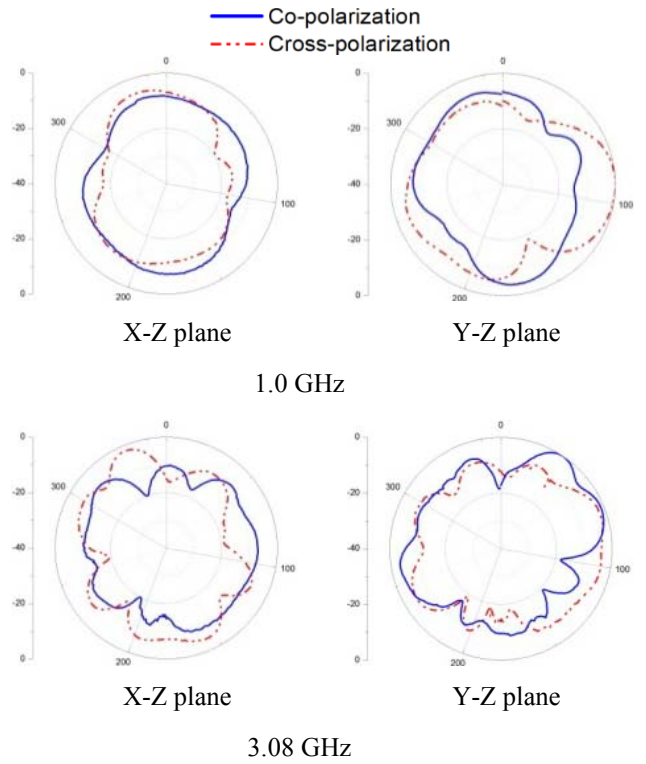


Fig. 6. Normalized measured radiation patterns of antenna 2A

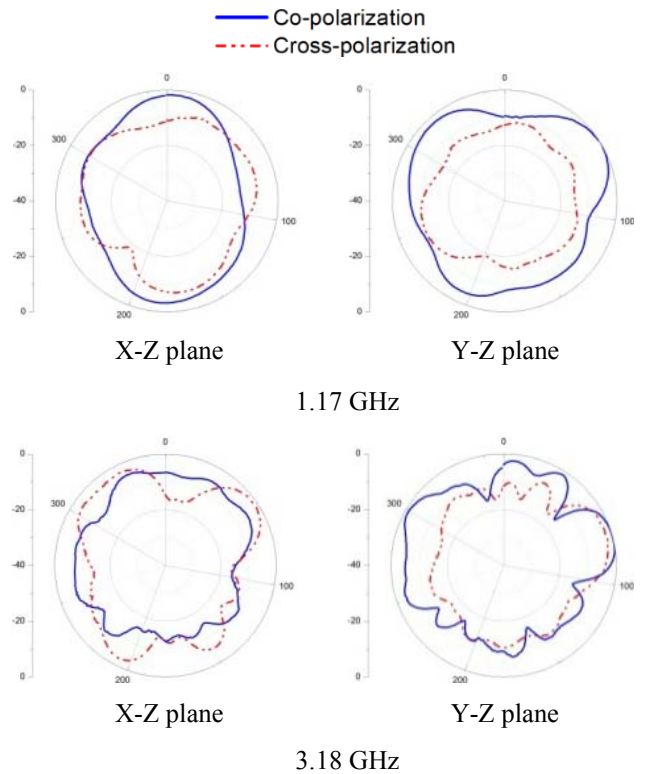


Fig. 7. Normalized measured radiation patterns of antenna 2B

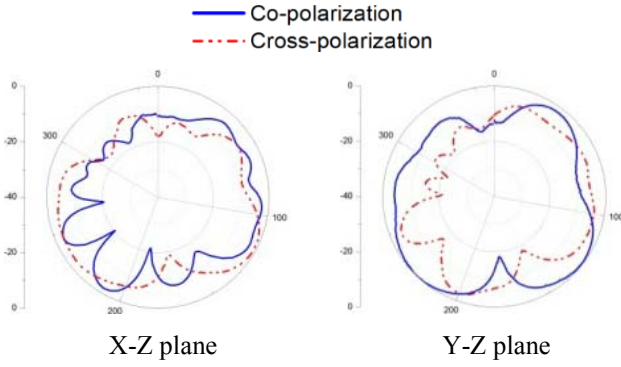


Fig. 8. Normalized measured radiation patterns of antenna 3A at 3.37 GHz

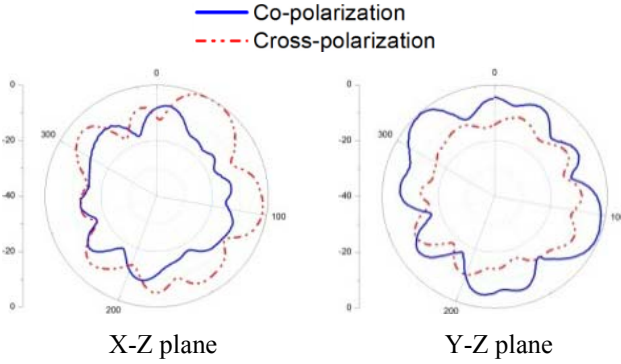


Fig. 9. Normalized measured radiation patterns of antenna 3B at 3.61 GHz

The measured radiation pattern results illustrates that on the x-z plane, the patch antennas with microstrip feeding (designs 1 and 2) have strongest radiation at its origin angle. Meanwhile, the radiation patterns on the y-z plane are tending to be stronger approximately 90° from its origin. This is because of the embroidery antenna body is much less conductive and with high material loss compared to bulk metal antenna except for the feeding point which has silver epoxy applied on SMA connector. Therefore, during the turning process on y-z plane, the radiated power reaches its higher level at the feeding faces to the transmitting antenna. Fig. 8 and Fig. 9 depict that there is not much difference between x-z plane and y-z plane since the antenna with design 3 has SMA feeding from the back-ground plane. The effect of small ground plane increases diffraction of radiation leading to the rise ripples [12]. Most antennas cross-polarization level is quite strong compared to co-polarization level due to its imperfect substrate thickness [13]. In fabrication process, conductive layers were unavoidable sunk slightly into the PDMS and the contribution of unbalance of PDMS mold during curing. It is clearly noticed that the embroidered structure does not affect the radiation pattern since the shape of patterns have not changed.

Table III shows the measured on-axis gains of proposed patch antennas from 1.7 GHz to 18 GHz range by using gain-transfer method. Among each antenna design (1, 2 and 3), structure A embroidered antenna are always have higher gain than structure B embroidered antenna regardless their identical

embroidery properties and similar electrical characteristics. This is because of structure A has most of its electronics charges at the bottom side which facing against the substrate and reduce the dielectric loss during radiation. The results show that the thicker the non-conductive layer facing the substrate, the lower the gain of the antenna.

TABLE III. MEASURED ON-AXIS GAIN OF PROPOSED ANTENNAS

Antenna	Resonant frequency (MHz)	S11 (dB)	On-axis gain (dB)
1A	3238	-25.442	-0.172
	4638	-25.036	1.866
1B	3050	-18.565	-12.975
	4469	-13.203	-3.936
1C	3250	-15.598	-4.654
	4488	-18.73	1.349
2A	3088	-14.307	-13.463
2B	3188	-10.1	-13.869
3A	3375	-15.329	-11.051
3B	3613	-12.407	-13.457

IV. CONCLUSION

With identical stitch density, stitch number, and conductive thread amount, single two-sided embroidery antenna gives similar conductivity with double one-sided embroidery. However, it performs better in term of reflection coefficient and gain. This is due to majority charges concentrate at the bottom of the patch and non-conductive layer facing downward against the substrate will give poorer performance regardless of its identical conductivity surface.

ACKNOWLEDGMENT

This research has been supported by Malaysia Government, Ministry of Science, Technology and Innovation (MOSTI), project no 06-02-12-SF0213.

REFERENCES

- [1] M. A. R. Osman, M. K. Abd Rahim, N. A. Samsur, H. A. M. Salim, and M. F. Ali, "Embroidered fully textile wearable antenna for medical monitoring applications," *Progress In Electromagnetics Research*, vol. 117, pp. 321–337, 2011.
- [2] L. Vallozzi, W. Vandendriessche, H. Rogier, C. Hertleer, and M. L. Scarpell, "Wearable textile GPS antenna for integration in protective garments," *Antennas and Propagation (EuCAP)*, 2010 4th European Conference, pp. 1–4, April 2010.
- [3] Zheyu Wang, Lanlin Zhang, Y. Bayram, and J. L. Volakis, "Multilayer printing of embroidered RF circuit on polymer composites," *Antennas and Propagation (APSURSI)*, pp. 278–281, July 2011.
- [4] A. Chauraya, Shiyu Zhang, W. Whittow, T. Acti, R. Seager, T. Dias, and Y. C. Varadaxoglou, "Addressing the challenges of fabricating microwave antennas using conductive threads," *Antennas and Propagation (EUCAP)*, 2012 6th European Conference, pp. 1365–1367, March 2012.
- [5] R. Jung-Sim, C. Yong-Seung, L. Jae-Hee, T. Youndo, N. Sangwook, and K. Tae Jin, "Embroidered wearable multiresonant folded dipole antenna for FM reception," *Antennas and Wireless Propagation Letters*, vol. 9, pp. 803–806, August 2010.
- [6] T. Maleszka and P. Kabacik, "Bandwidth properties of embroidered loop antenna for wearable applications," *Wireless Technology Conference (EuWIT)*, 2010 European Conference, pp. 89–92, Sept 2010.
- [7] E. Moradi, T. Bjorninen, L. Ukkonen, and Y. Rahmat-Samii, "Effects of sewing pattern on the performance of embroidered dipole-type RFID tag antennas" *Antennas and Wireless Propagation Letters*, vol. 11, pp. 1482–1485.

- [8] S. Koulouridis, G.Kiziltas, Yijun Zhou, D. J. Hansford, and J. L. Volakis, "Polymer-Ceramic composites for microwave applications: fabrication and performance assessment," *Microwave Theory and Techniques*, vol. 54, pp. 4202–4208, Dec 2006.
- [9] Lanlin Zhang, Zheyu Wang, and J. L. Volakis, "Textile antennas and sensors for body-worn applications," *Antennas and Wireless Propagation Letters*, vol. 11, pp. 1690–1693, Jan 2013.
- [10] Loc Ngo Quang Bao, Pei Cheng Ooi and Jit Kai Chin, "The effect of different structures of embroidery patch antenna on polymer substrate with identical embroidery properties," *IEEE Antennas and Propagation Society International Symposium (APSURSI)*, pp. 840-841, July 2014.
- [11] Yuehui Ouyang, W. J. Chappell, "High frequency properties of electro-textiles for wearable antenna applications," *IEEE Transaction on Antennas and Propagation*, vol. 56, iss. 2, pp. 381–389, Feb 2008.
- [12] C. A. Balanis, *Antenna theory analysis and design*, 3rd ed, John Wiley & Sons, New Jersey, 2005.
- [13] R. Garg, P. Bhartia, Inder Bahl and A. Ittipiboon, *Microstrip antenna design handbook*, Artech House, 2001.

Embroidery Patch Antennas Dyed with Nanopowders on Polymer Substrate

Loc Ngo Quang Bao, *Student Member, IEEE*, Pei Cheng Ooi, *Member, IEEE*, Jit Kai Chin, and Chuan Chin Pu

Abstract—This paper presents a method to improve the conductivity of embroidered patches used in antennas on polymer composite — polydimethylsiloxane (PDMS) substrate. Nanopowders which include graphene, zinc oxide (ZnO) and copper oxide (CuO) were dispersed in ethanol solvent to prepare as dyeing solutions. The effect of nanopowders on patch resistance has been studied. The measured results show that the patch conductivity improves 11.87% after 7 times dyeing with CuO and 8.14% after 10 times dyeing with ZnO. In contrast, graphene raises up the sheet resistance. The CuO and ZnO dyed conductive patch layers have been laminated and integrated on polymer substrate with embroidered ground plane to analyze the dyeing effect on antenna performance. Although dyeing effect reduces the resonant frequencies, the measured result indicates that dyed patch antennas perform better in term of reflection coefficient level.

Index terms—embroidery antenna, polymer antenna, patch antenna, graphene, zinc oxide, copper oxide.

I. INTRODUCTION

Wearable antenna with garment integration becomes essential nowadays in many applications such as in medical field, military development, mineworker tracking and environment monitoring. These antennas need not only possess good RF performance characteristics but also mechanical structure which is adaptable to conformity and durability [1-3]. The wearable antenna needs to be hidden and low profile. Therefore, microstrip patch antenna is suitable for any wearable application [4].

Embroidery patch antenna is a potential candidate that meets the requirements. Furthermore, computerized sewing machine can be used to fabricate textile antennas quickly and on mass manufacturing scales, highly flexible to change the design at minimal costs and time. Researches show that conductivity of embroidered layers can be improved by selecting high conductive thread with more metal concentration, considering stitch direction and spacing between stitches or increasing stitch density, stitch type [5-8]. However, these methods have the distinctive disadvantages of increasing stiffness and reducing elasticity. Higher thread friction could also generate excess heat at each of the contact points at high machine speeds and needles damages mainly due to the coarse nature of the conductive threads utilized [9]. As a result of this constraint, the conductivity can be improved by combining the antenna conductive layer with exceptional properties of ZnO, CuO or graphene, all of which are in nanostructure powder form.

Graphene is a basic building block for graphitic materials of all other dimensionalities [10]. It has attracted significant attention as a result of its outstanding electronic, mechanical and chemical properties [11]. Meanwhile, ZnO and CuO are important metal oxide nanostructures which have unique advantages in electronic devices, low processing cost, durability and strong energy [12]. For thousands of years, humans have been decorating clothing through immersion of fabrics in liquid dyes [13]. This process provides a useful pathway for incorporating nanopowder into porous, light and flexible embroidered layers which popular spin coating or vacuum coating method cannot achieve.

In this work, conductive patches layers have been designed, embroidered and applied dyeing method with CuO and ZnO nanopowders to improve its conductivity. The dyed patches have been integrated on PDMS substrate to analyze dyeing effect on antenna performance. The original patch antenna was also fabricated for reference purpose.

II. ANTENNA DESIGN AND DYEING PROCEDURE

The antenna design has been introduced in [14]. Fig. 1(a) shows the front view of the antenna structure and Fig. 1(b) is the photograph of antenna prototype. The antenna parameters are illustrated in Table I.

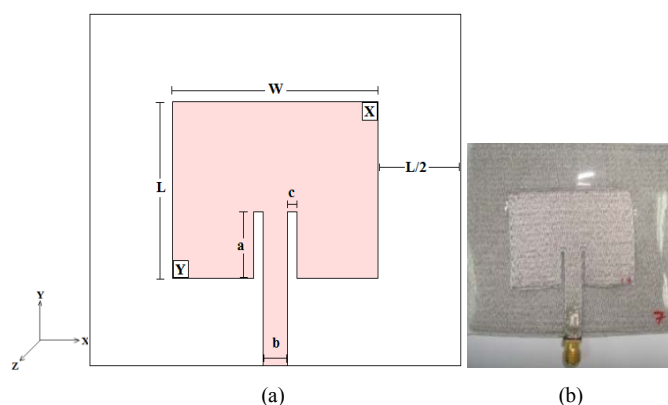


Fig 1. Antenna designs and photograph of prototypes.

TABLE I
PARAMETERS OF THE ANTENNA

Parameter	Value
W	43.29225 mm
L	34.6135 mm
a	13 mm
b	5 mm
c	2 mm

Substrate thickness	2 mm
Dielectric constant (ϵ_r)	3

A. Embroidered Conductive Layers

The conductive layers have been embroidered by using Shieldex 40-22/7 +110 PET 3ply. The thread lineal resistance is 800 Kohm/m. The conductive thread was embroidered with 2365 stitches and 0.4 mm density on very thin cotton fabric with 0.25 mm thickness. The minimal thickness of the fabric minimizes its effect on the antenna performance and its losses are very small compared to the losses of the sewing thread [15]. The resistances of patch layers were measured using Fluke PM 6304 by choosing the same reference points X and Y as shown in Fig. 1(a).

B. Dispersion and Dyeing Process

Dispersion and dyeing process were introduced in [16]. Graphene, ZnO and CuO nanopowders were dispersed in ethanol solvent to prepare as dyeing solution. According to [11], graphene achieves a maximum concentration of 0.05 mg/mL in aqueous solution containing 70 vol. % ethanol. The concentration of ZnO and CuO used in ethanol solvent is 0.5 mg/mL and 0.55 mg/mL respectively. The solutions were utilized ultrasonic irradiation in sonicating bath for two hours to obtain homogeneous dispersion as shown in Fig. 2.



Fig 2. Dyeing solution preparation process.

The embroidered patch layers were dipped 30 seconds in the dyeing dispersions then dried for 20 minutes at 70°C. This dyeing process was repeated five times for graphene and 11 times for ZnO and CuO solution to possess the resistance effect. The microscope zoom 4x view of graphene, ZnO and CuO dyeing solution after sonicating process is depicted in Fig. 3. The images show that homogeneous dispersion of nanopowder was achieved as nanoparticles were well distributed in ethanol solvent.

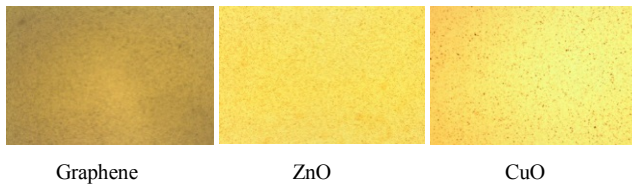


Fig 3. Microscope zoom 4x view of dyeing solution.

III. ANTENNA PERFORMANCE AND CHARACTERIZATIONS

A. Embroidered Patch Resistance

Fig. 4 shows the microscope zoom 4x view of different dyed embroidered patches with nanopowder solutions compared with original patch without dyeing under the same microscope setting condition.

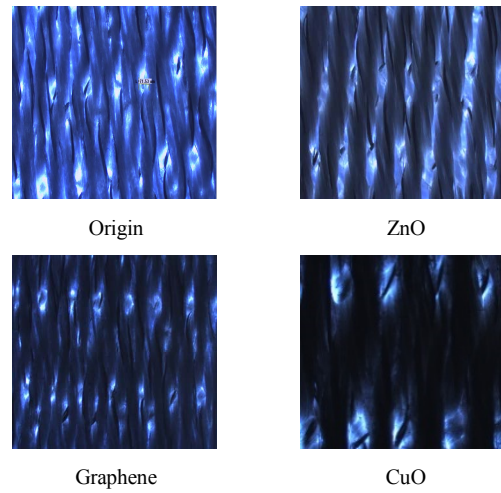


Fig 4. Microscope zoom 4x view of dyed embroidered antenna patch.

The changing color in Fig. 4 indicates that graphene and metal nanopowder were deposited on embroidered surfaces. The SEM images of all proposed dyed embroidered patches under zoom 150x and 2400x are illustrated in Fig. 5.

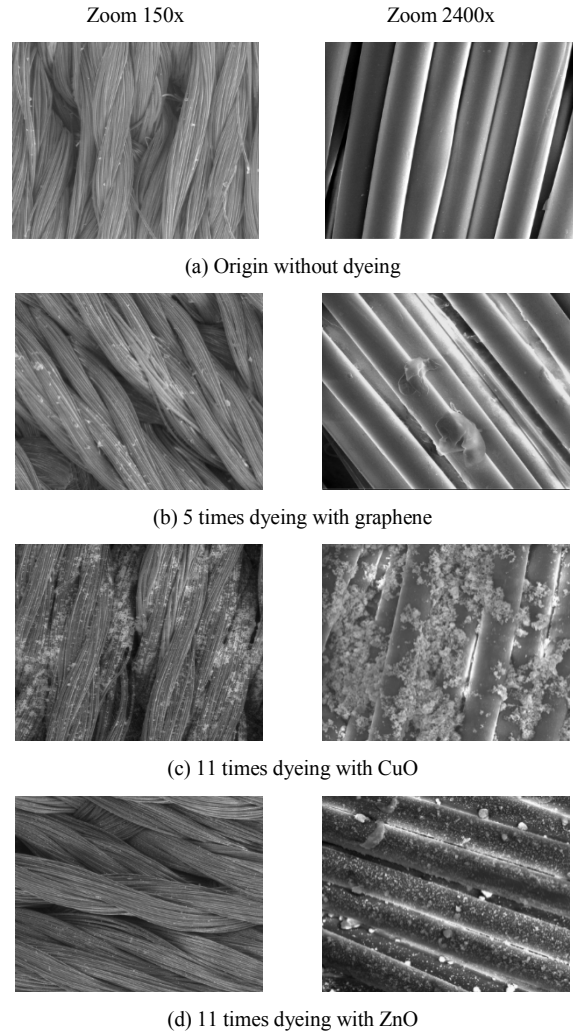


Fig 5. SEM images of proposed embroidered patches after dyeing effect.

The measured results of embroidered microstrip-fed rectangular patch antenna were presented as antenna 1A in [14] with original patch resistance is 28.363 Ohm. Fig. 6 illustrates the measured resistance results of embroidered patch layer dyed with graphene, ZnO, CuO solutions after multiple repeated dyeing processes. The result shows that ethanol solvent reacted with silver thread and this caused lost in conductivity. As a result, graphene dyed patch shows the tendency to increase its resistivity and graphene solution is therefore not strong enough to enhance the antenna patch conductivity [16]. Due to the increase of resistance, graphene dyeing process was stopped after five times immersion. In contrast, ZnO and CuO dispersion solutions contribute to the increase of conductivity up to 8.14% after 10 times dyeing for ZnO and 11.87% after seven times dyeing for CuO solution. The ZnO and CuO dyed antenna patches seemed to reach its limitation when the lowest patch resistance achieves at 26 and 25 Ohm respectively.

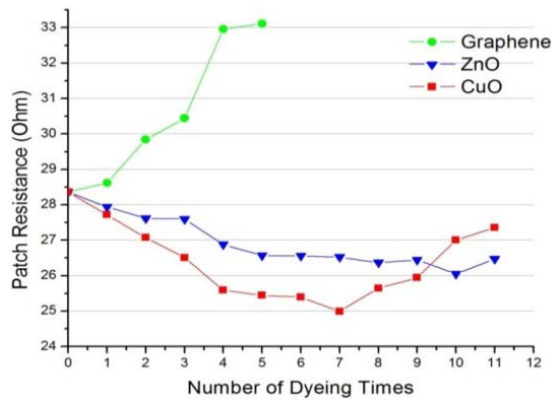


Fig 6. Resistances of graphene, ZnO and CuO dyed patches

B. Reflection Coefficient

Two embroidered patch antennas were fabricated by applying dyeing technique in CuO and ZnO solutions with seven and ten times immersion process respectively to achieve its best resistance. The nanopowder dyed patches were laminated and integrated on PDMS substrate followed by a two sided ground plane and compared with origin without dyeing version in Table II. Fig. 7 shows the measured reflection coefficient results of ZnO and CuO dyed antenna.

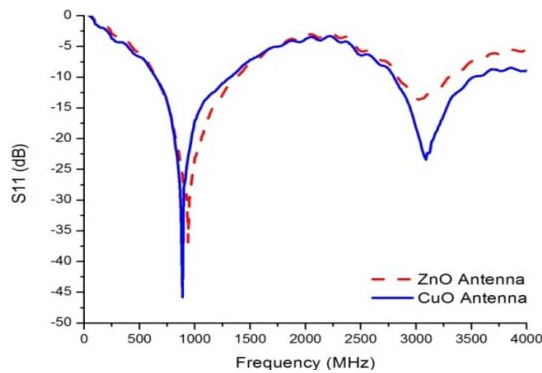


Fig 7. Measured reflection coefficient results of dyed embroidered patch antennas on PDMS substrate

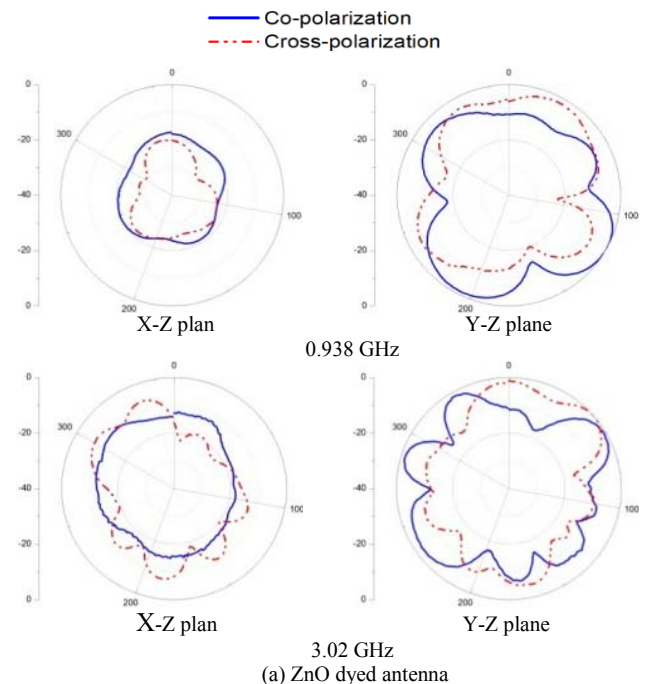
TABLE II
REFLECTION COEFFICIENT COMPARISONS BETWEEN WITH AND WITHOUT DYED PATCH ANTENNAS

Antenna	Patch Resistance (Ohm)	1 st		2 nd	
		Resonant frequency (MHz)	S11 (dB)	Resonant frequency (MHz)	S11 (dB)
Origin without dyeing	28.363	3238	-25.442	4638	-25.036
Dyed with ZnO	26.053	938	-36.874	3052	-13.648
Dyed with CuO	24.994	888	-45.817	3088	-23.426

The measured results in Table II show that higher conductive embroidered patch antenna gives better reflection coefficient level. Embroidery patch antenna on PDMS substrate without dyeing has patch resistance as 28.363 Ohm and its first resonant frequency at 3238 MHz with -25.442 dB. After dyeing, ZnO and CuO nanopowder were deposited respectively on embroidered surfaces. The process helps to improve the conductivity and reflection coefficient level improves to -36.874 dB and -45.817 dB respectively. However, the immersion process and the deposition of nanopowder have shifted the first resonant frequency down to 938 MHz for ZnO dyed antenna and 888 MHz for CuO dyed antenna compared to antenna without dyeing. Dyeing embroidery patch antenna with conductive nanopowder solution improves the conductivity of embroidered patch layer as well as the antenna performance in term of reflection coefficient level.

C. Radiation Patterns

The measured far-field radiation patterns of two dyed antenna at its first corresponding resonant frequencies are normalized and illustrated in Fig. 8.



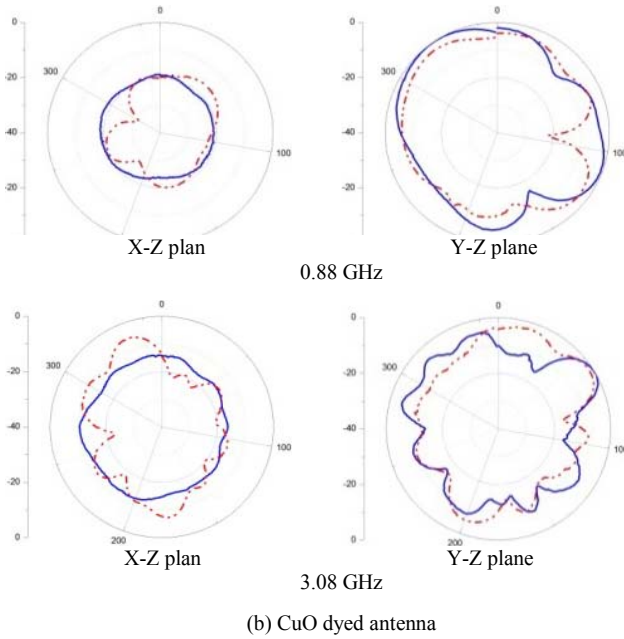


Fig. 8. Normalized measured radiation pattern of dyed antenna.

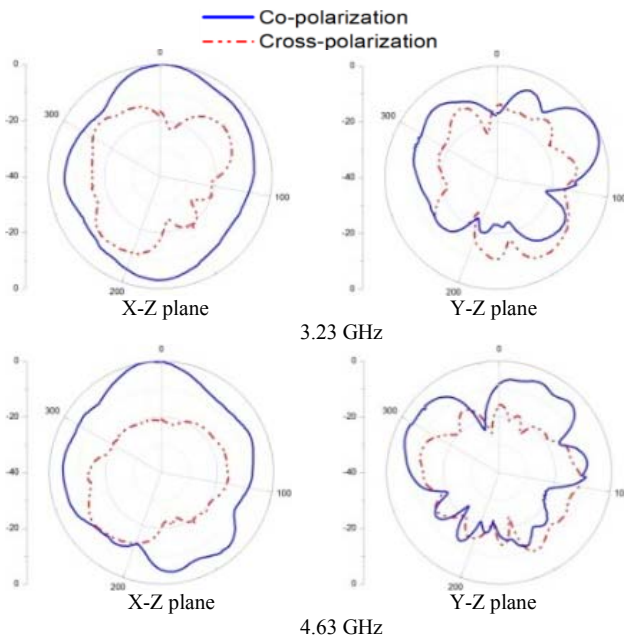


Fig. 9 Normalized measured radiation patterns of antenna without dyeing.

The measured radiation pattern results illustrate that on the x-z plane, the patch antennas have strongest radiation at its origin angle. Meanwhile, the radiation patterns on the y-z plane are tending to be stronger approximately 90° from its origin. This is because the embroidery antenna body is much less conductive and with high material loss compared to bulk metal antenna except for the feeding point which has silver epoxy applied on SMA connector. Therefore, during turning process on y-z plane, the radiated power reaches its higher level at the feeding faces to the transmitting antenna. The effect of small ground plane increases diffraction of radiation

leading to the rise ripples [17]. Most antennas cross-polarization level is strong compared to co-polarization level due to its imperfect substrate thickness [18]. In fabrication process, conductive layers were unavoidable sunk slightly into the PDMS and the contribution of unbalance of PDMS mold during curing. Fig. 8 indicates that dyed embroidery patch antenna with nanopowder has lower radiation on the x-z plane compared to antenna without dyeing in Fig. 9 because of the immersion process of embroidered patch in nanopowder dyeing solution.

TABLE III
MEASURED ON-AXIS GAIN OF PROPOSED ANTENNAS

Antenna	Resonant frequency (MHz)	S11 (dB)	On-axis gain (dB)
Origin	3238	-25.442	-0.172
	4638	-25.036	1.866
ZnO	3025	-13.648	-14.399
CuO	3088	-23.426	-15.4

Table III shows the measured on-axis gains of proposed patch antennas by using gain-transfer method. The effect of dyeing process has reduced the gain of original antenna at its operating frequency range due to the nanopowder deposited on radiating surfaces and the reaction of ethanol with silver thread.

IV. CONCLUSION

With dyeing method, ZnO and CuO dispersion solutions have improved the conductive characteristic of embroidered patch antenna and the level of reflection coefficient result. Although nanopowder is deposited, the graphene dyed patch raise up sheet resistance because of the existing process of ethanol and silver thread reaction.

ACKNOWLEDGMENT

This research has been supported by Malaysia Government, Ministry of Science, Technology and Innovation (MOSTI), project no 06-02-12-SF0213.

REFERENCES

- [1] M. A. R. Osman, M. K. Abd Rahim, N. A. Samsur, H. A. M. Salim, and M. F. Ali, "Embroidered fully textile wearable antenna for medical monitoring applications," *Progress In Electromagnetics Research*, vol. 117, pp. 321–337, 2011.
- [2] L. Vallozzi, W. Vandendriessche, H. Rogier, C. Hertleer, and M. L. Scarpell, "Wearable textile GPS antenna for integration in protective garments," *Antennas and Propagation (EuCAP)*, 4th European Conference, pp. 1–4, April 2010.
- [3] Zheyu Wang, Lanlin Zhang, Y. Bayram, and J. L. Volakis, "Multilayer printing of embroidered RF circuit on polymer composites," *Antennas and Propagation (APSURSI)*, pp. 278–281, July 2011.
- [4] S. Sankaralingam, S. Dasgupta, S. S. Roy, K. Monhanty, and B. Gupta, "A fully fabric wearable antenna for HiperLAN/2 applications," *India conference (INDICON)*, pp. 1–5, Dec 2011.
- [5] A. Chauraya, Shiyu Zhang, W. Whittow, T. Acti, R. Seager, T. Dias, and Y. C. Varadaxoglou, "Addressing the challenges of fabricating microwave antennas using conductive threads," *Antennas and Propagation (EUCAP)*, 6th European Conference, pp. 1365–1367, March 2012.
- [6] R. Jung-Sim, C. Yong-Seung, L. Jae-Hee, T. Youndo, N. Sangwook, and K. Tae Jin, "Embroidered wearable multiresonant folded dipole

- antenna for FM reception,” *Antennas and Wireless Propagation Letters*, vol. 9, pp. 803–806, August 2010.
- [7] T. Maleszka and P. Kabacik, “Bandwidth properties of embroidered loop antenna for wearable applications,” *Wireless Technology Conference (EuWIT), European Conference*, pp. 89–92, Sept 2010.
- [8] Shiyu Zhang, A. Chauraya, W. Whittow, R. Seager, T. Acti, T. Dias, and Y. Vardaxoglou, “Embroidered wearable antennas using conductive threads with different stitch spacings,” *Antennas and Propagation Conference (LAPC)*, pp. 1–4, 2012.
- [9] T. Acti, Shiyu Zhang, A. Chauraya, W. Whittow, R. Seager, T. Dias, and Y. Vardaxoglou, “High performance flexible fabric electronics for megahertz frequency communication,” *Antennas and Propagation Conference (LAPC)*, pp. 1–4, 2011.
- [10] A. K. Geim and K. S. Novoselov, “The rise of graphene,” *Nature materials* 6, pp. 183–191, 2007.
- [11] Wei-Wei Liu, Bao-Yu Xia, Xiao-Xia Wang, and Jian-Nong Wang, “Exfoliation and dispersion of graphene in ethanol-water mixtures,” *Fontiers of Materials Science*, vol. 6, Issue 2, pp. 176–182, June 2012.
- [12] Ahmad Umar, *Metal oxide nanostructures and their applications*, Amer Scientific Pub, October 2009
- [13] R. S. Horsfall and L. G. Lawrie, *The dyeing of textile fibres*, 2nded, Chapman & hall ltd, London, 1946.
- [14] Loc Ngo Quang Bao, Pei Cheng Ooi, and Jit Kai Chin, “The effect of different structures of embroidery patch antenna on polymer substrate with identical embroidery properties,” *Antennas and Propagation (APSURSI)*, July 2014.
- [15] E. Moradi, T. Bjorninen, L. Ukkonen, and Y. Rahmat-Samii, “Effects of sewing pattern on the performance of embroidered dipole-type RFID tag antennas,” *Antennas and Wireless Propagation Letters*, vol. 11, pp. 1482–1485, 2012.
- [16] Loc Ngo Quang bao, Pei Cheng Ooi and Jit Kai Chin, “Investigation of embroidery conductive layer dyed with graphene and ZnO,” to be presented in the 19th *International Symposium on Antenna and Propagation (ISAP)*, December 2014.
- [17] C. A. Balanis, *Antenna theory analysis and design*, 3rd ed, John Wiley & Sons, New Jersey, 2005.
- [18] R. Garg, P. Bhartia, Inder Bahl and A. Ittipiboon, *Microstrip antenna design handbook*, Artech House, 2001.